



HAL
open science

Measurement of event-plane correlations in $\sqrt{s_{NN}}=2.76$ TeV lead-lead collisions with the ATLAS detector

G. Aad, S. Albrand, J. Brown, J. Collot, S. Crépe-Renaudin, B. Dechenaux,
P.A. Delsart, C. Gabaldon, M.H. Genest, J.Y. Hostachy, et al.

► **To cite this version:**

G. Aad, S. Albrand, J. Brown, J. Collot, S. Crépe-Renaudin, et al.. Measurement of event-plane correlations in $\sqrt{s_{NN}}=2.76$ TeV lead-lead collisions with the ATLAS detector. Physical Review C, 2014, 90, pp.024905. 10.1103/PhysRevC.90.024905 . in2p3-00955165

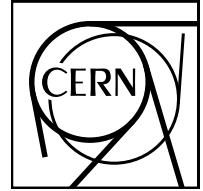
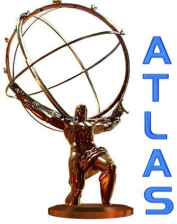
HAL Id: in2p3-00955165

<https://hal.in2p3.fr/in2p3-00955165>

Submitted on 21 Sep 2023

HAL is a multi-disciplinary open access archive for the deposit and dissemination of scientific research documents, whether they are published or not. The documents may come from teaching and research institutions in France or abroad, or from public or private research centers.

L'archive ouverte pluridisciplinaire **HAL**, est destinée au dépôt et à la diffusion de documents scientifiques de niveau recherche, publiés ou non, émanant des établissements d'enseignement et de recherche français ou étrangers, des laboratoires publics ou privés.



CERN-PH-EP-2014-021

Submitted to: Phys. Rev. C.

Measurement of event-plane correlations in $\sqrt{s_{NN}} = 2.76$ TeV lead–lead collisions with the ATLAS detector

The ATLAS Collaboration

Abstract

A measurement of event-plane correlations involving two or three event planes of different order is presented as a function of centrality for $7 \mu\text{b}^{-1}$ Pb+Pb collision data at $\sqrt{s_{NN}} = 2.76$ TeV, recorded by the ATLAS experiment at the LHC. Fourteen correlators are measured using a standard event-plane method and a scalar-product method, and the latter method is found to give a systematically larger correlation signal. Several different trends in the centrality dependence of these correlators are observed. These trends are not reproduced by predictions based on the Glauber model, which includes only the correlations from the collision geometry in the initial state. Calculations that include the final-state collective dynamics are able to describe qualitatively, and in some cases also quantitatively, the centrality dependence of the measured correlators. These observations suggest that both the fluctuations in the initial geometry and non-linear mixing between different harmonics in the final state are important for creating these correlations in momentum space.

Measurement of event-plane correlations in $\sqrt{s_{\text{NN}}} = 2.76$ TeV lead–lead collisions with the ATLAS detector

The ATLAS Collaboration

A measurement of event-plane correlations involving two or three event planes of different order is presented as a function of centrality for $7 \mu\text{b}^{-1}$ Pb+Pb collision data at $\sqrt{s_{\text{NN}}} = 2.76$ TeV, recorded by the ATLAS experiment at the LHC. Fourteen correlators are measured using a standard event-plane method and a scalar-product method, and the latter method is found to give a systematically larger correlation signal. Several different trends in the centrality dependence of these correlators are observed. These trends are not reproduced by predictions based on the Glauber model, which includes only the correlations from the collision geometry in the initial state. Calculations that include the final-state collective dynamics are able to describe qualitatively, and in some cases also quantitatively, the centrality dependence of the measured correlators. These observations suggest that both the fluctuations in the initial geometry and non-linear mixing between different harmonics in the final state are important for creating these correlations in momentum space.

PACS numbers: 25.75.Dw

I. INTRODUCTION

Heavy-ion collisions at the Relativistic Heavy Ion Collider (RHIC) and the Large Hadron Collider (LHC) create hot and dense matter that is thought to be composed of strongly interacting quarks and gluons. One striking observation that supports this picture is the large momentum anisotropy of particle emission in the transverse plane. This anisotropy is believed to be the result of anisotropic expansion of the created matter driven by the pressure gradients, with more particles emitted in the direction of the largest gradients [1]. The collective expansion of the matter can be modeled by relativistic viscous hydrodynamic theory [2]. The magnitude of the azimuthal anisotropy is sensitive to transport properties of the matter, such as the ratio of the shear viscosity to the entropy density and the equation of state [3].

The anisotropy of the particle distribution ($\frac{dN}{d\phi}$) in azimuthal angle ϕ is customarily characterized by a Fourier series:

$$\frac{dN}{d\phi} \propto 1 + 2 \sum_{n=1}^{\infty} v_n \cos n(\phi - \Phi_n), \quad (1)$$

where v_n and Φ_n represent the magnitude and phase (referred to as the event plane) of the n^{th} -order azimuthal anisotropy (or flow) at the corresponding angular scale. These quantities can also be conveniently represented in a two-dimensional vector format or in the standard complex form [4, 5]:

$$\vec{v}_n = (v_n \cos n\Phi_n, v_n \sin n\Phi_n) \text{ or } v_n e^{in\Phi_n}. \quad (2)$$

In non-central collisions, the overlap region of the initial geometry has an almost elliptic shape. The anisotropy is therefore dominated by the second harmonic term, v_2 . However, first-order ($n = 1$) and higher-order ($n > 2$) v_n coefficients have also been observed [6–8]. These coefficients have been related to additional shape components arising from the fluctuations of the positions of nucleons in the overlap region. The amplitude and the directions of these shape components can be estimated via a simple Glauber model [9] from the transverse positions (r, ϕ) of the participating nucleons relative to their center of mass [10]:

$$\epsilon_n = \frac{\sqrt{\langle r^n \cos n\phi \rangle^2 + \langle r^n \sin n\phi \rangle^2}}{\langle r^n \rangle}, \quad (3)$$

$$n\Phi_n^* = \arctan \left(\frac{\langle r^n \sin n\phi \rangle}{\langle r^n \cos n\phi \rangle} \right) + \pi, \quad (4)$$

where ϵ_n is the eccentricity and the angle Φ_n^* is commonly referred to as the participant-plane (PP) angle. These shape components are transferred via hydrodynamic evolution into higher-order azimuthal anisotropy in momentum space. For small ϵ_n values, one expects $v_n \propto \epsilon_n$, and the Φ_n to be correlated with the minor-axis direction given by Φ_n^* . However, model calculations show that the values of ϵ_n are large, and the alignment between Φ_n and Φ_n^* is

strongly violated for $n > 3$ due to non-linear effects in the hydrodynamic evolution [11].

Detailed measurements of v_n have been performed at RHIC and the LHC, and non-zero v_n values are observed for $n \leq 6$ [6–8, 12–16], consistent with the existence of sizable fluctuations in the initial state. Further information on these fluctuations can be obtained by studying the correlations between Φ_n of different order. If the fluctuations in ϵ_n are small and totally random, the orientations of Φ_n of different order are expected to be uncorrelated. Calculations based on the Glauber model reveal strong correlations between some PP angles such as Φ_2^* and Φ_4^* or Φ_2^* and Φ_6^* [10], and weak correlations between others such as Φ_2^* and Φ_3^* or Φ_2^* and Φ_5^* [17]. Previous measurements at RHIC and the LHC support a weak correlation between Φ_2 and Φ_3 [19, 20] and a strong correlation between Φ_2 and Φ_4 [18]. The former is consistent with no strong correlation between Φ_2^* and Φ_3^* and the dominance of linear response for elliptic flow and triangular flow, i.e. $\Phi_2 \approx \Phi_2^*$ and $\Phi_3 \approx \Phi_3^*$. The latter is consistent with a significant non-linear hydrodynamic response for quadrangular flow, which couples v_4 to v_2^2 . The correlations among three event planes of different order have also been investigated in a model framework and several significant correlators have been identified [10, 21–23]. However, no published experimental measurements on three-plane correlations exist to date. A measurement of the correlations between two and three event planes can shed light on the patterns of the fluctuations of the initial-state geometry and non-linear effects in the final state.

II. ATLAS DETECTOR AND TRIGGER

The ATLAS detector [24] provides nearly full solid angle coverage of the collision point with tracking detectors, calorimeters and muon chambers, which are well suited for measurements of azimuthal anisotropies over a large pseudorapidity range.¹ This analysis primarily uses three subsystems to measure the event plane: the inner detector (ID), the barrel and endcap electromagnetic calorimeters (ECal) and the forward calorimeter (FCal). The ID is contained within the 2 T field of a superconducting solenoid magnet, and measures the trajectories of charged particles in the pseudorapidity range $|\eta| < 2.5$ and over the full azimuth. A charged particle passing through the ID typically traverses three modules of the silicon pixel detector (Pixel), four double-sided silicon strip modules of the semiconductor tracker (SCT), and a transition radiation tracker for $|\eta| < 2$. The electromagnetic energy measurement in the ECal is based on a liquid-argon sampling technology. The FCal uses tungsten and copper absorbers with liquid argon as the active medium, and has a total thickness of about ten interaction lengths. The ECal covers the pseudorapidity range $|\eta| < 3.2$, and the FCal extends the calorimeter coverage to $|\eta| < 4.9$. The energies in the ECal and FCal are reconstructed and grouped into towers with segmentation in pseudorapidity and azimuthal angle of $\Delta\eta \times \Delta\phi = 0.1 \times 0.1$ to 0.2×0.2 , which are then used to calculate the event plane. The procedure for obtaining the event-plane correlations is found to be insensitive to the segmentation and energy calibration of the calorimeters.

The minimum-bias Level-1 trigger [25] used for this analysis requires a signal in each of two zero-degree calorimeters (ZDC) or a signal in either one of the two minimum-bias trigger scintillator (MBTS) counters. The ZDC is positioned at 140 m from the collision point, detecting neutrons and photons with $|\eta| > 8.3$, and the MBTS covers $2.1 < |\eta| < 3.9$. The ZDC Level-1 trigger thresholds on each side are set below the peak corresponding to a single neutron. A Level-2 timing requirement based on signals from each side of the MBTS is imposed to suppress beam backgrounds [25].

III. EVENT AND TRACK SELECTIONS

This paper is based on Pb+Pb collision data collected in 2010 at the LHC with a nucleon–nucleon center-of-mass energy $\sqrt{s_{NN}} = 2.76$ TeV. The data correspond to an integrated luminosity of approximately $7 \mu\text{b}^{-1}$. In order to suppress non-collision backgrounds, an offline event selection requires a reconstructed primary vertex with at least three associated charged tracks reconstructed in the ID and a time difference $|\Delta t| < 3$ ns between the MBTS trigger counters on either side of the interaction point. A coincidence between the two ZDCs at forward and backward pseudorapidity is required to reject a variety of background processes, while maintaining high efficiency for non-Coulomb processes. Events satisfying these conditions are required to have a reconstructed primary vertex with z_{vtx} within 150 mm of the nominal center of the ATLAS detector. The pile-up probability is estimated to be at the 10^{-4} level and is therefore negligible. About 48 million events pass the requirements for the analysis.

¹ ATLAS uses a right-handed coordinate system with its origin at the nominal interaction point (IP) in the center of the detector and the z -axis along the beam pipe. The x -axis points from the IP to the center of the LHC ring, and the y -axis points upward. Cylindrical coordinates (r, ϕ) are used in the transverse plane, ϕ being the azimuthal angle around the beam pipe. The pseudorapidity is defined in terms of the polar angle θ as $\eta = -\ln \tan(\theta/2)$.

The Pb+Pb event centrality is characterized using the total transverse energy (ΣE_T) deposited in the FCal over the pseudorapidity range $3.2 < |\eta| < 4.9$ and measured at the electromagnetic energy scale [26]. A larger ΣE_T value corresponds to a more central collision. From an analysis of the ΣE_T distribution after applying all trigger and event selection criteria, the sampled fraction of the total inelastic cross section has been estimated to be $(98 \pm 2)\%$ in a previous analysis [27]. The uncertainty in this estimate is evaluated by varying the trigger criteria, event selection and background rejection requirements on the FCal ΣE_T distribution [27]. The FCal ΣE_T distribution is divided into a set of 5%-wide percentile bins, together with five 1%-wide bins for the most central 5% of the events. A centrality interval refers to a percentile range, starting at 0% for the most central collisions. Thus the 0%–1% centrality interval corresponds to the most central 1% of the events. A standard Glauber model Monte Carlo analysis [9] is used to estimate the average number of participating nucleons, $\langle N_{\text{part}} \rangle$, and its associated systematic uncertainties for each centrality interval [27]. These numbers are summarized in Table I.

Centrality	0%–1%	1%–2%	2%–3%	3%–4%	4%–5%
$\langle N_{\text{part}} \rangle$	400.6 ± 1.3	392.6 ± 1.8	383.2 ± 2.1	372.6 ± 2.3	361.8 ± 2.5
Centrality	0%–5%	5%–10%	10%–15%	15%–20%	20%–25%
$\langle N_{\text{part}} \rangle$	382.2 ± 2.0	330.3 ± 3.0	281.9 ± 3.5	239.5 ± 3.8	202.6 ± 3.9
Centrality	25%–30%	30%–35%	35%–40%	40%–45%	45%–50%
$\langle N_{\text{part}} \rangle$	170.2 ± 4.0	141.7 ± 3.9	116.8 ± 3.8	95.0 ± 3.7	76.1 ± 3.5
Centrality	50%–55%	55%–60%	60%–65%	65%–70%	70%–75%
$\langle N_{\text{part}} \rangle$	59.9 ± 3.3	46.1 ± 3.0	34.7 ± 2.7	25.4 ± 2.3	18 ± 1.9

TABLE I: The list of centrality intervals and associated $\langle N_{\text{part}} \rangle$ values used in this paper. The systematic uncertainties are taken from Ref. [27].

The event plane is also measured by the ID, using reconstructed tracks with $p_T > 0.5$ GeV and $|\eta| < 2.5$ [8]. To improve the robustness of track reconstruction in the high-multiplicity environment of heavy-ion collisions, more stringent requirements on track quality, compared to those defined for proton–proton collisions [28], are used. At least nine hits in the silicon detectors are required for each track, with no missing Pixel hits and not more than one missing SCT hit, excluding the known non-operational modules. In addition, at its point of closest approach the track is required to be within 1 mm of the primary vertex in both the transverse and longitudinal directions [29]. The track reconstruction performance is studied by comparing data to Monte Carlo calculations based on the HIJING event generator [30] and a full GEANT4 simulation of the detector [31, 32]. The track reconstruction efficiency ranges from 72% at $\eta = 0$ to 51% for $|\eta| > 2$ in peripheral collisions, while it ranges from 72% at $\eta = 0$ to about 42% for $|\eta| > 2$ in central collisions [33]. However, the event-plane correlation results are found to be insensitive to the reconstruction efficiency (see Sec. IV D).

IV. DATA ANALYSIS

A. Experimental observables

The n^{th} -order harmonic has a n -fold symmetry in azimuth, and is thus invariant under the transformation $\Phi_n \rightarrow \Phi_n + 2\pi/n$. Therefore, a general definition of the relative angle between two event planes, $a_n \Phi_n + a_m \Phi_m$, has to be invariant under a phase shift $\Phi_l \rightarrow \Phi_l + 2\pi/l$. It should also be invariant under a global rotation by any angle. The first condition requires a_n (a_m) to be multiple of n (m), while the second condition requires the sum of the coefficients to vanish: $a_n + a_m = 0$. The relative angle $\Phi_{n,m} = k(\Phi_n - \Phi_m)$, with k being the least common multiple (LCM) of n and m , satisfies these constraints, as does any integer multiple of $\Phi_{n,m}$.

The correlation between Φ_n and Φ_m is completely described by the differential distribution of the event yield $dN_{\text{evts}}/d(k(\Phi_n - \Phi_m))$. This distribution must be an even function due to the symmetry of the underlying physics, and hence can be expanded into the following Fourier series:

$$\frac{dN_{\text{evts}}}{d(k(\Phi_n - \Phi_m))} \propto 1 + 2 \sum_{j=1}^{\infty} V_{n,m}^j \cos jk(\Phi_n - \Phi_m), \quad (5)$$

$$V_{n,m}^j = \langle \cos jk(\Phi_n - \Phi_m) \rangle. \quad (6)$$

The measurement of the two-plane correlation is thus equivalent to measuring a set of cosine functions $\langle \cos jk(\Phi_n - \Phi_m) \rangle$ averaged over many events [22].

This discussion can be generalized for correlations involving three or more event planes. The multi-plane correlators can be written as $\langle \cos(c_1\Phi_1 + 2c_2\Phi_2 + \dots + l_l\Phi_l) \rangle$ with the constraint [21, 23]:

$$c_1 + 2c_2 + \dots + l_l = 0, \quad (7)$$

where the coefficients c_n are integers. The two-plane correlators defined in Eq. (6) satisfy this constraint. For convenience, correlation involving two event planes Φ_n and Φ_m is referred to as “ n - m ” correlation, and one involving three event planes Φ_n , Φ_m and Φ_h as “ n - m - h ” correlation. The multi-plane correlators can always be decomposed into a linear combination of several two-plane relative angles and they carry additional information not accessible through two-plane correlators [22].

Experimentally the Φ_n angles are estimated from the observed event-plane angles, Ψ_n , defined as the directions of the “flow vectors” \vec{q}_n , which in turn are calculated from the azimuthal distribution of particles in the calorimeter or the ID:

$$\begin{aligned} \vec{q}_n &= (q_{x,n}, q_{y,n}) = \frac{1}{\sum u_i} (\Sigma[u_i \cos n\phi_i] - \langle \Sigma[u_i \cos n\phi_i] \rangle_{\text{evts}}, \Sigma[u_i \sin n\phi_i] - \langle \Sigma[u_i \sin n\phi_i] \rangle_{\text{evts}}), \\ \tan n\Psi_n &= \frac{q_{y,n}}{q_{x,n}}. \end{aligned} \quad (8)$$

Here the weight u_i is either the E_T of the i^{th} tower in the ECal and the FCal or the p_T of the i^{th} reconstructed track in the ID. Subtraction of the event-averaged centroid, $(\langle \Sigma[u_i \cos n\phi_i] \rangle_{\text{evts}}, \langle \Sigma[u_i \sin n\phi_i] \rangle_{\text{evts}})$, in Eq. (8) removes biases due to detector effects [34].² A standard flattening technique [35] is then used to remove the small residual non-uniformities in the distribution of Ψ_n . The \vec{q}_n defined this way, when averaged over events with the same Φ_n , is insensitive to the energy scale in the calorimeter or the momentum scale in the ID and to any random smearing effect. In the limit of infinite multiplicity it approaches the single-particle flow weighted by u : $\vec{q}_n \rightarrow (\vec{v}_n)_u = \Sigma u_i (\vec{v}_n)_i / \Sigma u_i$.

The correlators in terms of Φ_n can be obtained from the correlations between the measured angles Ψ_n divided by a resolution term [22]:

$$\begin{aligned} \langle \cos(c_1\Phi_1 + 2c_2\Phi_2 + \dots + l_l\Phi_l) \rangle &= \frac{\langle \cos(c_1\Psi_1 + 2c_2\Psi_2 + \dots + l_l\Psi_l) \rangle}{\text{Res}\{c_1\Psi_1\}\text{Res}\{c_2\Psi_2\}\dots\text{Res}\{c_l\Psi_l\}} \\ \text{Res}\{c_n\Psi_n\} &= \sqrt{\langle (\cos c_n n(\Psi_n - \Phi_n))^2 \rangle}. \end{aligned} \quad (9)$$

The resolution factors $\text{Res}\{c_n\Psi_n\}$ can be determined using the standard two-subevent or three-subevent methods [4] as discussed in Sec. IV B. To avoid auto-correlations, each Ψ_n needs to be measured using subevents covering different η ranges, preferably with a gap in between. Here a subevent refers to a collection of particles over a certain η range in the event. This method of obtaining the correlator is referred to as the event-plane or EP method.

In Eq. (9), all events are given equal weights in both the numerator (raw correlator) and the denominator (resolution). It was recently proposed [36, 37] that the potential bias in the EP method arising from the effects of event-by-event fluctuations of the flow and multiplicity can be removed by applying additional weight factors:

$$\begin{aligned} \langle \cos(c_1\Phi_1 + 2c_2\Phi_2 + \dots + l_l\Phi_l) \rangle_w &= \frac{\langle \cos(c_1\Psi_1 + 2c_2\Psi_2 + \dots + l_l\Psi_l) \rangle_w}{\text{Res}\{c_1\Psi_1\}_w \text{Res}\{c_2\Psi_2\}_w \dots \text{Res}\{c_l\Psi_l\}_w} \\ \langle \cos(c_1\Psi_1 + 2c_2\Psi_2 + \dots + l_l\Psi_l) \rangle_w &= \langle q_1^{c_1} q_2^{c_2} \dots q_l^{c_l} \cos(c_1\Psi_1 + 2c_2\Psi_2 + \dots + l_l\Psi_l) \rangle \\ \text{Res}\{c_n\Psi_n\}_w &= \sqrt{\langle (q_n^{c_n} \cos c_n n(\Psi_n - \Phi_n))^2 \rangle}, \end{aligned} \quad (10)$$

where the $q_n = |\vec{q}_n|$ represents the magnitude of the flow vector of the subevent used to calculate the Ψ_n (Eq. (8)), and the subscript “w” is used to indicate the q_n -weighting. This weighting method is often referred to as the “scalar-product” or SP method [38]. Correspondingly, the weighted version of the PP correlators can be obtained by using

² For example, a localized inefficiency over a ϕ region in the detector would lead to a non-zero average \vec{q}_n . The subtraction corrects this bias.

the eccentricity ϵ_n defined in Eq. (3) as the weight [21]:

$$\langle \cos(c_1\Phi_1^* + 2c_2\Phi_2^* + \dots + lc_l\Phi_l^*) \rangle_w = \frac{\langle \epsilon_1^{c_1} \epsilon_2^{c_2} \dots \epsilon_l^{c_l} \cos(c_1\Phi_1^* + 2c_2\Phi_2^* + \dots + lc_l\Phi_l^*) \rangle}{\sqrt{\langle \epsilon_1^{2c_1} \rangle \langle \epsilon_2^{2c_2} \rangle \dots \langle \epsilon_l^{2c_l} \rangle}}. \quad (11)$$

In Eq. (10), events with larger flow have bigger weights in the calculation of the raw correlation and the resolution factors. Other than the weighting, the procedure for obtaining the raw signal and resolution factors is identical in the EP and SP methods. Hence the discussion in the remainder of the paper should be regarded as applicable to both methods and the subscript “w” is dropped in all formulae, unless required for clarity.

It is worth emphasizing that the expression for the correlators in Eq. 10 is constructed to be insensitive to the details of the detector performance, such as the η -coverage, segmentation, energy calibration or the efficiency [4, 34]. This is because the angle Φ_n is a global property of the event that can be estimated from the Ψ_n from independent detectors, and the procedure for obtaining the correlators is “self-correcting”. A poor segmentation or energy calibration of the calorimeter, for example, increases the smearing of Ψ_n about Φ_n , and hence reduces the raw correlation (numerator of Eq. 10). This reduction in the raw correlation, however, is expected to be mostly compensated by smaller resolution terms $\text{Res}\{c_n n \Psi_n\}$ in the denominators.

A very large number of correlators could be studied. However, the measurability of these correlators is dictated by the values of $\text{Res}\{jn\Psi_n\}$ (c_n replaced by j for simplicity). A detailed study in this analysis shows that the values of $\text{Res}\{jn\Psi_n\}$ decrease very quickly for increasing n , but they decrease more slowly with j for fixed n [23]. The resolution factors are sufficiently good for $\text{Res}\{jn\Psi_n\}$ for $n = 2$ to 6 and j values up to $j = 6$ for $n = 2$. This defines the two- and three-plane correlators that can be measured.

Table II gives a summary of the set of two-plane correlators and resolution terms that need to be measured in this analysis for each centrality interval. The corresponding information for the three-plane correlators is shown in Table III. The first three correlators in Table II correspond to the first three Fourier coefficients ($j = 1, 2, 3$) in Eq. (6), and are derived from the observed distribution $dN_{\text{evts}}/d(4(\Psi_2 - \Psi_4))$. All the other correlators in Tables II and III only correspond to the first Fourier coefficient of the observed distribution. The two-plane and three-plane correlators are listed separately because different subdetectors are used (see Sec. IV B), and this requires separate evaluation of the resolution corrections.

$\langle \cos 4(\Phi_2 - \Phi_4) \rangle$	$\text{Res}\{4\Psi_2\}, \text{Res}\{4\Psi_4\}$
$\langle \cos 8(\Phi_2 - \Phi_4) \rangle$	$\text{Res}\{8\Psi_2\}, \text{Res}\{8\Psi_4\}$
$\langle \cos 12(\Phi_2 - \Phi_4) \rangle$	$\text{Res}\{12\Psi_2\}, \text{Res}\{12\Psi_4\}$
$\langle \cos 6(\Phi_2 - \Phi_3) \rangle$	$\text{Res}\{6\Psi_2\}, \text{Res}\{6\Psi_3\}$
$\langle \cos 6(\Phi_2 - \Phi_6) \rangle$	$\text{Res}\{6\Psi_2\}, \text{Res}\{6\Psi_6\}$
$\langle \cos 6(\Phi_3 - \Phi_6) \rangle$	$\text{Res}\{6\Psi_3\}, \text{Res}\{6\Psi_6\}$
$\langle \cos 12(\Phi_3 - \Phi_4) \rangle$	$\text{Res}\{12\Psi_3\}, \text{Res}\{12\Psi_4\}$
$\langle \cos 10(\Phi_2 - \Phi_5) \rangle$	$\text{Res}\{10\Psi_2\}, \text{Res}\{10\Psi_5\}$

TABLE II: The list of two-plane correlators and associated event-plane resolution factors that need to be measured.

$\langle \cos(2\Phi_2 + 3\Phi_3 - 5\Phi_5) \rangle$	$\text{Res}\{2\Psi_2\}, \text{Res}\{3\Psi_3\}, \text{Res}\{5\Psi_5\}$
$\langle \cos(-8\Phi_2 + 3\Phi_3 + 5\Phi_5) \rangle$	$\text{Res}\{8\Psi_2\}, \text{Res}\{3\Psi_3\}, \text{Res}\{5\Psi_5\}$
$\langle \cos(2\Phi_2 + 4\Phi_4 - 6\Phi_6) \rangle$	$\text{Res}\{2\Psi_2\}, \text{Res}\{4\Psi_4\}, \text{Res}\{6\Psi_6\}$
$\langle \cos(-10\Phi_2 + 4\Phi_4 + 6\Phi_6) \rangle$	$\text{Res}\{10\Psi_2\}, \text{Res}\{4\Psi_4\}, \text{Res}\{6\Psi_6\}$
$\langle \cos(2\Phi_2 - 6\Phi_3 + 4\Phi_4) \rangle$	$\text{Res}\{2\Psi_2\}, \text{Res}\{6\Psi_3\}, \text{Res}\{4\Psi_4\}$
$\langle \cos(-10\Phi_2 + 6\Phi_3 + 4\Phi_4) \rangle$	$\text{Res}\{10\Psi_2\}, \text{Res}\{6\Psi_3\}, \text{Res}\{4\Psi_4\}$

TABLE III: The list of three-plane correlators and associated event-plane resolution factors that need to be measured.

B. Analysis method

For two-plane correlation (2PC) measurements, the event is divided into two subevents symmetric around $\eta = 0$ with a gap in between, so they nominally have the same resolution. Each subevent provides its own estimate of the

event plane via Eq. (8): Ψ_n^P and Ψ_m^P for positive η and Ψ_n^N and Ψ_m^N for negative η . This leads to two statistically independent estimates of the correlator, which are averaged to obtain the final signal. Because of the symmetry of the subevents, the product of resolution factors in the denominator is identical for each measurement, and the event-averaged correlator can be written as:

$$\langle \cos k(\Phi_n - \Phi_m) \rangle = \frac{\langle \cos k(\Psi_n^P - \Psi_m^N) \rangle + \langle \cos k(\Psi_n^N - \Psi_m^P) \rangle}{\text{Res}\{k\Psi_n^P\}\text{Res}\{k\Psi_m^N\} + \text{Res}\{k\Psi_n^N\}\text{Res}\{k\Psi_m^P\}}. \quad (12)$$

To measure a three-plane correlation (3PC), three non-overlapping subevents, labeled as A, B and C, are chosen to have approximately the same η coverage. In this analysis, subevents A and C are chosen to be symmetric about $\eta = 0$, and hence have identical resolution, while the resolution of subevent B in general is different. There are $3! = 6$ independent ways of obtaining the same three-plane correlator. But the symmetry between A and C reduces this to three pairs of measurements, which are labeled as Type1, Type2 and Type3. For example, the Type1 measurement of the correlation $2\Phi_2 + 3\Phi_3 - 5\Phi_5$ is obtained from $2\Psi_2^B + 3\Psi_3^A - 5\Psi_5^C$ and $2\Psi_2^B + 3\Psi_3^C - 5\Psi_5^A$, i.e. by requiring the Ψ_2 angle to be given by subevent B:

$$\langle \cos(2\Phi_2 + 3\Phi_3 - 5\Phi_5) \rangle_{\text{Type1}} = \frac{\langle \cos(2\Psi_2^B + 3\Psi_3^A - 5\Psi_5^C) \rangle + \langle \cos(2\Psi_2^B + 3\Psi_3^C - 5\Psi_5^A) \rangle}{\text{Res}\{2\Psi_2^B\}\text{Res}\{3\Psi_3^A\}\text{Res}\{5\Psi_5^C\} + \text{Res}\{2\Psi_2^B\}\text{Res}\{3\Psi_3^C\}\text{Res}\{5\Psi_5^A\}}. \quad (13)$$

Similarly, the Type2 (Type3) measurement is obtained by requiring the Ψ_3 (Ψ_5) to be measured by subevent B. Since the three angles in each detector, e.g. Ψ_2^A , Ψ_3^A and Ψ_5^A , are obtained from orthogonal Fourier modes, the different types of estimates for a given correlator are expected to be statistically independent.

The resolution factors $\text{Res}\{jn\Psi_n\}$ are obtained from a two-subevent method (2SE) and a three-subevent method (3SE) [4]. The 2SE method follows almost identically the 2PC procedure described above: two subevents symmetric about $\eta = 0$ are chosen and used to make two measurements of the event plane at the same order n : Ψ_n^P and Ψ_n^N . The correlator $\langle \cos jn(\Psi_n^P - \Psi_n^N) \rangle$ is then calculated, and the square-root yields the desired resolution [8]:

$$\text{Res}\{jn\Psi_n\} = \sqrt{\langle \cos jn(\Psi_n^P - \Psi_n^N) \rangle} \equiv \text{Res}\{jn\Psi_n^P\} \equiv \text{Res}\{jn\Psi_n^N\}. \quad (14)$$

In the 3SE method, the value of $\text{Res}\{jn\Psi_n\}$ for a given subevent A is determined from angle correlations with two subevents B and C covering different regions in η :

$$\text{Res}\{jn\Psi_n^A\} = \sqrt{\frac{\langle \cos jn(\Psi_n^A - \Psi_n^B) \rangle \langle \cos jn(\Psi_n^A - \Psi_n^C) \rangle}{\langle \cos jn(\Psi_n^B - \Psi_n^C) \rangle}}. \quad (15)$$

The 3SE method does not rely on equal resolutions for the subevents, and hence there are many ways of choosing subevents B and C.

In the case of the weighted correlators given by the SP method, the resolution terms defined by Eqs. 14 and 15 are instead calculated as [36]:

$$\text{Res}\{jn\Psi_n\}_w = \sqrt{\langle (q_n^P q_n^N)^j \cos jn(\Psi_n^P - \Psi_n^N) \rangle}, \quad (16)$$

and

$$\text{Res}\{jn\Psi_n^A\}_w = \sqrt{\frac{\langle (q_n^A q_n^B)^j \cos jn(\Psi_n^A - \Psi_n^B) \rangle \langle (q_n^A q_n^C)^j \cos jn(\Psi_n^A - \Psi_n^C) \rangle}{\langle (q_n^B q_n^C)^j \cos jn(\Psi_n^B - \Psi_n^C) \rangle}}. \quad (17)$$

C. Analysis procedure

The large η coverage of the ID, ECal and FCal, with their fine segmentation, allows many choices of subevents for estimating the event planes and studying their correlations over about ten units in η . The edge towers of the FCal (approximately $4.8 < |\eta| < 4.9$) are excluded to minimize the non-uniformity of E_T in azimuth, as in a previous analysis [8]. These detectors are divided into a set of small segments in η , and the subevents are constructed by combining these segments. A large number of subevents can be used for measuring both the raw correlation signal

and the resolution corrections. A detailed set of cross-checks and estimations of systematic uncertainties can therefore be performed.

The guiding principle for choosing the subevents is that they should have large η acceptance, but still have a sufficiently large η gap from each other. For two-plane correlations, the default subevents are ECal+FCal at negative ($-4.8 < \eta < -0.5$) and positive ($0.5 < \eta < 4.8$) η , with a gap of one unit in between. For three-plane correlations, the default subevents are ECal_P ($0.5 < \eta < 2.7$), FCal ($3.3 < |\eta| < 4.8$), and ECal_N ($-2.7 < \eta < -0.5$). As an important consistency cross-check for the 2PC and 3PC analyses, subevents are also chosen only from the ID. These combinations are listed in Table IV. The resolution for each of these subevents is determined via the 2SE method and the 3SE method, and the latter typically involves measuring correlations with many other subevents not listed in Table IV, for example using smaller sections of the ECal or ID.

Subevents used for two-plane correlations and their η coverages			
Calorimeter-based	ECalFCal _P $\eta \in (0.5, 4.8)$		ECalFCal _N $\eta \in (-4.8, -0.5)$
ID-based	ID _P $\eta \in (0.5, 2.5)$		ID _N $\eta \in (-2.5, -0.5)$
Subevents used for three-plane correlations and their η coverages			
Calorimeter-based	ECal _P $\eta \in (0.5, 2.7)$	FCal $ \eta \in (3.3, 4.8)$	ECal _N $\eta \in (-2.7, -0.5)$
ID-based	ID _P $\eta \in (1.5, 2.5)$	ID $\eta \in (-1.0, 1.0)$	ID _N $\eta \in (-2.5, -1.5)$

TABLE IV: Combinations of subevents used in two-plane and three-plane correlation analysis. The calorimeter-based analysis is the default, while the ID-based result provides an important cross-check.

Figure 1 shows the two-plane relative angle distributions for the 20%–30% centrality interval. The signal or “foreground” distributions are calculated by combining event-plane angles from the same event. The “background” distributions are calculated from mixed events by combining the event-plane angles obtained from different events with similar centrality (matched within 5%) and z_{vtx} (matched within 3 cm). Ten mixed events are constructed for each foreground event. Both distributions are normalized so that the average of the entries is one. The background distributions provide an estimate of detector effects, while the foreground distributions contain both the detector effects and physics. The background distributions are almost flat, but do indicate some small variations at a level of about 10^{-3} . To cancel these non-physical structures, the correlation functions are obtained by dividing the foreground (S) by the background distributions (B):

$$C(k(\Psi_n - \Psi_m)) = \frac{S(k(\Psi_n - \Psi_m))}{B(k(\Psi_n - \Psi_m))}. \quad (18)$$

The correlation functions show significant positive signals for $4(\Psi_2 - \Psi_4)$, $6(\Psi_2 - \Psi_3)$, $6(\Psi_2 - \Psi_6)$ and $6(\Psi_3 - \Psi_6)$. The observed correlation signals (not corrected by resolution) in terms of the cosine average are calculated directly from these correlation functions.

Figure 2 shows the centrality dependence of the observed correlation signals for various two-plane correlators. The systematic uncertainty, shown as shaded bands, is estimated as the values of the sine terms $\langle \sin jk(\Psi_n - \Psi_m) \rangle$. Non-zero sine terms may arise from detector effects which lead to non-physical correlations between the two subevents. This uncertainty is calculated by averaging sine terms across the measured centrality range, giving uncertainties of $(0.2\text{--}1.5) \times 10^{-3}$ depending on the type of the correlator. This uncertainty is correlated with centrality and is significant only when the $\langle \cos jk(\Psi_n - \Psi_m) \rangle$ term is itself small, as in the rightmost four panels of Fig. 2. This uncertainty is included in the final results (see Sec. IV D).

A large number of resolution factors $\text{Res}\{jn\Psi_n\}$ needs to be determined using the 2SE and the 3SE methods, separately for each subevent listed in Table IV. For example, the resolution of ECalFCal_N can be obtained from its correlation with ECalFCal_P via Eq. (14) (2SE method), or from its correlation with any two non-overlapping reference subevents at $\eta > 0$ via Eq. (15) (3SE method) such as $0.5 < \eta < 1.5$ and $3.3 < \eta < 4.8$. Therefore, for a particular subevent in Table IV, there are usually several determinations of $\text{Res}\{jn\Psi_n\}$, one from the 2SE method and several from the 3SE method. The default value used is obtained from the 2SE method where available, or from the 3SE combination with the smallest uncertainty. The spread of these values is included in the systematic uncertainty, separately for each centrality interval. The relative differences between most of these estimates are found to be independent of the event centrality, except for the 50%–75% centrality range, where weak centrality dependences are observed in some cases.

All the cosine terms in the 2SE and 3SE formulae are calculated from the distributions similar to those in Eq. (18),

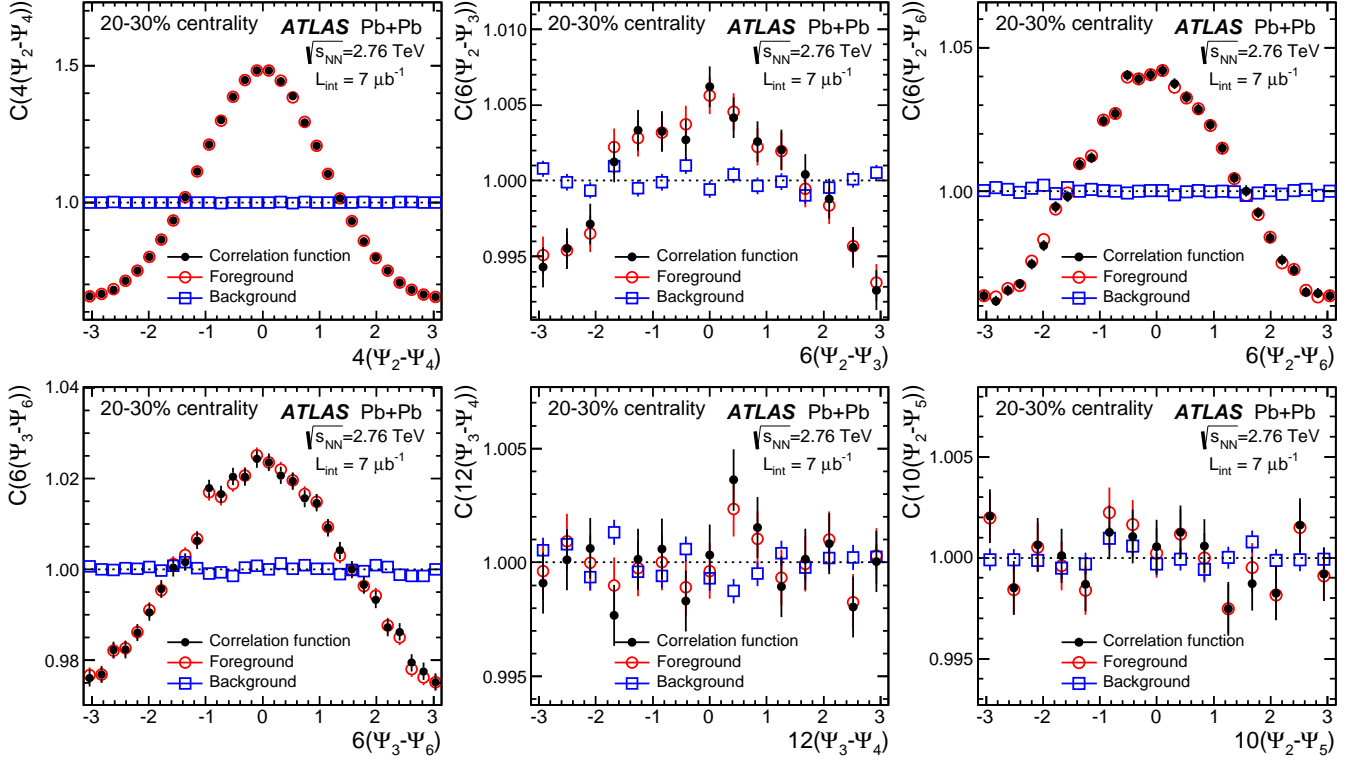


FIG. 1: (Color online) Relative angle distributions between two raw event planes from ECalFCal_N and ECalFCal_P defined in Table IV for the 20%–30% centrality interval for the foreground (open circles), background (open squares) and correlation function (filled circles) based on the EP method. The correlation functions give (via Eq. (12)) the two-plane correlators defined in Table II. The y -axis scales are not the same for all panels.

but at the same order n :

$$C(n(\Psi_n^A - \Psi_n^B)) = \frac{S(n(\Psi_n^A - \Psi_n^B))}{B(n(\Psi_n^A - \Psi_n^B))}, \quad (19)$$

where the background distribution is obtained by combining the Ψ_n of subevent A in one event with Ψ_n of subevent B from a different event with similar centrality and z_{vtx} . Furthermore, the non-zero sine values $\langle \sin jn(\Psi_n^A - \Psi_n^B) \rangle$ arising from the 2SE and 3SE analyses are also included in the uncertainty in the resolution factor. Once the individual resolution factors are determined for each subevent, the combined resolution factors are then calculated by multiplying the relevant individual $\text{Res}\{jn\Psi_n\}$ terms. They are shown in Fig. 3 as a function of centrality for the eight two-plane correlators listed in Table II. The systematic uncertainty is calculated via a simple error propagation from the individual resolution terms, and is nearly independent of the event centrality. This uncertainty is included in the final results (see Sec. IV D).

The analysis procedure and the systematic uncertainties discussed above are also valid for the three-plane correlation analysis. However, the 3PC is slightly more complicated because it has three independent measurements for each correlator, which also need to be combined. Figure 4 shows the relative angle distributions for various three-plane correlators from the Type1 measurement in the 20%–30% centrality interval. The observed correlation signals are calculated as cosine averages of the correlation functions in an obvious generalization of Eq. (18):

$$C(c_n n \Psi_n + c_m m \Psi_m + c_h h \Psi_h) = \frac{S(c_n n \Psi_n + c_m m \Psi_m + c_h h \Psi_h)}{B(c_n n \Psi_n + c_m m \Psi_m + c_h h \Psi_h)}, \quad (20)$$

where the background distribution is constructed by requiring that all three angles Ψ_n , Ψ_m , and Ψ_h are from different events. The correlation functions show significant positive signals for $2\Psi_2 + 3\Psi_3 - 5\Psi_5$, $2\Psi_2 + 4\Psi_4 - 6\Psi_6$, and $-10\Psi_2 + 4\Psi_4 + 6\Psi_6$, while the signal for $2\Psi_2 - 6\Psi_3 + 4\Psi_4$ is negative, and the signals for the remaining correlators are consistent with zero.

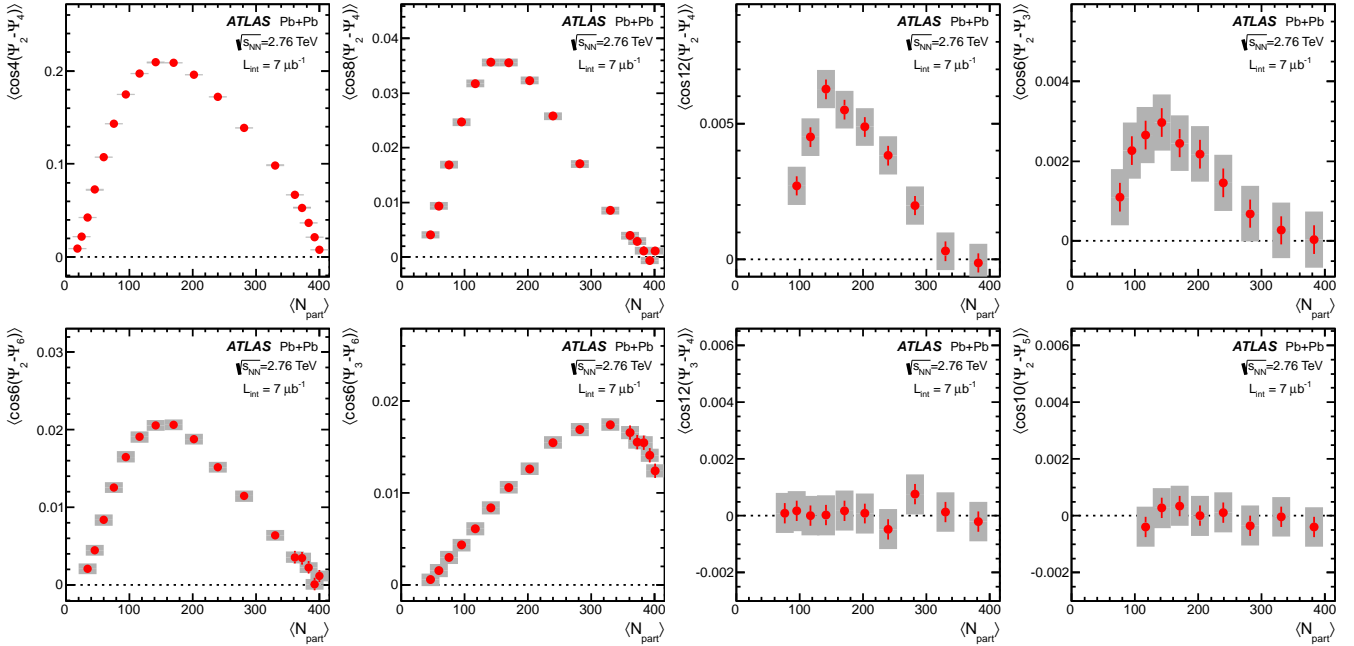


FIG. 2: (Color online) Observed correlation signals based on the EP method, $\langle \cos jk(\Psi_n - \Psi_m) \rangle$, calculated from the correlation functions such as those in Fig. 1 as a function of $\langle N_{part} \rangle$. The middle two panels in the top row have $j = 2$ and $j = 3$, while all other panels have $j = 1$. The error bars and shaded bands indicate the statistical and systematic uncertainties, respectively.

Figure 5 shows the centrality dependence of the observed correlation signals (left panel), combined resolutions (middle panel) and corrected signals (right panel) for Type1, Type2 and Type3 combinations of $\langle \cos(2\Psi_2 + 3\Psi_3 - 5\Psi_5) \rangle$. The systematic uncertainty in the observed correlation signals is estimated from the values of $\langle \sin(c_n n \Psi_n + c_m m \Psi_m + c_h h \Psi_h) \rangle$, and is calculated by averaging these sine terms over the measured centrality range. This uncertainty is $(0.2\text{--}1.5) \times 10^{-3}$ in absolute variation, depending on the type of three-plane correlator. The uncertainty in the combined resolution is obtained by propagation from those for the individual resolution factors. Both sources of uncertainties are strongly correlated with centrality, and they are included in the final results (see Sec. IV D). Figure 5 shows that all three types of measurements (Type1, Type2 and Type3) have similar values for the observed signal and the combined resolution. This behavior is expected since the three subevents cover similar rapidity ranges. The three corrected results are statistically combined, and the spreads between them are included in the total systematic uncertainty.

The same analysis procedure is repeated for event-plane correlations obtained via the SP method. The performance of the SP method is found to be very similar to that of the EP method. The magnitudes of the sine terms relative to the cosine terms for both the signal distributions in $k(\Psi_n - \Psi_m)$ and $c_n n \Psi_n + c_m m \Psi_m + c_h h \Psi_h$, as well as the distributions in $n(\Psi_n^A - \Psi_n^B)$ for calculating the resolution factors are found to be nearly the same as those for the EP method. This behavior is quite natural as the effects of detector acceptance are expected to be independent of the strength of the flow signal. The resolution factors and their associated systematic uncertainties are calculated with the same detector combinations as those used for the EP method. The spreads of the results between various detector combinations are included in the systematic uncertainty for the resolution factors. These uncertainties are also found to be strongly correlated between the two methods. The uncorrelated systematic uncertainties between the two methods are evaluated by calculating a double ratio for each detector “X” listed in Table IV:

$$R_X = \frac{\text{Res}\{jn\Psi_n\}_w(\text{X, other})/\text{Res}\{jn\Psi_n\}_w(\text{X, ref})}{\text{Res}\{jn\Psi_n\}(\text{X, other})/\text{Res}\{jn\Psi_n\}(\text{X, ref})}, \quad (21)$$

where the “ref” refers to the default detector combination used to calculate the resolution of “X”, and “other” refers to other detector combinations used to evaluate the systematic uncertainties in the resolution of “X” via the 2SE and 3SE methods as discussed above (see the paragraph before Eq. (19)). The spread of the R_X values provides an estimate of the uncorrelated uncertainty between the two methods for resolution factor $\text{Res}\{jn\Psi_n\}$. This uncorrelated uncertainty is typically much smaller than the total systematic uncertainty in the resolution factor in either method.

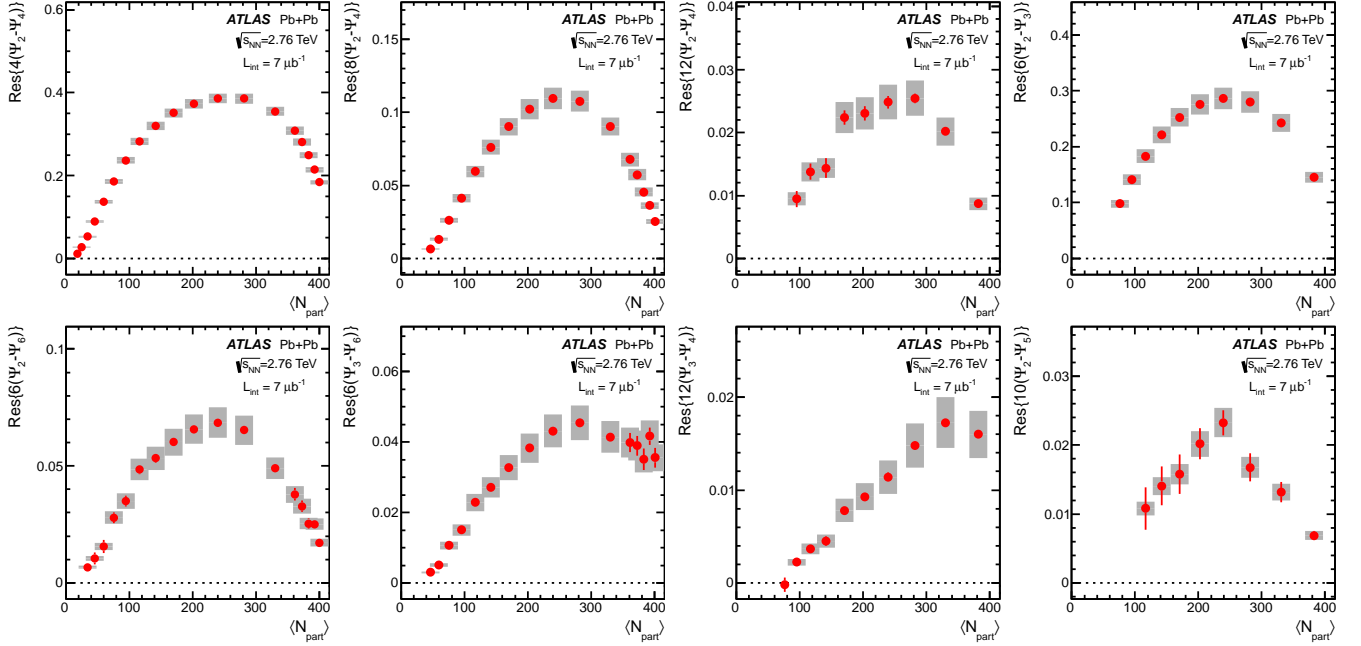


FIG. 3: (Color online) The combined resolution factors based on the EP method for two-plane correlators, $\text{Res}\{jk(\Psi_n - \Psi_m)\} \equiv \text{Res}\{jk\Psi_n\}\text{Res}\{jk\Psi_m\}$, as a function of $\langle N_{\text{part}} \rangle$. The middle two panels in the top row have $j = 2$ and $j = 3$, while all other panels have $j = 1$. The error bars and shaded bands indicate the statistical and systematic uncertainties, respectively.

D. Systematic uncertainties

The main systematic uncertainties in the result are introduced and discussed in Sec. IV C at various key steps of the analysis. This section gives a summary of these uncertainties, and then discusses any additional systematic uncertainties and cross-checks.

The systematic uncertainties associated with the analysis procedure are dominated by contributions from residual detector acceptance effects and uncertainties in the resolution factors. Most detector acceptance effects are expected to cancel in the raw correlation function by dividing the foreground and background distributions (Eqs. 18–20). The residual acceptance effects, estimated by the sine terms of the distributions, are found to be $(0.2\text{--}1.5) \times 10^{-3}$ of the average amplitude of the correlation functions, and are found to be independent of the event centrality. The uncertainties in the resolution factors are calculated from the differences between the 2SE estimate and various 3SE estimates, which are then propagated to give the total uncertainties for the combined resolution factor. These uncertainties are found to be quite similar in the EP and SP methods since they both rely on the same subevent correlations; the larger of the two is quoted as the total systematic uncertainty. The uncorrelated uncertainties are evaluated separately via Eq. (21), and are used for comparison between the two methods. The uncertainties in the resolution factors are found to depend only weakly on event centrality.

Additional systematic uncertainties include those associated with the trigger and event selections, as well as variations of resolution-corrected signals between different running periods. The former is evaluated by varying the full centrality range by $\pm 2\%$ according to the estimated efficiency of $(98 \pm 2)\%$ for selecting minimum-bias Pb+Pb events. The latter is evaluated by comparing the results obtained independently from three running periods each with $1/3$ of the total event statistics. All these uncertainties are generally small, and are quite similar between the EP method and the SP method. Both types of uncertainties are found to be independent of the event centrality.

Tables V and VI summarize the sources of systematic uncertainties for two-plane and three-plane correlations. The total systematic uncertainties are the quadrature sum of the three sources listed in these tables and the uncertainties associated with residual detector effects. The total uncertainties are found to be nearly independent of the event centrality over the 0% – 50% centrality range, although a small increase is observed for some of the correlators in the 50% – 75% centrality range. In most cases, the total systematic uncertainties are dominated by uncertainties associated with the resolution factors. The uncertainties in the resolution correction can become quite sizable when the angles Ψ_5 and Ψ_6 are involved. This is expected since the higher-order flow signals v_5 and v_6 are weak, leading to small values of $\text{Res}\{6\Psi_6\}$, $\text{Res}\{5\Psi_5\}$ and $\text{Res}\{10\Psi_5\}$ with large uncertainties.

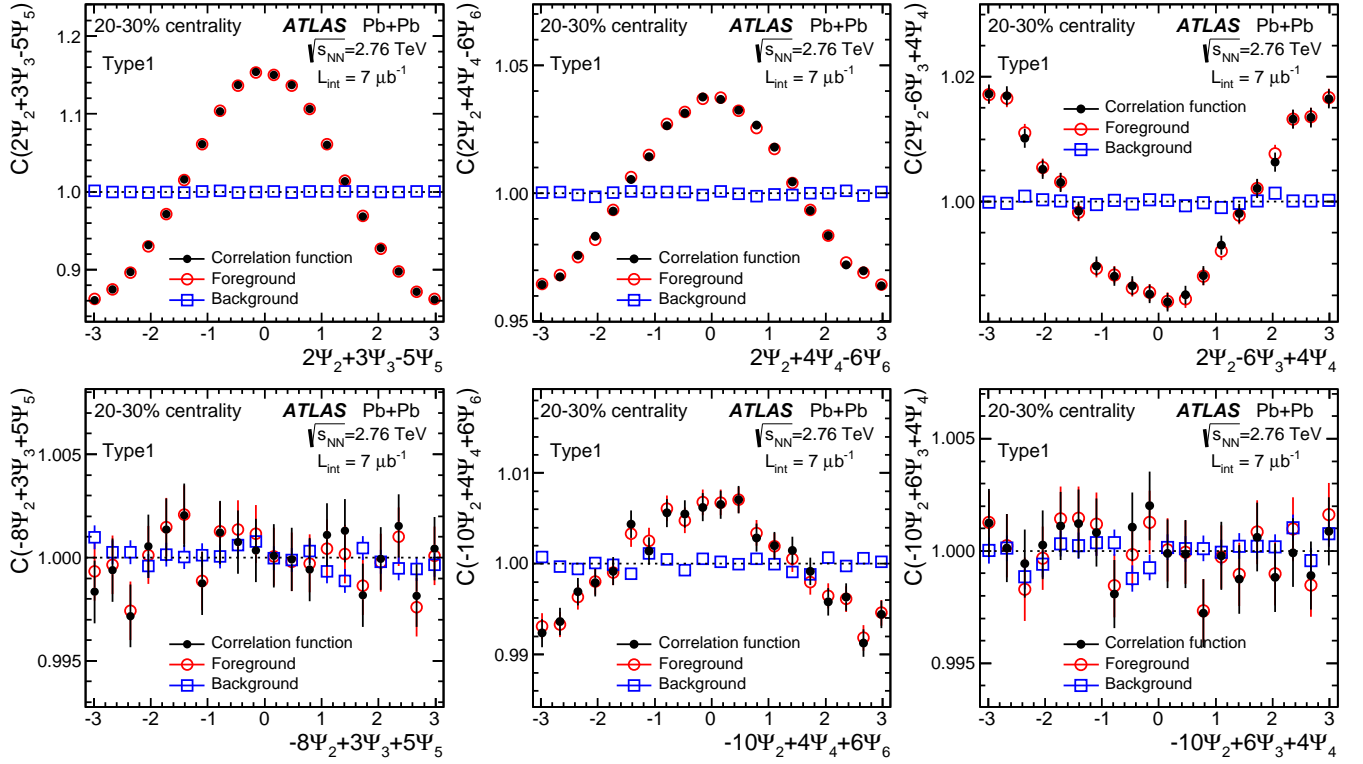


FIG. 4: (Color online) Relative angle distributions between three event planes from ECal_N , FCal and ECal_P defined in Table IV for Type1 correlation in the 20%–30% centrality interval for foreground (open circles), background (open squares) and correlation function (filled circles) based on the EP method. The correlation functions give (via equations similar to Eq. (13)) the three-plane correlators defined in Table III. The y -axis scales are not the same for all panels.

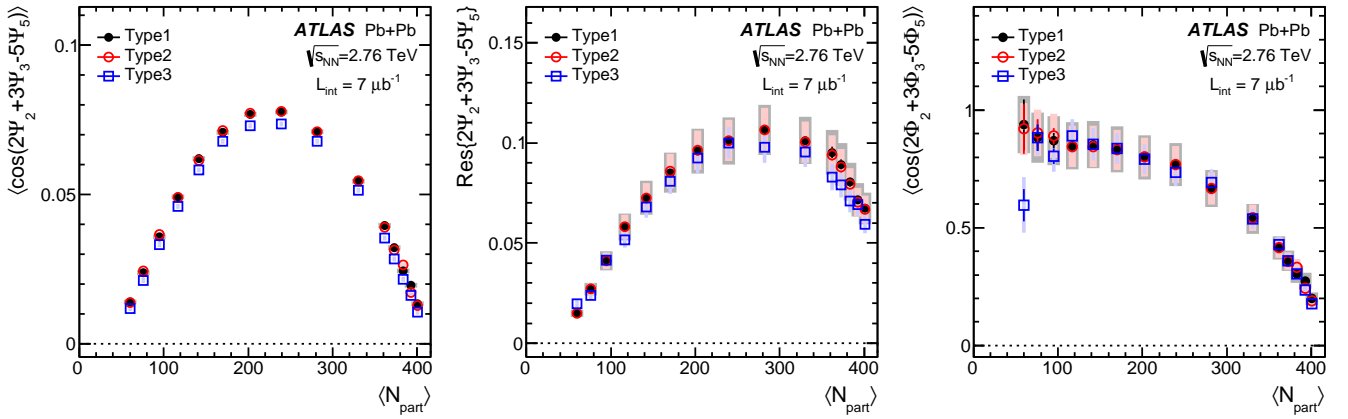


FIG. 5: (Color online) The $\langle N_{\text{part}} \rangle$ dependence of the observed correlation signals (left panel), combined resolutions (middle panel) and corrected signals (right panel) based on the EP method for the three types of event plane combinations for $2\Psi_2 + 3\Psi_3 - 5\Psi_5$ using the ATLAS calorimeters. The error bars and shaded bands indicate the statistical and systematic uncertainties, respectively.

One important issue in this analysis is the extent to which the measured correlations are biased by short-range correlations such as jet fragmentation, resonance decays and Bose–Einstein correlations. These short-range correlations may contribute to the observed correlation signals and the resolution factors and hence affect the measured correlations. The potential influence of these short-range correlations is studied for the eight two-plane correlators with the EP method. The η gap between the two symmetric subevents from ECalFCal , η_{min} , is varied in the range of

0 to 8. Seventeen symmetric pairs of subevents are chosen, each corresponding to a different η separation. For each case, the observed correlation signals and the resolution factors are obtained using the correlations between these two subevents. Both the observed correlation signals and combined resolutions decrease significantly (by up to a factor of four) as η_{\min} is increased. However, the final corrected correlation signals are relatively stable. For example, a gradual change of a few percent is observed for $\eta_{\min} < 4$ where the statistical and systematic uncertainties are not very large. This observation strongly suggests that the measurement indeed reflects long-range correlations between the event planes. In most cases, the raw correlation signals decrease smoothly with η_{\min} . In contrast, the estimated resolution factors have a sharp increase towards small η_{\min} in many cases, leading to a suppression of the corrected correlation signals at small η_{\min} . This behavior suggests that short-range correlations can influence individual harmonics, and hence the resolution factors, but their influences are weak for correlations between EP angles of different order. In all cases, the influences of these short-range correlations are negligible for $\eta_{\min} > 0.4$. The choices of the subevents in Table IV have a minimum η gap of 0.6, and hence are sufficient to suppress these short-range correlations.

The event-plane correlators measured by the calorimeters are also compared with those obtained independently from the ID for both the EP method and the SP method (see Table IV for the definition of the subevents). Despite the larger fluctuations due to the limited η range of its subevents, the results from the ID are consistent with those from the calorimeters (see Appendix). Since the ID is an entirely different type of detector and measures only charged particles, this consistency gives confidence that the measured results are robust. It is argued in Ref. [37] that the SP method as defined in Eq. (10) is insensitive to various smearing effects on the weighting factors, such as energy or momentum resolution or multiplicity fluctuations, and as long as these smearings are random and isotropic, they should cancel after averaging over events in the numerator and denominator of Eq. (10). This behavior was checked explicitly in the ID by calculating \vec{q}_n given by Eq. (8) in several different ways: (1) instead of $u = p_T$ as in the default calculation, the charged particles are set to have equal weight $u = 1$, (2) the weight u is randomly set to be zero for half of the charged particles, or (3) the \vec{q}_n is redefined as $\vec{q}_n \Sigma u_i$ to include explicitly the event-by-event multiplicity fluctuations. The results of all of these cross-checks are consistent with the results of the default calculation.

$\Sigma\Phi$	$4(\Phi_2 - \Phi_4)$	$8(\Phi_2 - \Phi_4)$	$12(\Phi_2 - \Phi_4)$	$6(\Phi_2 - \Phi_3)$	$6(\Phi_2 - \Phi_6)$	$6(\Phi_3 - \Phi_6)$	$12(\Phi_3 - \Phi_4)$	$10(\Phi_2 - \Phi_5)$
Resolution	3%	7%	11%	7%	10%	11%	16%	9%
Trigger & event sel.	1-2%	1-4%	3%	3%	1-2%	1-2%	< 1%	< 1%
Run periods	< 1%	1%	5%	5%	3%	3%	2%	2%

TABLE V: Three sources of uncertainties for the two-plane correlators, $\langle \cos(\Sigma\Phi) \rangle$, where $\Sigma\Phi = jk(\Phi_n - \Phi_m)$. They are given as percentage uncertainties.

$\Sigma\Phi$	$2\Phi_2 + 3\Phi_3 - 5\Phi_5$	$2\Phi_2 + 4\Phi_4 - 6\Phi_6$	$2\Phi_2 - 6\Phi_3 + 4\Phi_4$
Resolution	10%	21%	11%
Trigger & event sel.	1-2%	1%	3-4%
Run periods	2%	5%	5%
$\Sigma\Phi$	$-8\Phi_2 + 3\Phi_3 + 5\Phi_5$	$-10\Phi_2 + 4\Phi_4 + 6\Phi_6$	$-10\Phi_2 + 6\Phi_3 + 4\Phi_4$
Resolution	13%	24%	16%
Trigger & event sel.	1-3%	1-3%	1-3%
Run periods	1%	5%	5%

TABLE VI: Three sources of uncertainties for the three-plane correlators, $\langle \cos(\Sigma\Phi) \rangle$, where $\Sigma\Phi = c_n n\Phi_n + c_m m\Phi_m + c_h h\Phi_h$. They are given as percentage uncertainties.

V. RESULTS AND DISCUSSIONS

Figures 6 and 7 show the centrality dependence of the two-plane and three-plane correlators, respectively. The results from both the EP method and SP method are shown with their respective systematic uncertainties. These systematic uncertainties are similar in the two methods and are strongly correlated across the centrality range. Strong positive values are observed in most cases and their magnitudes usually decrease with increasing $\langle N_{\text{part}} \rangle$, such as $\langle \cos 4(\Phi_2 - \Phi_4) \rangle$, $\langle \cos 8(\Phi_2 - \Phi_4) \rangle$, $\langle \cos 12(\Phi_2 - \Phi_4) \rangle$, $\langle \cos 6(\Phi_2 - \Phi_6) \rangle$, $\langle \cos(2\Phi_2 + 3\Phi_3 - 5\Phi_5) \rangle$, $\langle \cos(2\Phi_2 + 4\Phi_4 - 6\Phi_6) \rangle$ and $\langle \cos(-10\Phi_2 + 4\Phi_4 + 6\Phi_6) \rangle$. The value of $\langle \cos 6(\Phi_2 - \Phi_3) \rangle$ is small (< 0.02), yet exhibits

a similar dependence on $\langle N_{\text{part}} \rangle$. A small $\langle \cos 6(\Phi_2 - \Phi_3) \rangle$ value in this analysis is a consequence of dividing a small $\langle \cos 6(\Psi_2 - \Psi_3) \rangle$ signal (Figure 2) by a relatively large combined resolution factor (Fig. 3). Two other correlators show very different trends: the value of $\langle \cos 6(\Phi_3 - \Phi_6) \rangle$ increases with $\langle N_{\text{part}} \rangle$, and the value of $\langle \cos(2\Phi_2 - 6\Phi_3 + 4\Phi_4) \rangle$ is negative and its magnitude decreases with $\langle N_{\text{part}} \rangle$. The values of the remaining correlators are consistent with zero.

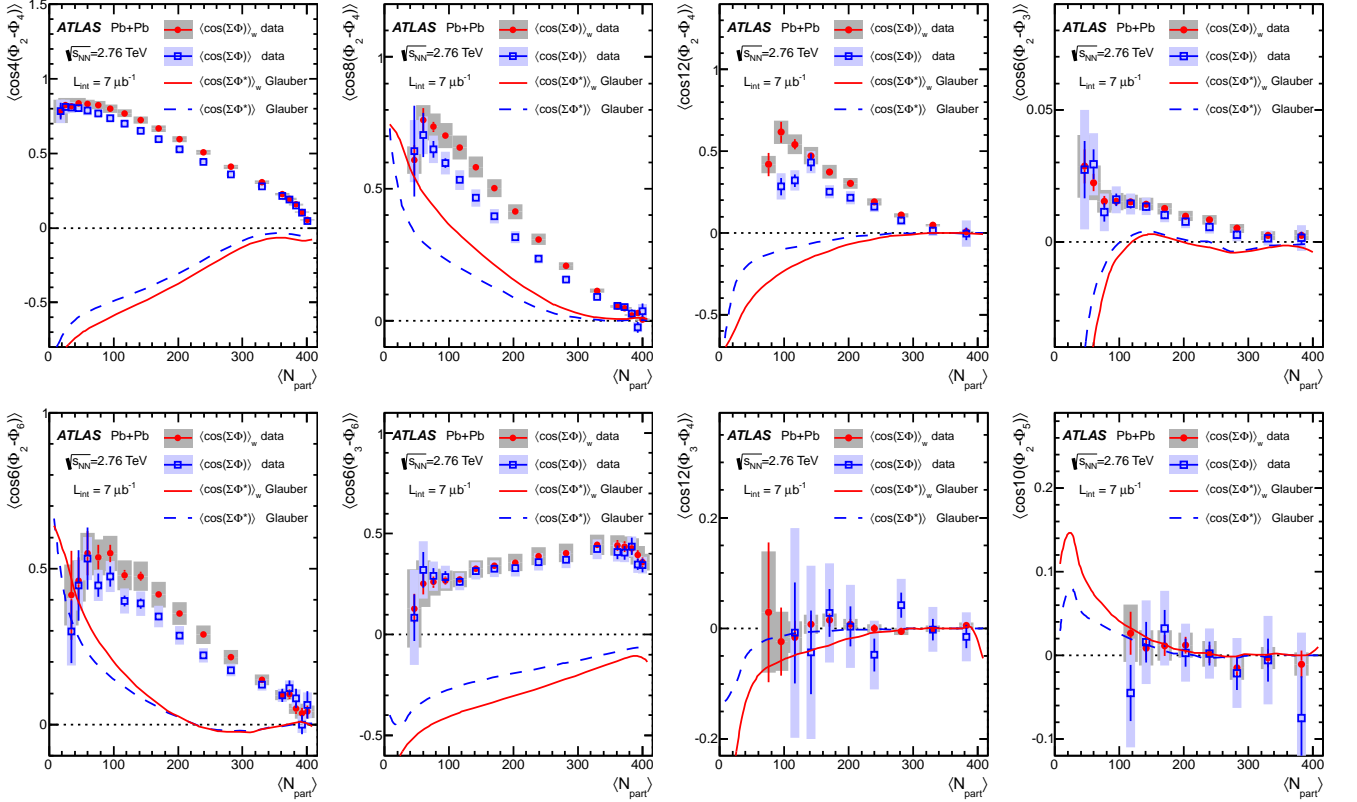


FIG. 6: (Color online) The centrality dependence of eight two-plane correlators, $\langle \cos(\Sigma\Phi) \rangle$ with $\Sigma\Phi = jk(\Phi_n - \Phi_m)$ obtained via the SP method (solid symbols) and the EP method (open symbols). The middle two panels in the top row have $j = 2$ and $j = 3$, respectively, while all other panels have $j = 1$. The error bars and shaded bands indicate the statistical uncertainties and total systematic uncertainties, respectively. The expected correlations among participant-plane angles Φ_n from a Glauber model are indicated by the solid curves for weighted case (Eq. (11)) and dashed lines for the unweighted case.

Figures 6 and 7 also suggest that the magnitude of the correlations from the SP method is always larger than that from the EP method. To better quantify their differences, Figures 8 and 9 show the ratio (SP/EP) for some selected two-plane and three-plane correlators, respectively. As discussed in Sec. IV D, the nature of the systematic uncertainties is very similar in the EP and SP methods, and hence these uncertainties mostly cancel in the ratio. The results from the SP method are larger than those from the EP method, and their ratios reach a maximum at around $100 < \langle N_{\text{part}} \rangle < 300$ range or 10%–40% centrality range. The maximum difference is about 10–15% for most two-plane correlators, but reaches 20–30% in mid-central collisions for $\langle \cos 8(\Phi_2 - \Phi_4) \rangle$ and $\langle \cos 6(\Phi_2 - \Phi_6) \rangle$. The differences are smaller for the three-plane correlators, except for $\langle \cos(-10\Phi_2 + 4\Phi_4 + 6\Phi_6) \rangle$.

Figures 6 and 7 also compare the data with the correlators calculated using the participant-plane angles defined in Eq. (4) from the Glauber model [9]. Thirty million events were generated and grouped into centrality intervals according to the impact parameter. If each flow harmonic is driven solely by the corresponding geometric component and the Φ_n aligns with the Φ_n^* , then the event-plane correlation and participant-plane correlation are expected to have the same sign and show similar centrality dependence. The results in Figs. 6 and 7 show that for several correlators the centrality dependence of the Glauber model predictions show trends similar to the data, although in some cases the sign is opposite, e.g. $\langle \cos 4(\Phi_2 - \Phi_4) \rangle$ and $\langle \cos(2\Phi_2 + 3\Phi_3 - 5\Phi_5) \rangle$. In some cases, even the magnitudes of the correlators show opposite centrality dependence between the Glauber model and the data in addition to the sign-flip, such as $\langle \cos 6(\Phi_3 - \Phi_6) \rangle$. These discrepancies suggest that in general Φ_n may not align with Φ_n^* . Indeed, large misalignments between Φ_n and Φ_n^* have been observed in event-by-event hydrodynamic model calculations for flow harmonics with $n > 3$, and these have been ascribed to the non-linear response of the medium to the fluctuations in

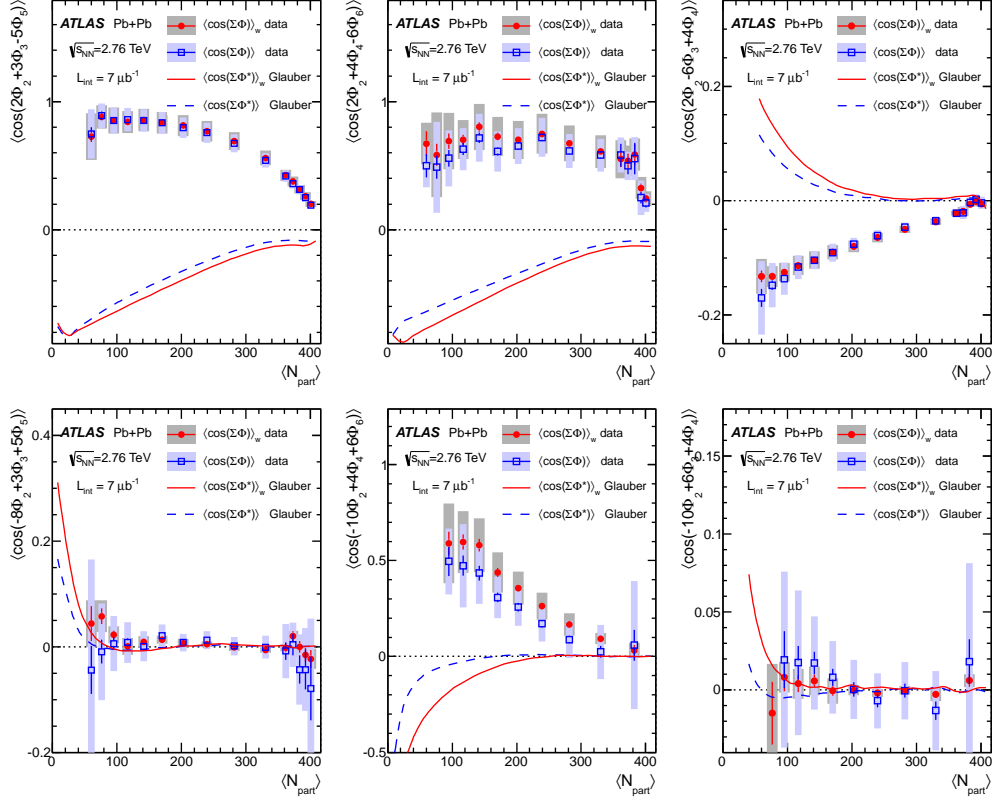


FIG. 7: (Color online) The centrality dependence of six three-plane correlators, $\langle \cos(\Sigma\Phi) \rangle$ with $\Sigma\Phi = c_n n\Phi_n + c_m m\Phi_m + c_h h\Phi_h$ obtained via the SP method (solid symbols) and the EP method (open symbols). The error bars and shaded bands indicate the statistical uncertainty and total systematic uncertainty, respectively. The expected correlations among participant-plane angles Φ_n^* from a Glauber model are indicated by the solid curves for weighted case (Eq. (11)) and dashed lines for the unweighted case.

the initial geometry [11, 39]. The non-linear effects are found to be small for lower-order harmonics [11, 40], such that $\Phi_n \approx \Phi_n^*$ and $v_n \propto \epsilon_n$ for $n = 2$ and 3 or equivalently in the form introduced in Eq. (2):

$$v_2 e^{i2\Phi_2} \propto \epsilon_2 e^{i2\Phi_2^*}, \quad v_3 e^{i3\Phi_3} \propto \epsilon_3 e^{i3\Phi_3^*}. \quad (22)$$

Recently, motivated by the preliminary version [41] of the results presented in this paper, several theory groups calculated the centrality dependence of EP correlators based on hydrodynamic models [5, 42–45]. The results of these calculations are in qualitative agreement with the experimental data. The dynamical origin of these correlators has been explained using the so-called single-shot hydrodynamics [42, 44, 45], where small fluctuations are imposed on a smooth average geometry profile, and the hydrodynamic response to these small fluctuations is then derived analytically using a cumulant expansion method. In this analytical approach, the v_4 signal comprises a term proportional to the ϵ_4 (linear response term) and a leading non-linear term that is proportional to ϵ_2^2 [5, 44]:

$$\begin{aligned} v_4 e^{i4\Phi_4} &= \alpha_4 \epsilon_4 e^{i4\Phi_4^*} + \alpha_{2,4} \left(\epsilon_2 e^{i2\Phi_2^*} \right)^2 + \dots \\ &= \alpha_4 \epsilon_4 e^{i4\Phi_4^*} + \beta_{2,4} v_2^2 e^{i4\Phi_2} + \dots, \end{aligned} \quad (23)$$

where the second line of the equation is derived from Eq. (22), and the coefficients α_4 , $\alpha_{2,4}$ and $\beta_{2,4}$ are all weak functions of centrality. Since v_2 increases rapidly for smaller $\langle N_{\text{part}} \rangle$ [8], the angle Φ_4 becomes more closely aligned with Φ_2 . Hence the centrality dependence of $\langle \cos j4(\Phi_2 - \Phi_4) \rangle$ reflects mainly the increase of the v_2 as $\langle N_{\text{part}} \rangle$ decreases.

Similarly, the correlations between Φ_2 and Φ_6 or between Φ_3 and Φ_6 have been explained by the following decom-

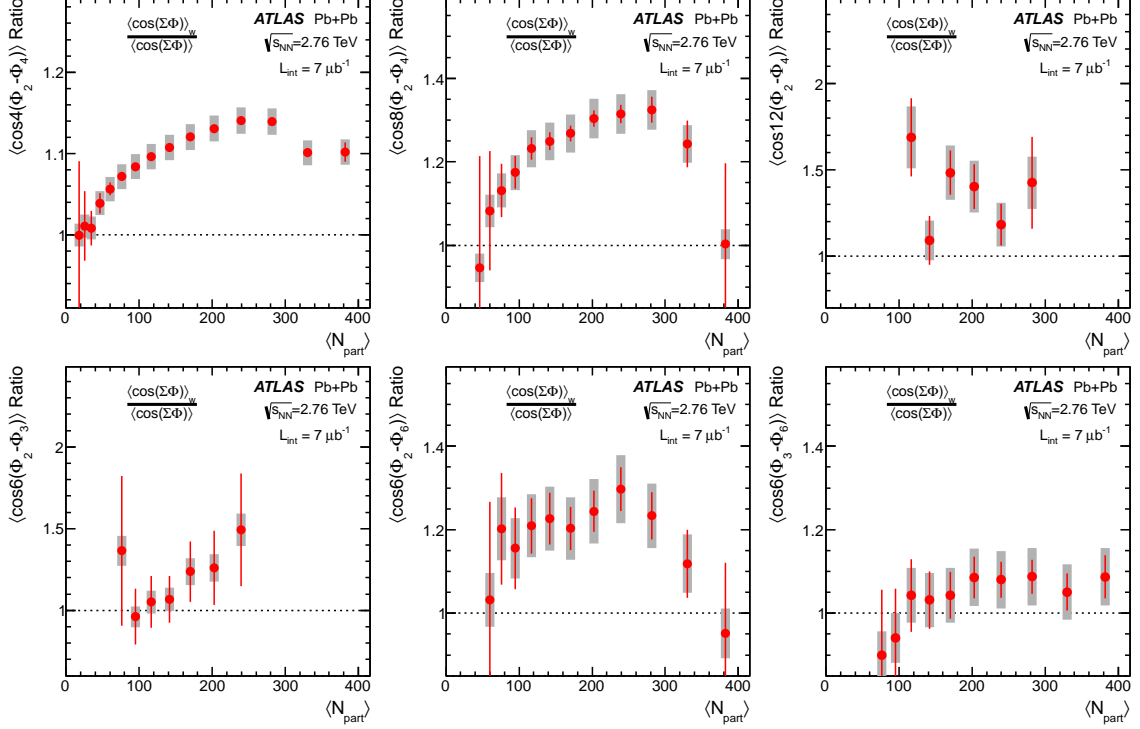


FIG. 8: (Color online) The ratios of the SP-method correlators to the EP-method correlators, $\langle \cos(\Sigma\Phi) \rangle_w / \langle \cos(\Sigma\Phi) \rangle$ for several two-plane correlators i.e with $\Sigma\Phi = jk(\Phi_n - \Phi_m)$. The error bars and shaded bands indicate the statistical uncertainties and total systematic uncertainties, respectively.

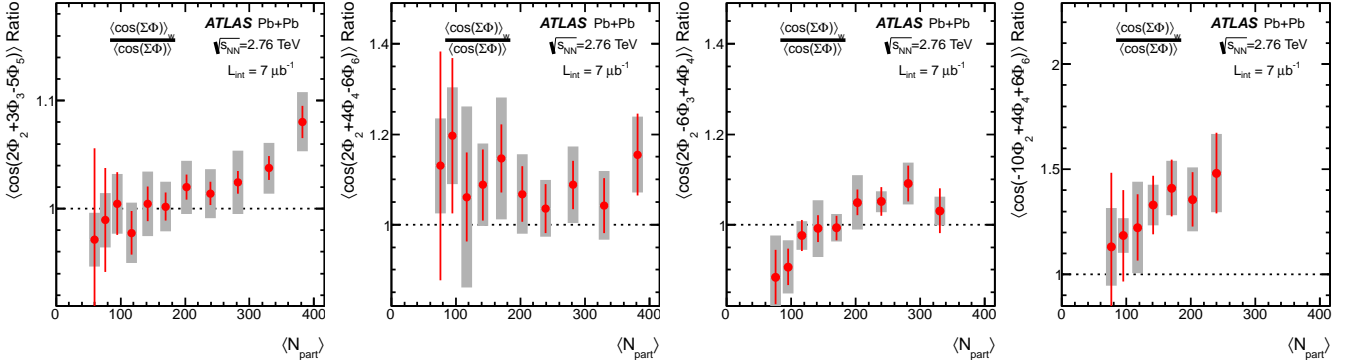


FIG. 9: (Color online) The ratios of the SP-method correlators to the EP-method correlators, $\langle \cos(\Sigma\Phi) \rangle_w / \langle \cos(\Sigma\Phi) \rangle$ for several three-plane correlators i.e with $\Sigma\Phi = c_n n\Phi_n + c_m m\Phi_m + c_h h\Phi_h$. The error bars and shaded bands indicate the statistical uncertainties and total systematic uncertainties, respectively.

position of the v_6 signal [5, 44]:

$$\begin{aligned}
 v_6 e^{i6\Phi_6} &= \alpha_6 \epsilon_6 e^{i6\Phi_6^*} + \alpha_{2,6} \left(\epsilon_2 e^{i2\Phi_2^*} \right)^3 + \alpha_{3,6} \left(\epsilon_3 e^{i3\Phi_3^*} \right)^2 + \dots \\
 &= \alpha_6 \epsilon_6 e^{i6\Phi_6^*} + \beta_{2,6} v_2^3 e^{i6\Phi_2} + \beta_{3,6} v_3^2 e^{i6\Phi_3} + \dots .
 \end{aligned} \tag{24}$$

Due to the non-linear contributions, Φ_6 becomes correlated with Φ_2 and Φ_3 , even though Φ_2 and Φ_3 are only very weakly correlated. The centrality dependences of $\langle \cos 6(\Phi_2 - \Phi_6) \rangle$ and $\langle \cos 6(\Phi_3 - \Phi_6) \rangle$ are strongly influenced by the centrality dependence of v_2 and v_3 : since v_2 increases for smaller $\langle N_{\text{part}} \rangle$ and v_3 is relatively independent of $\langle N_{\text{part}} \rangle$ [8],

the relative contribution of the second term increases and that of the third term decreases for smaller $\langle N_{\text{part}} \rangle$, i.e. the collisions become more peripheral. This behavior explains the opposite centrality dependence of $\langle \cos 6(\Phi_2 - \Phi_6) \rangle$ and $\langle \cos 6(\Phi_3 - \Phi_6) \rangle$.

In the same manner, the correlation between Φ_2, Φ_3 and Φ_5 has been explained by the following decomposition of the v_5 signal [5, 44]:

$$\begin{aligned} v_5 e^{i5\Phi_5} &= \alpha_5 \epsilon_5 e^{i5\Phi_5^*} + \alpha_{2,3,5} \epsilon_2 e^{i2\Phi_2^*} \epsilon_3 e^{i3\Phi_3^*} + \dots \\ &= \alpha_5 \epsilon_5 e^{i5\Phi_5^*} + \beta_{2,3,5} v_2 v_3 e^{i(2\Phi_2+3\Phi_3)} + \dots \end{aligned} \quad (25)$$

The coupling between v_5 and $v_2 v_3$ explains qualitatively the centrality dependence of the correlator $\langle \cos(2\Phi_2 + 3\Phi_3 - 5\Phi_5) \rangle$.

A multi-phase transport (AMPT) model [46] is frequently used to study the harmonic flow coefficients v_n and to study the relation of v_n to the initial geometry. The AMPT model combines the initial-state geometry fluctuations of the Glauber model and final-state interactions through a parton and hadron transport model. The AMPT model generates collective flow by elastic scatterings in the partonic and hadronic phase and was shown to reproduce the v_n values [47] and the particle multiplicity [48] reasonably well. As a full event generator, the AMPT model allows the generated events to be analyzed with the same procedures as in the data. Figures 10 and 11 compare some selected correlators (six two-plane correlators and four three-plane correlators) with a prediction [37] from the AMPT model. Good agreement is observed between the data and the calculation, and in particular the model predicts correctly the stronger signal observed with the SP method.

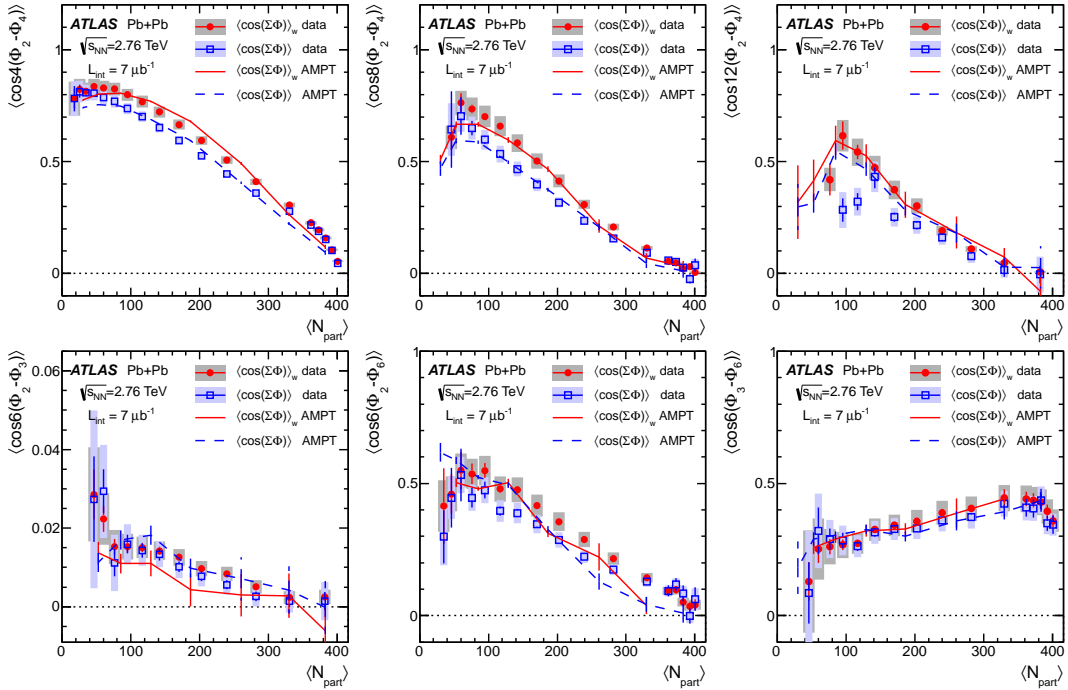


FIG. 10: (Color online) Comparison of six two-plane correlators, $\langle \cos(\Sigma\Phi) \rangle$ with $\Sigma\Phi = jk(\Phi_n - \Phi_m)$, with results from the AMPT model calculated via the SP method (solid lines) and the EP method (dashed lines) from Ref. [37]. The error bars on the lines represent the statistical uncertainties in the calculation.

VI. CONCLUSIONS

Measurements of fourteen correlators between two and three event planes, $\langle \cos jk(\Phi_n - \Phi_m) \rangle$ and $\langle \cos(c_n n \Psi_n + c_m m \Psi_m + c_h h \Psi_h) \rangle$, respectively, are presented using $7 \mu\text{b}^{-1}$ of Pb+Pb collision data at $\sqrt{s_{\text{NN}}} = 2.76 \text{ TeV}$ collected by the ATLAS experiment at the LHC. These correlations are estimated from correlations of observed event-plane angles measured in the calorimeters over a large pseudorapidity range $|\eta| < 4.8$ using both a

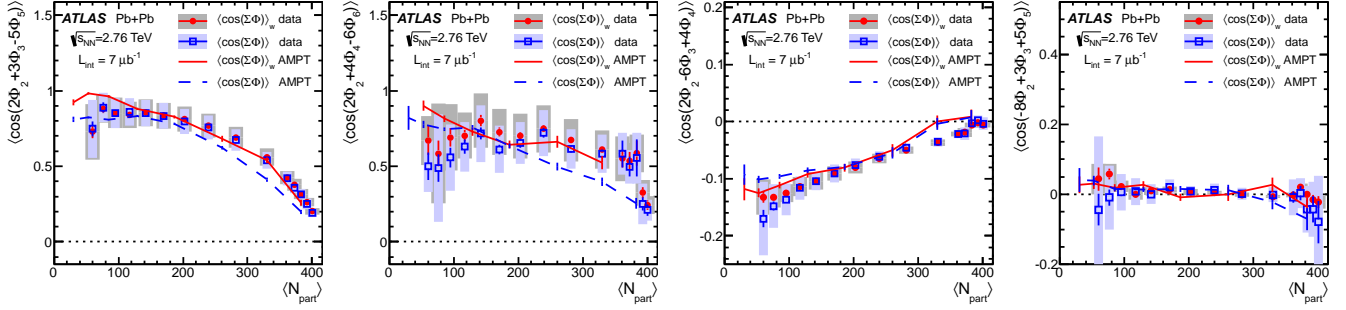


FIG. 11: (Color online) Comparison of four three-plane correlators, $\langle \cos(\Sigma\Phi) \rangle$ with $\Sigma\Phi = c_n n\Phi_n + c_m m\Phi_m + c_h h\Phi_h$, with results from the AMPT model calculated via the SP method (solid lines) and the EP method (dashed lines) from Ref. [37]. The error bars on the curves represent the statistical uncertainties in the calculation.

standard event-plane method and a scalar-product method. Significant positive correlation signals are observed for $4(\Phi_2 - \Phi_4)$, $6(\Phi_2 - \Phi_6)$, $6(\Phi_3 - \Phi_6)$, $2\Phi_2 + 3\Phi_3 - 5\Phi_5$, $2\Phi_2 + 4\Phi_4 - 6\Phi_6$ and $-10\Phi_2 + 4\Phi_4 + 6\Phi_6$. The correlation signals are negative for $2\Phi_2 - 6\Phi_3 + 4\Phi_4$. The magnitudes of the correlations from the scalar-product method are observed to be systematically larger than those obtained from the event-plane method. The centrality dependence of most correlators is found to be very different from that predicted by a Glauber model. However, calculations based on the same Glauber model, but including the final-state collective dynamics, are able to describe qualitatively, and in many cases also quantitatively, the centrality dependence of the measured correlators. These observations suggest that both the fluctuations in the initial geometry and non-linear mixing between different harmonics in the final state are important for creating these correlations in momentum space. A detailed theoretical description of these correlations can improve our present understanding of the space-time evolution of the hot and dense matter created in heavy-ion collisions.

Acknowledgments

We thank CERN for the very successful operation of the LHC, as well as the support staff from our institutions without whom ATLAS could not be operated efficiently.

We acknowledge the support of ANPCyT, Argentina; YerPhI, Armenia; ARC, Australia; BMWF and FWF, Austria; ANAS, Azerbaijan; SSTC, Belarus; CNPq and FAPESP, Brazil; NSERC, NRC and CFI, Canada; CERN; CONICYT, Chile; CAS, MOST and NSFC, China; COLCIENCIAS, Colombia; MSMT CR, MPO CR and VSC CR, Czech Republic; DNRF, DNSRC and Lundbeck Foundation, Denmark; EPLANET, ERC and NSRF, European Union; IN2P3-CNRS, CEA-DSM/IRFU, France; GNSF, Georgia; BMBF, DFG, HGF, MPG and AvH Foundation, Germany; GSRT and NSRF, Greece; ISF, MINERVA, GIF, I-CORE and Benoziyo Center, Israel; INFN, Italy; MEXT and JSPS, Japan; CNRST, Morocco; FOM and NWO, Netherlands; BRF and RCN, Norway; MNiSW and NCN, Poland; GRICES and FCT, Portugal; MNE/IFA, Romania; MES of Russia and ROSATOM, Russian Federation; JINR; MSTD, Serbia; MSSR, Slovakia; ARRS and MIZŠ, Slovenia; DST/NRF, South Africa; MINECO, Spain; SRC and Wallenberg Foundation, Sweden; SER, SNSF and Cantons of Bern and Geneva, Switzerland; NSC, Taiwan; TAEK, Turkey; STFC, the Royal Society and Leverhulme Trust, United Kingdom; DOE and NSF, United States of America.

The crucial computing support from all WLCG partners is acknowledged gratefully, in particular from CERN and the ATLAS Tier-1 facilities at TRIUMF (Canada), NDGF (Denmark, Norway, Sweden), CC-IN2P3 (France), KIT/GridKA (Germany), INFN-CNAF (Italy), NL-T1 (Netherlands), PIC (Spain), ASGC (Taiwan), RAL (UK) and BNL (USA) and in the Tier-2 facilities worldwide.

-
- [1] S. A. Voloshin, A. M. Poskanzer, and R. Snellings, [arXiv:0809.2949 \[nucl-ex\]](#).
 - [2] U. Heinz and R. Snellings, [Ann. Rev. Nucl. Part. Sci. **63**, 123 \(2013\)](#), [arXiv:1301.2826 \[nucl-th\]](#).
 - [3] D. A. Teaney, [arXiv:0905.2433 \[nucl-th\]](#).
 - [4] A. M. Poskanzer and S. Voloshin, [Phys. Rev. **C 58**, 1671 \(1998\)](#), [arXiv:nucl-ex/9805001 \[nucl-ex\]](#).
 - [5] F. G. Gardim, F. Grassi, M. Luzum, and J.-Y. Ollitrault, [Phys. Rev. **C 85**, 024908 \(2012\)](#), [arXiv:1111.6538 \[nucl-th\]](#).
 - [6] ALICE Collaboration, [Phys. Lett. **B 708**, 249 \(2012\)](#), [arXiv:1109.2501 \[nucl-ex\]](#).

- [7] CMS Collaboration, *Eur. Phys. J. C* **72**, 2012 (2012), arXiv:1201.3158 [nucl-ex] .
- [8] ATLAS Collaboration, *Phys. Rev. C* **86**, 014907 (2012), arXiv:1203.3087 [hep-ex] .
- [9] M. L. Miller, K. Reygers, S. J. Sanders, and P. Steinberg, *Ann. Rev. Nucl. Part. Sci.* **57**, 205 (2007), arXiv:nucl-ex/0701025 [nucl-ex] .
- [10] D. Teaney and L. Yan, *Phys. Rev. C* **83**, 064904 (2011), arXiv:1010.1876 [nucl-th] .
- [11] Z. Qiu and U. W. Heinz, *Phys. Rev. C* **84**, 024911 (2011), arXiv:1104.0650 [nucl-th] .
- [12] A. Adare *et al.* (PHENIX Collaboration), *Phys. Rev. Lett.* **107**, 252301 (2011), arXiv:1105.3928 [nucl-ex] .
- [13] L. Adamczyk *et al.* (STAR Collaboration), *Phys. Rev. C* **88**, 014904 (2013), arXiv:1301.2187 [nucl-ex] .
- [14] ALICE Collaboration, *Phys. Rev. Lett.* **105**, 252302 (2010), arXiv:1011.3914 [nucl-ex] .
- [15] ATLAS Collaboration, *J. High Energy Phys.* **1311**, 183 (2013), arXiv:1305.2942 [hep-ex] .
- [16] CMS Collaboration, *Phys. Rev. C* **89**, 044906 (2014), arXiv:1310.8651 [nucl-ex] .
- [17] J. L. Nagle and M. P. McCumber, *Phys. Rev. C* **83**, 044908 (2011), arXiv:1011.1853 [nucl-ex] .
- [18] A. Adare *et al.* (PHENIX Collaboration), *Phys. Rev. Lett.* **105**, 062301 (2010), arXiv:1003.5586 [nucl-ex] .
- [19] ALICE Collaboration, *Phys. Rev. Lett.* **107**, 032301 (2011), arXiv:1105.3865 [nucl-ex] .
- [20] R. Bhaleerao, M. Luzum, and J. Ollitrault, *J. Phys. G* **38**, 124055 (2011), arXiv:1106.4940 [nucl-ex] .
- [21] R. S. Bhaleerao, M. Luzum, and J.-Y. Ollitrault, *Phys. Rev. C* **84**, 034910 (2011), arXiv:1104.4740 [nucl-th] .
- [22] J. Jia and S. Mohapatra, *Eur. Phys. J. C* **73**, 2510 (2013), arXiv:1203.5095 [nucl-th] .
- [23] J. Jia and D. Teaney, *Eur. Phys. J. C* **73**, 2558 (2013), arXiv:1205.3585 [nucl-ex] .
- [24] ATLAS Collaboration, *JINST* **3**, S08003 (2008).
- [25] ATLAS Collaboration, *Eur. Phys. J. C* **72**, 1849 (2012), arXiv:1110.1530 [hep-ex] .
- [26] ATLAS Collaboration, *Eur. Phys. J. C* **73**, 2304 (2013), arXiv:1112.6426 [hep-ex] .
- [27] ATLAS Collaboration, *Phys. Lett. B* **710**, 363 (2012), arXiv:1108.6027 [hep-ex] .
- [28] ATLAS Collaboration, *New J. Phys.* **13**, 053033 (2011), arXiv:1012.5104 [hep-ex] .
- [29] ATLAS Collaboration, *Phys. Lett. B* **707**, 330 (2012), arXiv:1108.6018 [hep-ex] .
- [30] M. Gyulassy and X.-N. Wang, *Comput. Phys. Commun.* **83**, 307 (1994), arXiv:nucl-th/9502021 [nucl-th] .
- [31] ATLAS Collaboration, *Eur. Phys. J. C* **70**, 823 (2010).
- [32] S. Agostinelli *et al.* (GEANT4), *Nucl. Instrum. Methods Phys. Res., Sect. A* **506**, 250 (2003).
- [33] ATLAS Collaboration, ATLAS-CONF-2011-079, <http://cdsweb.cern.ch/record/1355702>.
- [34] S. Afanasiev *et al.* (PHENIX Collaboration), *Phys. Rev. C* **80**, 024909 (2009), arXiv:0905.1070 [nucl-ex] .
- [35] J. Barrette *et al.* (E877 Collaboration), *Phys. Rev. C* **56**, 3254 (1997), arXiv:nucl-ex/9707002 [nucl-ex] .
- [36] M. Luzum and J.-Y. Ollitrault, *Phys. Rev. C* **87**, 044907 (2013), arXiv:1209.2323 [nucl-ex] .
- [37] R. S. Bhaleerao, J.-Y. Ollitrault, and S. Pal, *Phys. Rev. C* **88**, 024909 (2013), arXiv:1307.0980 [nucl-th] .
- [38] C. Adler *et al.* (STAR Collaboration), *Phys. Rev. C* **66**, 034904 (2002), arXiv:nucl-ex/0206001 [nucl-ex] .
- [39] R. Andrade, F. Grassi, Y. Hama, and W.-L. Qian, *Nucl. Phys. A* **854**, 81 (2011), arXiv:1008.0139 [hep-ph] .
- [40] H. Niemi, G. Denicol, H. Holopainen, and P. Huovinen, *Phys. Rev. C* **87**, 054901 (2013), arXiv:1212.1008 [nucl-th] .
- [41] ATLAS Collaboration, ATLAS-CONF-2012-049, <https://cds.cern.ch/record/1451882> .
- [42] D. Teaney and L. Yan, *Phys. Rev. C* **86**, 044908 (2012), arXiv:1206.1905 [nucl-th] .
- [43] Z. Qiu and U. Heinz, *Phys. Lett. B* **717**, 261 (2012), arXiv:1208.1200 [nucl-th] .
- [44] D. Teaney and L. Yan, *Nucl. Phys. A* **904**, 365c (2013), arXiv:1210.5026 [nucl-th] .
- [45] D. Teaney and L. Yan, arXiv:1312.3689 [nucl-th] .
- [46] Z.-W. Lin, C. M. Ko, B.-A. Li, B. Zhang, and S. Pal, *Phys. Rev. C* **72**, 064901 (2005), arXiv:nucl-th/0411110 [nucl-th] .
- [47] J. Xu and C. M. Ko, *Phys. Rev. C* **84**, 044907 (2011), arXiv:1108.0717 [nucl-th] .
- [48] J. Xu and C. M. Ko, *Phys. Rev. C* **83**, 034904 (2011), arXiv:1101.2231 [nucl-th] .

Appendix

Figures 12–15 compare results between the calorimeter and the ID for the two-plane and three-plane correlations. As discussed at the end of Sec. IV D, the results are consistent between the calorimeter and the ID within their respective systematic uncertainties.

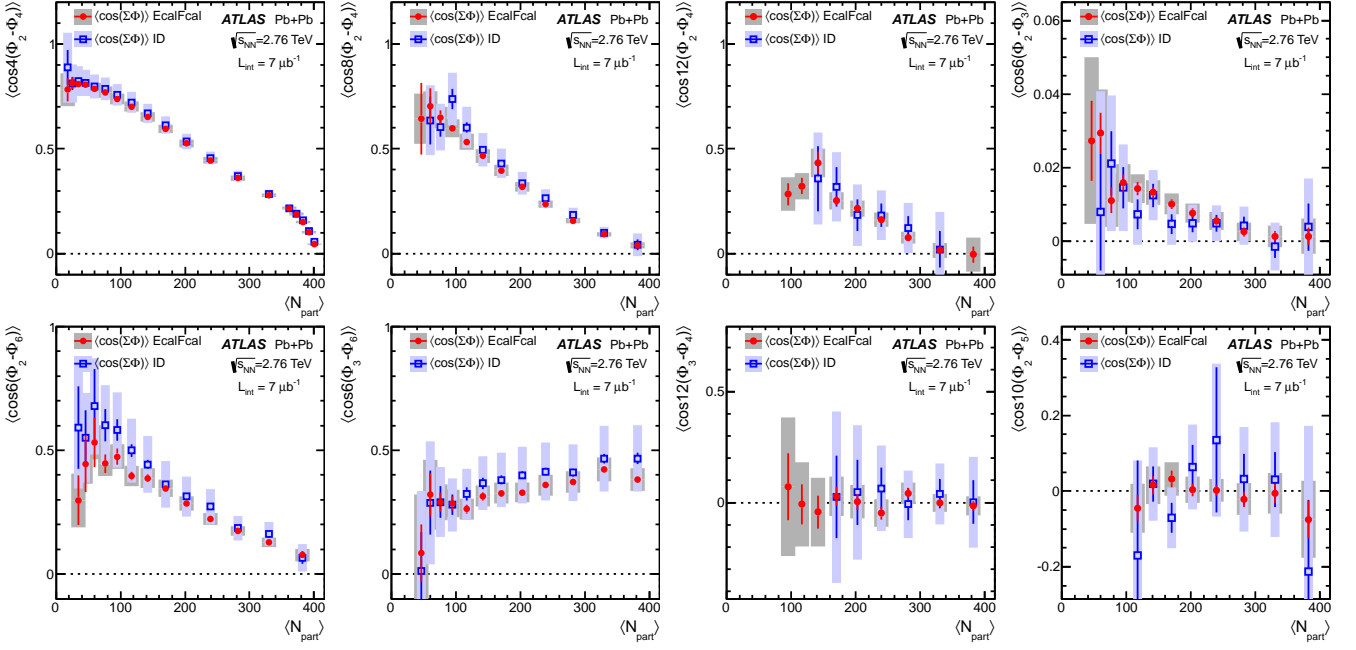


FIG. 12: (Color online) The comparison of the eight two-plane correlators between the calorimeters (default) and ID (cross-check) as a function of $\langle N_{\text{part}} \rangle$, both obtained from the EP method. The error bars and the shaded bands indicate the statistical and total systematic uncertainties, respectively.

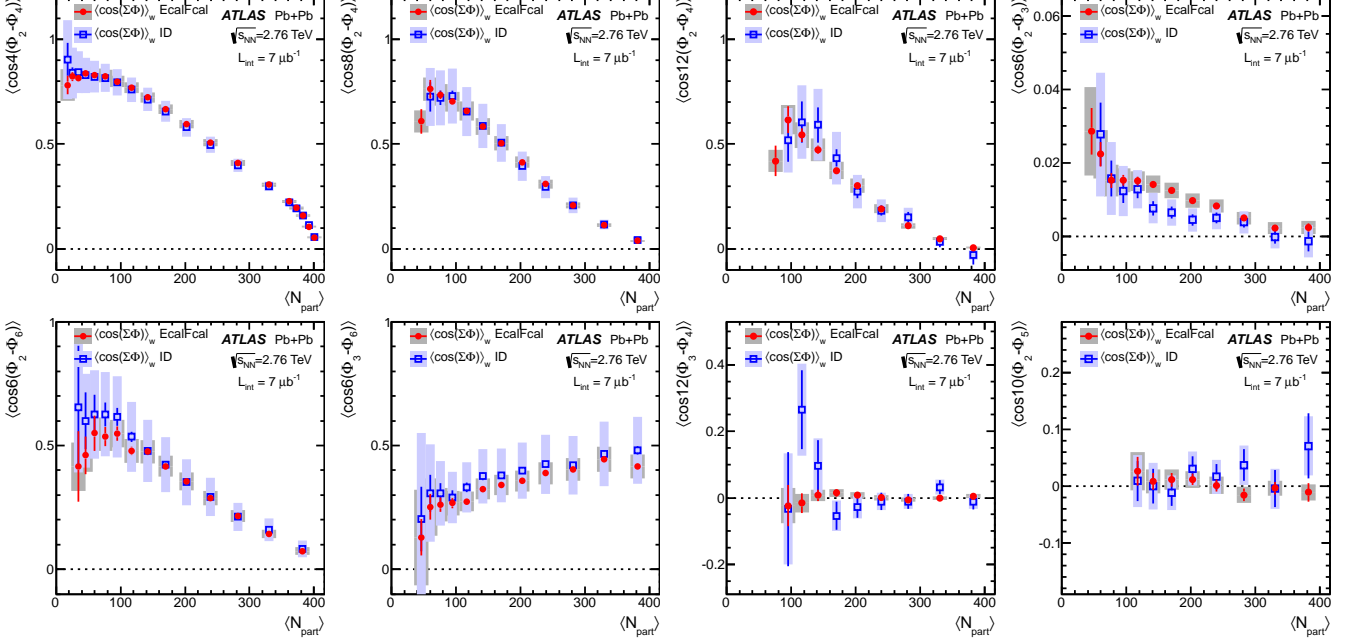


FIG. 13: The comparison of the eight two-plane correlators between the calorimeters (default) and ID (cross-check) as a function of $\langle N_{\text{part}} \rangle$, both obtained from the SP method. The error bars and the shaded bands indicate the statistical and total systematic uncertainties, respectively.

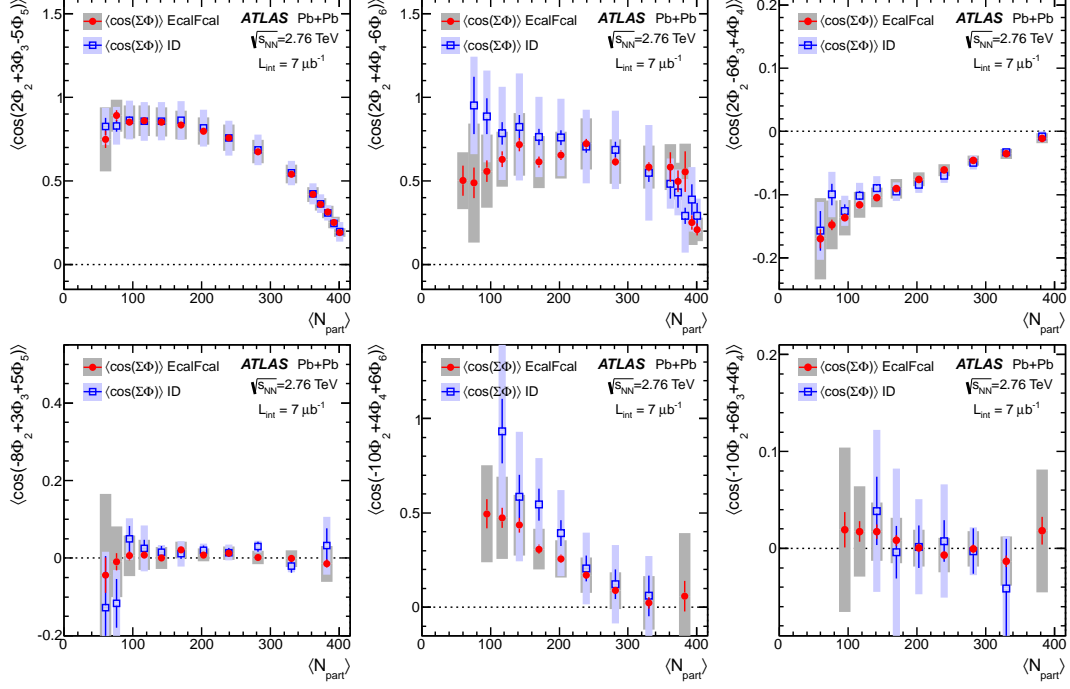


FIG. 14: (Color online) The comparison of the six three-plane correlators between the calorimeters (default) and ID (cross-check) as a function of $\langle N_{\text{part}} \rangle$, both obtained from the EP method. The error bars and the shaded bands indicate the statistical and total systematic uncertainty, respectively.

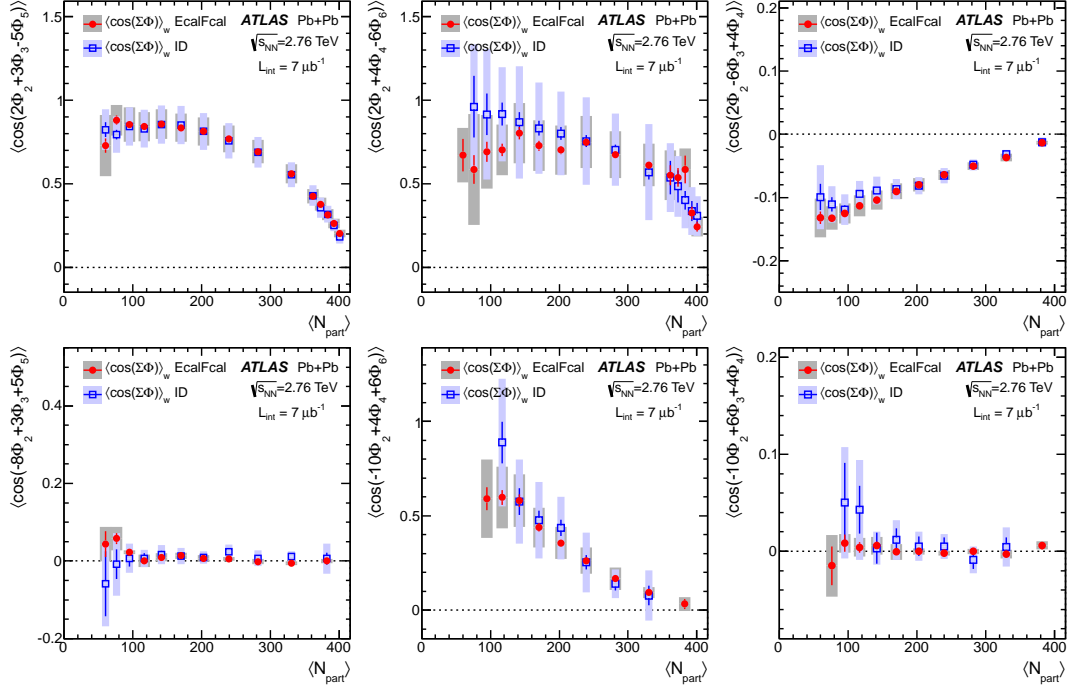


FIG. 15: (Color online) The comparison of the six three-plane correlators between the calorimeters (default) and ID (cross-check) as a function of $\langle N_{\text{part}} \rangle$, both obtained from the SP method. The error bars and the shaded bands indicate the statistical and total systematic uncertainties, respectively.

The ATLAS Collaboration

G. Aad⁸⁴, B. Abbott¹¹², J. Abdallah¹⁵², S. Abdel Khalek¹¹⁶, O. Abdinov¹¹, R. Aben¹⁰⁶, B. Abi¹¹³, M. Abolins⁸⁹, O.S. AbouZeid¹⁵⁹, H. Abramowicz¹⁵⁴, H. Abreu¹³⁷, R. Abreu³⁰, Y. Abulaiti^{147a,147b}, B.S. Acharya^{165a,165b,a}, L. Adamczyk^{38a}, D.L. Adams²⁵, J. Adelman¹⁷⁷, S. Adomeit⁹⁹, T. Adye¹³⁰, T. Agatonovic-Jovin^{13b}, J.A. Aguilar-Saavedra^{125f,125a}, M. Agustoni¹⁷, S.P. Ahlen²², A. Ahmad¹⁴⁹, F. Ahmadov^{64,b}, G. Aielli^{134a,134b}, T.P.A. Åkesson⁸⁰, G. Akimoto¹⁵⁶, A.V. Akimov⁹⁵, J. Albert¹⁷⁰, S. Albrand⁵⁵, M.J. Alconada Verzini⁷⁰, M. Aleksa³⁰, I.N. Aleksandrov⁶⁴, C. Alexa^{26a}, G. Alexander¹⁵⁴, G. Alexandre⁴⁹, T. Alexopoulos¹⁰, M. Alhroob^{165a,165c}, G. Alimonti^{90a}, L. Alio⁸⁴, J. Alison³¹, B.M.M. Allbrooke¹⁸, L.J. Allison⁷¹, P.P. Allport⁷³, S.E. Allwood-Spiers⁵³, J. Almond⁸³, A. Aloisio^{103a,103b}, A. Alonso³⁶, F. Alonso⁷⁰, C. Alpigiani⁷⁵, A. Altheimer³⁵, B. Alvarez Gonzalez⁸⁹, M.G. Alviggi^{103a,103b}, K. Amako⁶⁵, Y. Amaral Coutinho^{24a}, C. Amelung²³, D. Amidei⁸⁸, S.P. Amor Dos Santos^{125a,125c}, A. Amorim^{125a,125b}, S. Amoroso⁴⁸, N. Amram¹⁵⁴, G. Amundsen²³, C. Anastopoulos¹⁴⁰, L.S. Ancu⁴⁹, N. Andari³⁰, T. Andeen³⁵, C.F. Anders^{58b}, G. Anders³⁰, K.J. Anderson³¹, A. Andreazza^{90a,90b}, V. Andrei^{58a}, X.S. Anduaga⁷⁰, S. Angelidakis⁹, I. Angelozzi¹⁰⁶, P. Anger⁴⁴, A. Angerami³⁵, F. Anghinolfi³⁰, A.V. Anisenkov¹⁰⁸, N. Anjos^{125a}, A. Annovi⁴⁷, A. Antonaki⁹, M. Antonelli⁴⁷, A. Antonov⁹⁷, J. Antos^{145b}, F. Anulli^{133a}, M. Aoki⁶⁵, L. Aperio Bella¹⁸, R. Apolle^{119,c}, G. Arabidze⁸⁹, I. Aracena¹⁴⁴, Y. Arai⁶⁵, J.P. Araque^{125a}, A.T.H. Arce⁴⁵, J-F. Arguin⁹⁴, S. Argyropoulos⁴², M. Arik^{19a}, A.J. Armbruster³⁰, O. Arnaez⁸², V. Arnal⁸¹, H. Arnold⁴⁸, O. Arslan²¹, A. Artamonov⁹⁶, G. Artoni²³, S. Asai¹⁵⁶, N. Asbah⁹⁴, A. Ashkenazi¹⁵⁴, S. Ask²⁸, B. Åsman^{147a,147b}, L. Asquith⁶, K. Assamagan²⁵, R. Astalos^{145a}, M. Atkinson¹⁶⁶, N.B. Atlay¹⁴², B. Auerbach⁶, K. Augsten¹²⁷, M. Aourousseau^{146b}, G. Avolio³⁰, G. Azuelos^{94,d}, Y. Azuma¹⁵⁶, M.A. Baak³⁰, C. Bacci^{135a,135b}, H. Bachacou¹³⁷, K. Bachas¹⁵⁵, M. Backes³⁰, M. Backhaus³⁰, J. Backus Mayes¹⁴⁴, E. Badescu^{26a}, P. Bagiacchi^{133a,133b}, P. Bagnaia^{133a,133b}, Y. Bai^{33a}, T. Bain³⁵, J.T. Baines¹³⁰, O.K. Baker¹⁷⁷, S. Baker⁷⁷, P. Balek¹²⁸, F. Balli¹³⁷, E. Banas³⁹, Sw. Banerjee¹⁷⁴, D. Banfi³⁰, A. Bangert¹⁵¹, A.A.E. Bannoura¹⁷⁶, V. Bansal¹⁷⁰, H.S. Bansil¹⁸, L. Barak¹⁷³, S.P. Baranov⁹⁵, E.L. Barberio⁸⁷, D. Barberis^{50a,50b}, M. Barbero⁸⁴, T. Barillari¹⁰⁰, M. Barisonzi¹⁷⁶, T. Barklow¹⁴⁴, N. Barlow²⁸, B.M. Barnett¹³⁰, R.M. Barnett¹⁵, Z. Barnovska⁵, A. Baroncelli^{135a}, G. Barone⁴⁹, A.J. Barr¹¹⁹, F. Barreiro⁸¹, J. Barreiro Guimarães da Costa⁵⁷, R. Bartoldus¹⁴⁴, A.E. Barton⁷¹, P. Bartos^{145a}, V. Bartsch¹⁵⁰, A. Bassalat¹¹⁶, A. Basye¹⁶⁶, R.L. Bates⁵³, L. Batkova^{145a}, J.R. Batley²⁸, M. Battistin³⁰, F. Bauer¹³⁷, H.S. Bawa^{144,e}, T. Beau⁷⁹, P.H. Beauchemin¹⁶², R. Beccherle^{123a,123b}, P. Bechtel²¹, H.P. Beck¹⁷, K. Becker¹⁷⁶, S. Becker⁹⁹, M. Beckingham¹³⁹, C. Becot¹¹⁶, A.J. Beddall^{19c}, A. Beddall^{19c}, S. Bedikian¹⁷⁷, V.A. Bednyakov⁶⁴, C.P. Bee¹⁴⁹, L.J. Beemster¹⁰⁶, T.A. Beermann¹⁷⁶, M. Beger²⁵, K. Behr¹¹⁹, C. Belanger-Champagne⁸⁶, P.J. Bell⁴⁹, W.H. Bell⁴⁹, G. Bella¹⁵⁴, L. Bellagamba^{20a}, A. Bellerive²⁹, M. Bellomo⁸⁵, A. Belloni⁵⁷, O.L. Beloborodova^{108,f}, K. Belotskiy⁹⁷, O. Beltramello³⁰, O. Benary¹⁵⁴, D. Bencheikroun^{136a}, K. Bendtz^{147a,147b}, N. Benekos¹⁶⁶, Y. Benhammou¹⁵⁴, E. Benhar Nocchioli⁴⁹, J.A. Benitez Garcia^{160b}, D.P. Benjamin⁴⁵, J.R. Bensinger²³, K. Benslama¹³¹, S. Bentvelsen¹⁰⁶, D. Berge¹⁰⁶, E. Bergeas Kuutmann¹⁶, N. Berger⁵, F. Berghaus¹⁷⁰, E. Berglund¹⁰⁶, J. Beringer¹⁵, C. Bernard²², P. Bernat⁷⁷, C. Bernius⁷⁸, F.U. Bernlochner¹⁷⁰, T. Berry⁷⁶, P. Berta¹²⁸, C. Bertella⁸⁴, F. Bertolucci^{123a,123b}, M.I. Besana^{90a}, G.J. Besjes¹⁰⁵, O. Bessidskaia^{147a,147b}, N. Besson¹³⁷, C. Betancourt⁴⁸, S. Bethke¹⁰⁰, W. Bhimji⁴⁶, R.M. Bianchi¹²⁴, L. Bianchini²³, M. Bianco³⁰, O. Biebel⁹⁹, S.P. Bieniek⁷⁷, K. Bierwagen⁵⁴, J. Biesiada¹⁵, M. Biglietti^{135a}, J. Bilbao De Mendizabal⁴⁹, H. Bilokon⁴⁷, M. Bindi⁵⁴, S. Binet¹¹⁶, A. Bingul^{19c}, C. Bini^{133a,133b}, C.W. Black¹⁵¹, J.E. Black¹⁴⁴, K.M. Black²², D. Blackburn¹³⁹, R.E. Blair⁶, J.-B. Blanchard¹³⁷, T. Blazek^{145a}, I. Bloch⁴², C. Blocker²³, W. Blum^{82,*}, U. Blumenschein⁵⁴, G.J. Bobbink¹⁰⁶, V.S. Bobrovnikov¹⁰⁸, S.S. Bocchetta⁸⁰, A. Bocci⁴⁵, C.R. Boddy¹¹⁹, M. Boehler⁴⁸, J. Boek¹⁷⁶, T.T. Boek¹⁷⁶, J.A. Bogaerts³⁰, A.G. Bogdanchikov¹⁰⁸, A. Bogouch^{91,*}, C. Boehm^{147a}, J. Bohm¹²⁶, V. Boisvert⁷⁶, T. Bold^{38a}, V. Boldea^{26a}, A.S. Boldyrev⁹⁸, M. Bomben⁷⁹, M. Bona⁷⁵, M. Boonekamp¹³⁷, A. Borisov¹²⁹, G. Borissov⁷¹, M. Borri⁸³, S. Borroni⁴², J. Bortfeldt⁹⁹, V. Bortolotto^{135a,135b}, K. Bos¹⁰⁶, D. Boscherini^{20a}, M. Bosman¹², H. Boterenbrood¹⁰⁶, J. Boudreau¹²⁴, J. Bouffard², E.V. Bouhova-Thacker⁷¹, D. Boumediene³⁴, C. Bourdarios¹¹⁶, N. Bousson¹¹³, S. Boutouil^{136d}, A. Boveia³¹, J. Boyd³⁰, I.R. Boyko⁶⁴, I. Bozovic-Jelisavcic^{13b}, J. Bracinik¹⁸, P. Branchini^{135a}, A. Brandt⁸, G. Brandt¹⁵, O. Brandt^{58a}, U. Bratzler¹⁵⁷, B. Brau⁸⁵, J.E. Brau¹¹⁵, H.M. Braun^{176,*}, S.F. Brazzale^{165a,165c}, B. Brelier¹⁵⁹, K. Brendlinger¹²¹, A.J. Brennan⁸⁷, R. Brenner¹⁶⁷, S. Bressler¹⁷³, K. Bristow^{146c}, T.M. Bristow⁴⁶, D. Britton⁵³, F.M. Brochu²⁸, I. Brock²¹, R. Brock⁸⁹, C. Bromberg⁸⁹, J. Bronner¹⁰⁰, G. Brooijmans³⁵, T. Brooks⁷⁶, W.K. Brooks^{32b}, J. Brosamer¹⁵, E. Brost¹¹⁵, G. Brown⁸³, J. Brown⁵⁵, P.A. Bruckman de Renstrom³⁹, D. Bruncko^{145b}, R. Bruneliere⁴⁸, S. Brunet⁶⁰, A. Bruni^{20a}, G. Bruni^{20a}, M. Bruschi^{20a}, L. Bryngemark⁸⁰, T. Buanes¹⁴, Q. Buat¹⁴³, F. Bucci⁴⁹, P. Buchholz¹⁴², R.M. Buckingham¹¹⁹, A.G. Buckley⁵³, S.I. Buda^{26a}, I.A. Budagov⁶⁴, F. Buehrer⁴⁸, L. Bugge¹¹⁸, M.K. Bugge¹¹⁸, O. Bulekov⁹⁷, A.C. Bundock⁷³, H. Burckhart³⁰, S. Burdin⁷³, B. Burghgrave¹⁰⁷, S. Burke¹³⁰, I. Burmeister⁴³, E. Busato³⁴, D. Büscher⁴⁸, V. Büscher⁸², P. Bussey⁵³, C.P. Buszello¹⁶⁷, B. Butler⁵⁷, J.M. Butler²², A.I. Butt³, C.M. Buttar⁵³, J.M. Butterworth⁷⁷, P. Butti¹⁰⁶, W. Buttinger²⁸, A. Buzatu⁵³, M. Byszewski¹⁰, S. Cabrera Urbán¹⁶⁸, D. Caforio^{20a,20b}, O. Cakir^{4a}, P. Calafiura¹⁵, A. Calandri¹³⁷, G. Calderini⁷⁹, P. Calfayan⁹⁹, R. Calkins¹⁰⁷, L.P. Caloba^{24a}, D. Calvet³⁴, S. Calvet³⁴, R. Camacho Toro⁴⁹, S. Camarda⁴², D. Cameron¹¹⁸,

L.M. Caminada¹⁵, R. Caminal Armadans¹², S. Campana³⁰, M. Campanelli⁷⁷, A. Campoverde¹⁴⁹, V. Canale^{103a,103b}, A. Canepa^{160a}, J. Cantero⁸¹, R. Cantrill⁷⁶, T. Cao⁴⁰, M.D.M. Capeans Garrido³⁰, I. Caprini^{26a}, M. Caprini^{26a}, M. Capua^{37a,37b}, R. Caputo⁸², R. Cardarelli^{134a}, T. Carli³⁰, G. Carlino^{103a}, L. Carminati^{90a,90b}, S. Caron¹⁰⁵, E. Carquin^{32a}, G.D. Carrillo-Montoya^{146c}, A.A. Carter⁷⁵, J.R. Carter²⁸, J. Carvalho^{125a,125c}, D. Casadei⁷⁷, M.P. Casado¹², E. Castaneda-Miranda^{146b}, A. Castelli¹⁰⁶, V. Castillo Gimenez¹⁶⁸, N.F. Castro^{125a}, P. Catastini⁵⁷, A. Catinaccio³⁰, J.R. Catmore¹¹⁸, A. Cattai³⁰, G. Cattani^{134a,134b}, S. Caughron⁸⁹, V. Cavaliere¹⁶⁶, D. Cavalli^{90a}, M. Cavalli-Sforza¹², V. Cavasinni^{123a,123b}, F. Ceradini^{135a,135b}, B. Cerio⁴⁵, K. Cerny¹²⁸, A.S. Cerqueira^{24b}, A. Cerri¹⁵⁰, L. Cerrito⁷⁵, F. Cerutti¹⁵, M. Cerv³⁰, A. Cervelli¹⁷, S.A. Cetin^{19b}, A. Chafaq^{136a}, D. Chakraborty¹⁰⁷, I. Chalupkova¹²⁸, K. Chan³, P. Chang¹⁶⁶, B. Chapleau⁸⁶, J.D. Chapman²⁸, D. Charfeddine¹¹⁶, D.G. Charlton¹⁸, C.C. Chau¹⁵⁹, C.A. Chavez Barajas¹⁵⁰, S. Cheatham⁸⁶, A. Chegwiddden⁸⁹, S. Chekanov⁶, S.V. Chekulaev^{160a}, G.A. Chelkov⁶⁴, M.A. Chelstowska⁸⁸, C. Chen⁶³, H. Chen²⁵, K. Chen¹⁴⁹, L. Chen^{33d,g}, S. Chen^{33c}, X. Chen^{146c}, Y. Chen³⁵, H.C. Cheng⁸⁸, Y. Cheng³¹, A. Cheplakov⁶⁴, R. Cherkaoui El Moursli^{136e}, V. Chernyatin^{25,*}, E. Cheu⁷, L. Chevalier¹³⁷, V. Chiarella⁴⁷, G. Chiefari^{103a,103b}, J.T. Childers⁶, A. Chilingarov⁷¹, G. Chiodini^{72a}, A.S. Chisholm¹⁸, R.T. Chislett⁷⁷, A. Chitan^{26a}, M.V. Chizhov⁶⁴, S. Chouridou⁹, B.K.B. Chow⁹⁹, I.A. Christidi⁷⁷, D. Chromek-Burckhart³⁰, M.L. Chu¹⁵², J. Chudoba¹²⁶, J.C. Chwastowski³⁹, L. Chytka¹¹⁴, G. Ciapetti^{133a,133b}, A.K. Ciftci^{4a}, R. Ciftci^{4a}, D. Cinca⁶², V. Cindro⁷⁴, A. Ciocio¹⁵, P. Cirkovic^{13b}, Z.H. Citron¹⁷³, M. Citterio^{90a}, M. Ciubancan^{26a}, A. Clark⁴⁹, P.J. Clark⁴⁶, R.N. Clarke¹⁵, W. Cleland¹²⁴, J.C. Clemens⁸⁴, C. Clement^{147a,147b}, Y. Coadou⁸⁴, M. Cobal^{165a,165c}, A. Cocco¹³⁹, J. Cochran⁶³, L. Coffey²³, J.G. Cogan¹⁴⁴, J. Coggeshall¹⁶⁶, B. Cole³⁵, S. Cole¹⁰⁷, A.P. Colijn¹⁰⁶, C. Collins-Tooth⁵³, J. Collot⁵⁵, T. Colombo^{58c}, G. Colon⁸⁵, G. Compostella¹⁰⁰, P. Conde Muiño^{125a,125b}, E. Coniavitis¹⁶⁷, M.C. Conidi¹², S.H. Connell^{146b}, I.A. Connelly⁷⁶, S.M. Consonni^{90a,90b}, V. Consorti⁴⁸, S. Constantinescu^{26a}, C. Conta^{120a,120b}, G. Conti⁵⁷, F. Conventi^{103a,h}, M. Cooke¹⁵, B.D. Cooper⁷⁷, A.M. Cooper-Sarkar¹¹⁹, N.J. Cooper-Smith⁷⁶, K. Copic¹⁵, T. Cornelissen¹⁷⁶, M. Corradi^{20a}, F. Corriveau^{86,i}, A. Corso-Radu¹⁶⁴, A. Cortes-Gonzalez¹², G. Cortiana¹⁰⁰, G. Costa^{90a}, M.J. Costa¹⁶⁸, D. Costanzo¹⁴⁰, D. Côté⁸, G. Cottin²⁸, G. Cowan⁷⁶, B.E. Cox⁸³, K. Cranmer¹⁰⁹, G. Cree²⁹, S. Crépe-Renaudin⁵⁵, F. Crescioli⁷⁹, M. Crispin Ortuzar¹¹⁹, M. Cristinziani²¹, V. Croft¹⁰⁵, G. Crosetti^{37a,37b}, C.-M. Cuciuc^{26a}, C. Cuenca Almenar¹⁷⁷, T. Cuhadar Donszelmann¹⁴⁰, J. Cummings¹⁷⁷, M. Curatolo⁴⁷, C. Cuthbert¹⁵¹, H. Czirr¹⁴², P. Czodrowski³, Z. Czyczula¹⁷⁷, S. D'Auria⁵³, M. D'Onofrio⁷³, M.J. Da Cunha Sargedas De Sousa^{125a,125b}, C. Da Via⁸³, W. Dabrowski^{38a}, A. Dafinca¹¹⁹, T. Dai⁸⁸, O. Dale¹⁴, F. Dallahire⁹⁴, C. Dallapiccola⁸⁵, M. Dam³⁶, A.C. Daniells¹⁸, M. Dano Hoffmann¹³⁷, V. Dao¹⁰⁵, G. Darbo^{50a}, G.L. Darlea^{26c}, S. Darmora⁸, J.A. Dassoulas⁴², A. Dattagupta⁶⁰, W. Davey²¹, C. David¹⁷⁰, T. Davidek¹²⁸, E. Davies^{119,c}, M. Davies¹⁵⁴, O. Davignon⁷⁹, A.R. Davison⁷⁷, P. Davison⁷⁷, Y. Davygora^{58a}, E. Dawe¹⁴³, I. Dawson¹⁴⁰, R.K. Daya-Ishmukhametova²³, K. De⁸, R. de Asmundis^{103a}, S. De Castro^{20a,20b}, S. De Cecco⁷⁹, J. de Graat⁹⁹, N. De Groot¹⁰⁵, P. de Jong¹⁰⁶, H. De la Torre⁸¹, F. De Lorenzi⁶³, L. De Nooij¹⁰⁶, D. De Pedis^{133a}, A. De Salvo^{133a}, U. De Sanctis^{165a,165b}, A. De Santo¹⁵⁰, J.B. De Vivie De Regie¹¹⁶, G. De Zorzi^{133a,133b}, W.J. Dearnaley⁷¹, R. Debbé²⁵, C. Debenedetti⁴⁶, B. Dechenaux⁵⁵, D.V. Dedovich⁶⁴, J. Degenhardt¹²¹, I. Deigaard¹⁰⁶, J. Del Peso⁸¹, T. Del Prete^{123a,123b}, F. Deliot¹³⁷, C.M. Delitzsch⁴⁹, M. Deliyergiyev⁷⁴, A. Dell'Acqua³⁰, L. Dell'Asta²², M. Dell'Orso^{123a,123b}, M. Della Pietra^{103a,h}, D. della Volpe⁴⁹, M. Delmastro⁵, P.A. Delsart⁵⁵, C. Deluca¹⁰⁶, S. Demers¹⁷⁷, M. Demichev⁶⁴, A. Demilly⁷⁹, S.P. Denisov¹²⁹, D. Derendarz³⁹, J.E. Derkaoui^{136d}, F. Derue⁷⁹, P. Dervan⁷³, K. Desch²¹, C. Deterre⁴², P.O. Deviveiros¹⁰⁶, A. Dewhurst¹³⁰, S. Dhaliwal¹⁰⁶, A. Di Ciaccio^{134a,134b}, L. Di Ciaccio⁵, A. Di Domenico^{133a,133b}, C. Di Donato^{103a,103b}, A. Di Girolamo³⁰, B. Di Girolamo³⁰, A. Di Mattia¹⁵³, B. Di Micco^{135a,135b}, R. Di Nardo⁴⁷, A. Di Simone⁴⁸, R. Di Sipio^{20a,20b}, D. Di Valentino²⁹, M.A. Diaz^{32a}, E.B. Diehl⁸⁸, J. Dietrich⁴², T.A. Dietzsch^{58a}, S. Diglio⁸⁴, A. Dimitrievska^{13a}, J. Dingfelder²¹, C. Dionisi^{133a,133b}, P. Dita^{26a}, S. Dita^{26a}, F. Dittus³⁰, F. Djama⁸⁴, T. Djobava^{51b}, M.A.B. do Vale^{24c}, A. Do Valle Wemans^{125a,125g}, T.K.O. Doan⁵, D. Dobos³⁰, E. Dobson⁷⁷, C. Doglioni⁴⁹, T. Doherty⁵³, T. Dohmae¹⁵⁶, J. Dolejsi¹²⁸, Z. Dolezal¹²⁸, B.A. Dolgoshein^{97,*}, M. Donadelli^{24d}, S. Donati^{123a,123b}, P. Dondero^{120a,120b}, J. Donini³⁴, J. Dopke³⁰, A. Doria^{103a}, A. Dos Anjos¹⁷⁴, M.T. Dova⁷⁰, A.T. Doyle⁵³, M. Dris¹⁰, J. Dubbert⁸⁸, S. Dube¹⁵, E. Dubreuil³⁴, E. Duchovni¹⁷³, G. Duckeck⁹⁹, O.A. Ducu^{26a}, D. Duda¹⁷⁶, A. Dudarev³⁰, F. Dudziak⁶³, L. Dufflot¹¹⁶, L. Duguid⁷⁶, M. Dührssen³⁰, M. Dunford^{58a}, H. Duran Yildiz^{4a}, M. Düren⁵², A. Durglishvili^{51b}, M. Dwuznik^{38a}, M. Dyndal^{38a}, J. Ebke⁹⁹, W. Edson², N.C. Edwards⁴⁶, W. Ehrenfeld²¹, T. Eifert¹⁴⁴, G. Eigen¹⁴, K. Einsweiler¹⁵, T. Ekelof¹⁶⁷, M. El Kacimi^{136c}, M. Ellert¹⁶⁷, S. Elles⁵, F. Ellinghaus⁸², N. Ellis³⁰, J. Elmsheuser⁹⁹, M. Elsing³⁰, D. Emel'yanov¹³⁰, Y. Enari¹⁵⁶, O.C. Endner⁸², M. Endo¹¹⁷, R. Engelmann¹⁴⁹, J. Erdmann¹⁷⁷, A. Ereditato¹⁷, D. Eriksson^{147a}, G. Ernis¹⁷⁶, J. Ernst², M. Ernst²⁵, J. Ernwein¹³⁷, D. Errede¹⁶⁶, S. Errede¹⁶⁶, E. Ertel⁸², M. Escalier¹¹⁶, H. Esch⁴³, C. Escobar¹²⁴, B. Esposito⁴⁷, A.I. Etienvre¹³⁷, E. Etzion¹⁵⁴, H. Evans⁶⁰, L. Fabbri^{20a,20b}, G. Facini³⁰, R.M. Fakhruddinov¹²⁹, S. Falciano^{133a}, Y. Fang^{33a}, M. Fantini^{90a,90b}, A. Farbin⁸, A. Farilla^{135a}, T. Farooque¹², S. Farrell¹⁶⁴, S.M. Farrington¹⁷¹, P. Farthouat³⁰, F. Fassi¹⁶⁸, P. Fassnacht³⁰, D. Fassouliotis⁹, A. Favareto^{50a,50b}, L. Fayard¹¹⁶, P. Federic^{145a}, O.L. Fedin¹²², W. Fedorko¹⁶⁹, M. Fehling-Kaschek⁴⁸, S. Feigl³⁰, L. Feligioni⁸⁴, C. Feng^{33d}, E.J. Feng⁶, H. Feng⁸⁸, A.B. Fenyuk¹²⁹, S. Fernandez Perez³⁰, S. Ferrag⁵³, J. Ferrando⁵³, A. Ferrari¹⁶⁷, P. Ferrari¹⁰⁶, R. Ferrari^{120a}, D.E. Ferreira de Lima⁵³, A. Ferrer¹⁶⁸, D. Ferrere⁴⁹, C. Ferretti⁸⁸,

A. Ferretto Parodi^{50a,50b}, M. Fiascaris³¹, F. Fiedler⁸², A. Filipčić⁷⁴, M. Filipuzzi⁴², F. Filthaut¹⁰⁵,
 M. Fincke-Keeler¹⁷⁰, K.D. Finelli¹⁵¹, M.C.N. Fiolhais^{125a,125c}, L. Fiorini¹⁶⁸, A. Firan⁴⁰, J. Fischer¹⁷⁶,
 W.C. Fisher⁸⁹, E.A. Fitzgerald²³, M. Flechl⁴⁸, I. Fleck¹⁴², P. Fleischmann¹⁷⁵, S. Fleischmann¹⁷⁶, G.T. Fletcher¹⁴⁰,
 G. Fletcher⁷⁵, T. Flick¹⁷⁶, A. Floderus⁸⁰, L.R. Flores Castillo¹⁷⁴, A.C. Florez Bustos^{160b}, M.J. Flowerdew¹⁰⁰,
 A. Formica¹³⁷, A. Forti⁸³, D. Fortin^{160a}, D. Fournier¹¹⁶, H. Fox⁷¹, S. Fracchia¹², P. Francavilla⁷⁹,
 M. Franchini^{20a,20b}, S. Franchino³⁰, D. Francis³⁰, M. Franklin⁵⁷, S. Franz⁶¹, M. Fraternali^{120a,120b}, S.T. French²⁸,
 C. Friedrich⁴², F. Friedrich⁴⁴, D. Froidevaux³⁰, J.A. Frost²⁸, C. Fukunaga¹⁵⁷, E. Fullana Torregrosa⁸²,
 B.G. Fulsom¹⁴⁴, J. Fuster¹⁶⁸, C. Gabaldon⁵⁵, O. Gabizon¹⁷³, A. Gabrielli^{20a,20b}, A. Gabrielli^{133a,133b},
 S. Gadatsch¹⁰⁶, S. Gadomski⁴⁹, G. Gagliardi^{50a,50b}, P. Gagnon⁶⁰, C. Galea¹⁰⁵, B. Galhardo^{125a,125c}, E.J. Gallas¹¹⁹,
 V. Gallo¹⁷, B.J. Gallop¹³⁰, P. Gallus¹²⁷, G. Galster³⁶, K.K. Gan¹¹⁰, R.P. Gandrajula⁶², J. Gao^{33b,g}, Y.S. Gao^{144,e},
 F.M. Garay Walls⁴⁶, F. Garberson¹⁷⁷, C. García¹⁶⁸, J.E. García Navarro¹⁶⁸, M. Garcia-Sciveres¹⁵, R.W. Gardner³¹,
 N. Garelli¹⁴⁴, V. Garonne³⁰, C. Gatti⁴⁷, G. Gaudio^{120a}, B. Gaur¹⁴², L. Gauthier⁹⁴, P. Gauzzi^{133a,133b},
 I.L. Gavrilenko⁹⁵, C. Gay¹⁶⁹, G. Gaycken²¹, E.N. Gazis¹⁰, P. Ge^{33d}, Z. Gecse¹⁶⁹, C.N.P. Gee¹³⁰, D.A.A. Geerts¹⁰⁶,
 Ch. Geich-Gimbel²¹, K. Gellerstedt^{147a,147b}, C. Gemme^{50a}, A. Gemmell⁵³, M.H. Genest⁵⁵, S. Gentile^{133a,133b},
 M. George⁵⁴, S. George⁷⁶, D. Gerbaudo¹⁶⁴, A. Gershon¹⁵⁴, H. Ghazlane^{136b}, N. Ghodbane³⁴, B. Giacobbe^{20a},
 S. Giagu^{133a,133b}, V. Giangiobbe¹², P. Giannetti^{123a,123b}, F. Gianotti³⁰, B. Gibbard²⁵, S.M. Gibson⁷⁶,
 M. Gilchiese¹⁵, T.P.S. Gillam²⁸, D. Gillberg³⁰, G. Gilles³⁴, D.M. Gingrich^{3,d}, N. Giokaris⁹, M.P. Giordani^{165a,165c},
 R. Giordano^{103a,103b}, F.M. Giorgi¹⁶, P.F. Giraud¹³⁷, D. Giugni^{90a}, C. Giuliani⁴⁸, M. Giulini^{58b}, B.K. Gjelsten¹¹⁸,
 I. Gkialas^{155,j}, L.K. Gladilin⁹⁸, C. Glasman⁸¹, J. Glatzer³⁰, P.C.F. Glaysheer⁴⁶, A. Glazov⁴², G.L. Glonti⁶⁴,
 M. Goblirsch-Kolb¹⁰⁰, J.R. Goddard⁷⁵, J. Godfrey¹⁴³, J. Godlewski³⁰, C. Goeringer⁸², S. Goldfarb⁸⁸, T. Golling¹⁷⁷,
 D. Golubkov¹²⁹, A. Gomes^{125a,125b,125d}, L.S. Gomez Fajardo⁴², R. Gonçalo^{125a},
 J. Goncalves Pinto Firmino Da Costa⁴², L. Gonella²¹, S. González de la Hoz¹⁶⁸, G. Gonzalez Parra¹²,
 M.L. Gonzalez Silva²⁷, S. Gonzalez-Sevilla⁴⁹, L. Goossens³⁰, P.A. Gorbounov⁹⁶, H.A. Gordon²⁵, I. Gorelov¹⁰⁴,
 G. Gorfine¹⁷⁶, B. Gorini³⁰, E. Gorini^{72a,72b}, A. Gorišek⁷⁴, E. Gornicki³⁹, A.T. Goshaw⁶, C. Gössling⁴³,
 M.I. Gostkin⁶⁴, M. Gouighri^{136a}, D. Goujdami^{136c}, M.P. Goulette⁴⁹, A.G. Goussiou¹³⁹, C. Goy⁵, S. Gozpinar²³,
 H.M.X. Grabas¹³⁷, L. Graber⁵⁴, I. Grabowska-Bold^{38a}, P. Grafström^{20a,20b}, K.-J. Grahn⁴², J. Gramling⁴⁹,
 E. Gramstad¹¹⁸, S. Grancagnolo¹⁶, V. Grassi¹⁴⁹, V. Gratchev¹²², H.M. Gray³⁰, E. Graziani^{135a}, O.G. Grebenyuk¹²²,
 Z.D. Greenwood^{78,k}, K. Gregersen⁷⁷, I.M. Gregor⁴², P. Grenier¹⁴⁴, J. Griffiths⁸, N. Grigalashvili⁶⁴, A.A. Grillo¹³⁸,
 K. Grimm⁷¹, S. Grinstein^{12,l}, Ph. Gris³⁴, Y.V. Grishkevich⁹⁸, J.-F. Grivaz¹¹⁶, J.P. Grohs⁴⁴, A. Grohsjean⁴²,
 E. Gross¹⁷³, J. Grosse-Knetter⁵⁴, G.C. Grossi^{134a,134b}, J. Groth-Jensen¹⁷³, Z.J. Grout¹⁵⁰, K. Grybel¹⁴², L. Guan^{33b},
 F. Guescini⁴⁹, D. Guest¹⁷⁷, O. Gueta¹⁵⁴, C. Guicheney³⁴, E. Guido^{50a,50b}, T. Guillemin¹¹⁶, S. Guindon², U. Gul⁵³,
 C. Gumpert⁴⁴, J. Gunther¹²⁷, J. Guo³⁵, S. Gupta¹¹⁹, P. Gutierrez¹¹², N.G. Gutierrez Ortiz⁵³, C. Gutsche⁷⁷,
 N. Guttman¹⁵⁴, C. Guyot¹³⁷, C. Gwenlan¹¹⁹, C.B. Gwilliam⁷³, A. Haas¹⁰⁹, C. Haber¹⁵, H.K. Hadavand⁸,
 N. Haddad^{136e}, P. Haefner²¹, S. Hageboeck²¹, Z. Hajduk³⁹, H. Hakobyan¹⁷⁸, M. Haleem⁴², D. Hall¹¹⁹,
 G. Halladjian⁸⁹, K. Hamacher¹⁷⁶, P. Hamal¹¹⁴, K. Hamano⁸⁷, M. Hamer⁵⁴, A. Hamilton^{146a}, S. Hamilton¹⁶²,
 P.G. Hamnett⁴², L. Han^{33b}, K. Hanagaki¹¹⁷, K. Hanawa¹⁵⁶, M. Hance¹⁵, P. Hanke^{58a}, J.R. Hansen³⁶,
 J.B. Hansen³⁶, J.D. Hansen³⁶, P.H. Hansen³⁶, K. Hara¹⁶¹, A.S. Hard¹⁷⁴, T. Harenberg¹⁷⁶, S. Harkusha⁹¹,
 D. Harper⁸⁸, R.D. Harrington⁴⁶, O.M. Harris¹³⁹, P.F. Harrison¹⁷¹, F. Hartjes¹⁰⁶, S. Hasegawa¹⁰², Y. Hasegawa¹⁴¹,
 A. Hasib¹¹², S. Hassani¹³⁷, S. Haug¹⁷, M. Hauschild³⁰, R. Hauser⁸⁹, M. Havranek¹²⁶, C.M. Hawkes¹⁸,
 R.J. Hawkings³⁰, A.D. Hawkins⁸⁰, T. Hayashi¹⁶¹, D. Hayden⁸⁹, C.P. Hays¹¹⁹, H.S. Hayward⁷³, S.J. Haywood¹³⁰,
 S.J. Head¹⁸, T. Heck⁸², V. Hedberg⁸⁰, L. Heelan⁸, S. Heim¹²¹, T. Heim¹⁷⁶, B. Heinemann¹⁵, L. Heinrich¹⁰⁹,
 S. Heisterkamp³⁶, J. Hejbal¹²⁶, L. Helary²², C. Heller⁹⁹, M. Heller³⁰, S. Hellman^{147a,147b}, D. Hellmich²¹,
 C. Helsen³⁰, J. Henderson¹¹⁹, R.C.W. Henderson⁷¹, C. Hengler⁴², A. Henrichs¹⁷⁷, A.M. Henriques Correia³⁰,
 S. Henrot-Versille¹¹⁶, C. Hensel⁵⁴, G.H. Herbert¹⁶, Y. Hernández Jiménez¹⁶⁸, R. Herrberg-Schubert¹⁶, G. Hertel⁴⁸,
 R. Hertenberger⁹⁹, L. Hervas³⁰, G.G. Hesketh⁷⁷, N.P. Hesse¹⁰⁶, R. Hickling⁷⁵, E. Higón-Rodríguez¹⁶⁸, J.C. Hill²⁸,
 K.H. Hiller⁴², S. Hillert²¹, S.J. Hillier¹⁸, I. Hinchliffe¹⁵, E. Hines¹²¹, M. Hirose¹¹⁷, D. Hirschbuehl¹⁷⁶, J. Hobbs¹⁴⁹,
 N. Hod¹⁰⁶, M.C. Hodgkinson¹⁴⁰, P. Hodgson¹⁴⁰, A. Hoecker³⁰, M.R. Hoefkamp¹⁰⁴, J. Hoffman⁴⁰, D. Hoffmann⁸⁴,
 J.I. Hofmann^{58a}, M. Hohlfeld⁸², T.R. Holmes¹⁵, T.M. Hong¹²¹, L. Hooft van Huysduyven¹⁰⁹, J.-Y. Hostachy⁵⁵,
 S. Hou¹⁵², A. Hoummada^{136a}, J. Howard¹¹⁹, J. Howarth⁴², M. Hrabovsky¹¹⁴, I. Hristova¹⁶, J. Hrivnac¹¹⁶,
 T. Hryn'ova⁵, P.J. Hsu⁸², S.-C. Hsu¹³⁹, D. Hu³⁵, X. Hu²⁵, Y. Huang⁴², Z. Hubacek³⁰, F. Hubaut⁸⁴, F. Huegging²¹,
 T.B. Huffman¹¹⁹, E.W. Hughes³⁵, G. Hughes⁷¹, M. Huhtinen³⁰, T.A. Hülsing⁸², M. Hurwitz¹⁵, N. Huseynov^{64,b},
 J. Huston⁸⁹, J. Huth⁵⁷, G. Iacobucci⁴⁹, G. Iakovidis¹⁰, I. Ibragimov¹⁴², L. Iconomidou-Fayard¹¹⁶, J. Idarraga¹¹⁶,
 E. Ideal¹⁷⁷, P. Inengo^{103a}, O. Igonkina¹⁰⁶, T. Iizawa¹⁷², Y. Ikegami⁶⁵, K. Ikematsu¹⁴², M. Ikeno⁶⁵, D. Iliadis¹⁵⁵,
 N. Ilic¹⁵⁹, Y. Inamaru⁶⁶, T. Ince¹⁰⁰, P. Ioannou⁹, M. Iodice^{135a}, K. Iordanidou⁹, V. Ippolito⁵⁷, A. Irls Quiles¹⁶⁸,
 C. Isaksson¹⁶⁷, M. Ishino⁶⁷, M. Ishitsuka¹⁵⁸, R. Ishmukhametov¹¹⁰, C. Issever¹¹⁹, S. Istin^{19a}, J.M. Iturbe Ponce⁸³,
 J. Ivarsson⁸⁰, A.V. Ivashin¹²⁹, W. Iwanski³⁹, H. Iwasaki⁶⁵, J.M. Izen⁴¹, V. Izzo^{103a}, B. Jackson¹²¹, J.N. Jackson⁷³,
 M. Jackson⁷³, P. Jackson¹, M.R. Jaekel³⁰, V. Jain², K. Jakobs⁴⁸, S. Jakobsen³⁰, T. Jakoubek¹²⁶, J. Jakubek¹²⁷,
 D.O. Jamin¹⁵², D.K. Jana⁷⁸, E. Jansen⁷⁷, H. Jansen³⁰, J. Janssen²¹, M. Janus¹⁷¹, G. Jarlskog⁸⁰, N. Javadov^{64,b},

T. Javůrek⁴⁸, L. Jeanty¹⁵, G.-Y. Jeng¹⁵¹, D. Jennens⁸⁷, P. Jenni^{48,m}, J. Jentzsch⁴³, C. Jeske¹⁷¹, S. Jézéquel⁵, H. Ji¹⁷⁴, W. Ji⁸², J. Jia¹⁴⁹, Y. Jiang^{33b}, M. Jimenez Belenguer⁴², S. Jin^{33a}, A. Jinaru^{26a}, O. Jinnouchi¹⁵⁸, M.D. Joergensen³⁶, K.E. Johansson^{147a}, P. Johansson¹⁴⁰, K.A. Johns⁷, K. Jon-And^{147a,147b}, G. Jones¹⁷¹, R.W.L. Jones⁷¹, T.J. Jones⁷³, J. Jongmanns^{58a}, P.M. Jorge^{125a,125b}, K.D. Joshi⁸³, J. Jovicevic¹⁴⁸, X. Ju¹⁷⁴, C.A. Jung⁴³, R.M. Jungst³⁰, P. Jussel⁶¹, A. Juste Rozas^{12,l}, M. Kaci¹⁶⁸, A. Kaczmarska³⁹, M. Kado¹¹⁶, H. Kagan¹¹⁰, M. Kagan¹⁴⁴, E. Kajomovitz⁴⁵, S. Kama⁴⁰, N. Kanaya¹⁵⁶, M. Kaneda³⁰, S. Kaneti²⁸, T. Kanno¹⁵⁸, V.A. Kantserov⁹⁷, J. Kanzaki⁶⁵, B. Kaplan¹⁰⁹, A. Kapliy³¹, D. Kar⁵³, K. Karakostas¹⁰, N. Karastathis¹⁰, M. Karnevskiy⁸², S.N. Karpov⁶⁴, K. Karthik¹⁰⁹, V. Kartvelishvili⁷¹, A.N. Karyukhin¹²⁹, L. Kashif¹⁷⁴, G. Kasieczka^{58b}, R.D. Kass¹¹⁰, A. Kastanas¹⁴, Y. Kataoka¹⁵⁶, A. Katre⁴⁹, J. Katzy⁴², V. Kaushik⁷, K. Kawagoe⁶⁹, T. Kawamoto¹⁵⁶, G. Kawamura⁵⁴, S. Kazama¹⁵⁶, V.F. Kazanin¹⁰⁸, M.Y. Kazarinov⁶⁴, R. Keeler¹⁷⁰, P.T. Keener¹²¹, R. Kehoe⁴⁰, M. Keil⁵⁴, J.S. Keller⁴², H. Keoshkerian⁵, O. Kepka¹²⁶, B.P. Kerševan⁷⁴, S. Kersten¹⁷⁶, K. Kessoku¹⁵⁶, J. Keung¹⁵⁹, F. Khalil-zada¹¹, H. Khandanyan^{147a,147b}, A. Khanov¹¹³, A. Khodinov⁹⁷, A. Khomich^{58a}, T.J. Khoo²⁸, G. Khoriauli²¹, A. Khoroshilov¹⁷⁶, V. Khovanskii⁹⁶, E. Khramov⁶⁴, J. Khubua^{51b}, H.Y. Kim⁸, H. Kim^{147a,147b}, S.H. Kim¹⁶¹, N. Kimura¹⁷², O. Kind¹⁶, B.T. King⁷³, M. King¹⁶⁸, R.S.B. King¹¹⁹, S.B. King¹⁶⁹, J. Kirk¹³⁰, A.E. Kiryunin¹⁰⁰, T. Kishimoto⁶⁶, D. Kisielewska^{38a}, F. Kiss⁴⁸, T. Kitamura⁶⁶, T. Kittelmann¹²⁴, K. Kiuchi¹⁶¹, E. Kladiva^{145b}, M. Klein⁷³, U. Klein⁷³, K. Kleinknecht⁸², P. Klimek^{147a,147b}, A. Klimentov²⁵, R. Klingenberg⁴³, J.A. Klinger⁸³, T. Klioutchnikova³⁰, P.F. Klok¹⁰⁵, E.-E. Kluge^{58a}, P. Kluit¹⁰⁶, S. Kluth¹⁰⁰, E. Kneringer⁶¹, E.B.F.G. Knoops⁸⁴, A. Knue⁵³, T. Kobayashi¹⁵⁶, M. Kobel⁴⁴, M. Kocian¹⁴⁴, P. Kodys¹²⁸, P. Koevesarki²¹, T. Koffas²⁹, E. Koffeman¹⁰⁶, L.A. Kogan¹¹⁹, S. Kohlmann¹⁷⁶, Z. Kohout¹²⁷, T. Kohriki⁶⁵, T. Koi¹⁴⁴, H. Kolanoski¹⁶, I. Koletsou⁵, J. Koll⁸⁹, A.A. Komar^{95,*}, Y. Komori¹⁵⁶, T. Kondo⁶⁵, N. Kondrashova⁴², K. Köneke⁴⁸, A.C. König¹⁰⁵, S. König⁸², T. Kono^{65,n}, R. Konoplich^{109,o}, N. Konstantinidis⁷⁷, R. Kopeliansky¹⁵³, S. Koperny^{38a}, L. Köpke⁸², A.K. Kopp⁴⁸, K. Korcyl³⁹, K. Kordas¹⁵⁵, A. Korn⁷⁷, A.A. Korol¹⁰⁸, I. Korolkov¹², E.V. Korolkova¹⁴⁰, V.A. Korotkov¹²⁹, O. Kortner¹⁰⁰, S. Kortner¹⁰⁰, V.V. Kostyukhin²¹, S. Kotov¹⁰⁰, V.M. Kotov⁶⁴, A. Kotwal⁴⁵, C. Kourkoumelis⁹, V. Kouskoura¹⁵⁵, A. Koutsman^{160a}, R. Kowalewski¹⁷⁰, T.Z. Kowalski^{38a}, W. Kozanecki¹³⁷, A.S. Kozhin¹²⁹, V. Kral¹²⁷, V.A. Kramarenko⁹⁸, G. Kramberger⁷⁴, D. Krasnopevtsev⁹⁷, M.W. Krasny⁷⁹, A. Krasznahorkay³⁰, J.K. Kraus²¹, A. Kravchenko²⁵, S. Kreiss¹⁰⁹, M. Kretz^{58c}, J. Kretzschmar⁷³, K. Kreutzfeldt⁵², P. Krieger¹⁵⁹, K. Kroeninger⁵⁴, H. Kroha¹⁰⁰, J. Kroll¹²¹, J. Kroseberg²¹, J. Krstic^{13a}, U. Kruchonak⁶⁴, H. Krüger²¹, T. Kruker¹⁷, N. Krumnack⁶³, Z.V. Krumshteyn⁶⁴, A. Kruse¹⁷⁴, M.C. Kruse⁴⁵, M. Kruschal²², T. Kubota⁸⁷, S. Kudah^{4a}, S. Kuehn⁴⁸, A. Kugel^{58c}, A. Kuhl¹³⁸, T. Kuhl⁴², V. Kukhtin⁶⁴, Y. Kulchitsky⁹¹, S. Kuleshov^{32b}, M. Kuna^{133a,133b}, J. Kunkle¹²¹, A. Kupco¹²⁶, H. Kurashige⁶⁶, Y.A. Kurochkin⁹¹, R. Kurumida⁶⁶, V. Kus¹²⁶, E.S. Kuwertz¹⁴⁸, M. Kuze¹⁵⁸, J. Kvita¹¹⁴, A. La Rosa⁴⁹, L. La Rotonda^{37a,37b}, C. Lacasta¹⁶⁸, F. Lacava^{133a,133b}, J. Lacey²⁹, H. Lacker¹⁶, D. Lacour⁷⁹, V.R. Lacuesta¹⁶⁸, E. Ladygin⁶⁴, R. Lafaye⁵, B. Laforge⁷⁹, T. Lagouri¹⁷⁷, S. Lai⁴⁸, H. Laier^{58a}, L. Lambourne⁷⁷, S. Lammers⁶⁰, C.L. Lampen⁷, W. Lampl⁷, E. Lançon¹³⁷, U. Landgraf⁴⁸, M.P.J. Landon⁷⁵, V.S. Lang^{58a}, C. Lange⁴², A.J. Lankford¹⁶⁴, F. Lanni²⁵, K. Lantzsck³⁰, A. Lanza^{120a}, S. Laplace⁷⁹, C. Lapoire²¹, J.F. Laporte¹³⁷, T. Lari^{90a}, M. Lassnig³⁰, P. Laurelli⁴⁷, W. Lavrijsen¹⁵, A.T. Law¹³⁸, P. Laycock⁷³, B.T. Le⁵⁵, O. Le Dortz⁷⁹, E. Le Guirriec⁸⁴, E. Le Menedeu¹², T. LeCompte⁶, F. Ledroit-Guillon⁵⁵, C.A. Lee¹⁵², H. Lee¹⁰⁶, J.S.H. Lee¹¹⁷, S.C. Lee¹⁵², L. Lee¹⁷⁷, G. Lefebvre⁷⁹, M. Lefebvre¹⁷⁰, F. Legger⁹⁹, C. Leggett¹⁵, A. Lehan⁷³, M. Lehmacher²¹, G. Lehmann Miotto³⁰, X. Lei⁷, A.G. Leister¹⁷⁷, M.A.L. Leite^{24d}, R. Leitner¹²⁸, D. Lellouch¹⁷³, B. Lemmer⁵⁴, K.J.C. Leney⁷⁷, T. Lenz¹⁰⁶, G. Lenzen¹⁷⁶, B. Lenzi³⁰, R. Leone⁷, K. Leonhardt⁴⁴, S. Leontsinis¹⁰, C. Leroy⁹⁴, C.G. Lester²⁸, C.M. Lester¹²¹, M. Levchenko¹²², J. Levêque⁵, D. Levin⁸⁸, L.J. Levinson¹⁷³, M. Levy¹⁸, A. Lewis¹¹⁹, G.H. Lewis¹⁰⁹, A.M. Leyko²¹, M. Leyton⁴¹, B. Li^{33b,p}, B. Li⁸⁴, H. Li¹⁴⁹, H.L. Li³¹, L. Li^{33e}, S. Li⁴⁵, Y. Li^{116,q}, Z. Liang^{119,r}, H. Liao³⁴, B. Liberti^{134a}, P. Lichard³⁰, K. Lie¹⁶⁶, J. Liebal²¹, W. Liebig¹⁴, C. Limbach²¹, A. Limosani⁸⁷, M. Limper⁶², S.C. Lin^{152,s}, F. Linde¹⁰⁶, B.E. Lindquist¹⁴⁹, J.T. Linnemann⁸⁹, E. Lipeles¹²¹, A. Lipniacka¹⁴, M. Lisovsky⁴², T.M. Liss¹⁶⁶, D. Lissauer²⁵, A. Lister¹⁶⁹, A.M. Litke¹³⁸, B. Liu¹⁵², D. Liu¹⁵², J.B. Liu^{33b}, K. Liu^{33b,t}, L. Liu⁸⁸, M. Liu⁴⁵, M. Liu^{33b}, Y. Liu^{33b}, M. Livan^{120a,120b}, S.S.A. Livermore¹¹⁹, A. Lleres⁵⁵, J. Llorente Merino⁸¹, S.L. Lloyd⁷⁵, F. Lo Sterzo¹⁵², E. Lobodzinska⁴², P. Loch⁷, W.S. Lockman¹³⁸, T. Loddenkoetter²¹, F.K. Loebinger⁸³, A.E. Loevschall-Jensen³⁶, A. Loginov¹⁷⁷, C.W. Loh¹⁶⁹, T. Lohse¹⁶, K. Lohwasser⁴⁸, M. Lokajicek¹²⁶, V.P. Lombardo⁵, B.A. Long²², J.D. Long⁸⁸, R.E. Long⁷¹, L. Lopes^{125a}, D. Lopez Mateos⁵⁷, B. Lopez Paredes¹⁴⁰, J. Lorenz⁹⁹, N. Lorenzo Martinez⁶⁰, M. Losada¹⁶³, P. Loscutoff¹⁵, X. Lou⁴¹, A. Lounis¹¹⁶, J. Love⁶, P.A. Love⁷¹, A.J. Lowe^{144,e}, F. Lu^{33a}, H.J. Lubatti¹³⁹, C. Luci^{133a,133b}, A. Lucotte⁵⁵, F. Luehring⁶⁰, W. Lukas⁶¹, L. Luminari^{133a}, O. Lundberg^{147a,147b}, B. Lund-Jensen¹⁴⁸, M. Lungwitz⁸², D. Lynn²⁵, R. Lysak¹²⁶, E. Lytken⁸⁰, H. Ma²⁵, L.L. Ma^{33d}, G. Maccarrone⁴⁷, A. Macchiolo¹⁰⁰, J. Machado Miguens^{125a,125b}, D. Macina³⁰, D. Madaffari⁸⁴, R. Madar⁴⁸, H.J. Maddocks⁷¹, W.F. Mader⁴⁴, A. Madsen¹⁶⁷, M. Maeno⁸, T. Maeno²⁵, E. Magradze⁵⁴, K. Mahboubi⁴⁸, J. Mahlstedt¹⁰⁶, S. Mahmoud⁷³, C. Maiani¹³⁷, C. Maidantchik^{24a}, A. Maio^{125a,125b,125d}, S. Majewski¹¹⁵, Y. Makida⁶⁵, N. Makovec¹¹⁶, P. Mal^{137,u}, B. Malaescu⁷⁹, Pa. Malecki³⁹, V.P. Maleev¹²², F. Malek⁵⁵, U. Mallik⁶², D. Malon⁶, C. Malone¹⁴⁴, S. Maltezos¹⁰, V.M. Malyshev¹⁰⁸, S. Malyukov³⁰, J. Mamuzic^{13b}, B. Mandelli³⁰, L. Mandelli^{90a}, I. Mandić⁷⁴, R. Mandrysch⁶², J. Maneira^{125a,125b}, A. Manfredini¹⁰⁰,

L. Manhaes de Andrade Filho^{24b}, J.A. Manjarres Ramos^{160b}, A. Mann⁹⁹, P.M. Manning¹³⁸,
A. Manousakis-Katsikakis⁹, B. Mansoulie¹³⁷, R. Mantifel⁸⁶, L. Mapelli³⁰, L. March¹⁶⁸, J.F. Marchand²⁹,
G. Marchiori⁷⁹, M. Marcisovsky¹²⁶, C.P. Marino¹⁷⁰, C.N. Marques^{125a}, F. Marroquin^{24a}, S.P. Marsden⁸³,
Z. Marshall¹⁵, L.F. Marti¹⁷, S. Marti-Garcia¹⁶⁸, B. Martin³⁰, B. Martin⁸⁹, J.P. Martin⁹⁴, T.A. Martin¹⁷¹,
V.J. Martin⁴⁶, B. Martin dit Latour¹⁴, H. Martinez¹³⁷, M. Martinez^{12,l}, S. Martin-Haugh¹³⁰, A.C. Martyniuk⁷⁷,
M. Marx¹³⁹, F. Marzano^{133a}, A. Marzin³⁰, L. Masetti⁸², T. Mashimo¹⁵⁶, R. Mashinistov⁹⁵, J. Masik⁸³,
A.L. Maslennikov¹⁰⁸, I. Massa^{20a,20b}, N. Massol⁵, P. Mastrandrea¹⁴⁹, A. Mastroberardino^{37a,37b}, T. Masubuchi¹⁵⁶,
P. Matricon¹¹⁶, H. Matsunaga¹⁵⁶, T. Matsushita⁶⁶, P. Mättig¹⁷⁶, S. Mättig⁴², J. Mattmann⁸², J. Maurer^{26a},
S.J. Maxfield⁷³, D.A. Maximov^{108,f}, R. Mazini¹⁵², L. Mazzaferro^{134a,134b}, G. Mc Goldrick¹⁵⁹, S.P. Mc Kee⁸⁸,
A. McCarn⁸⁸, R.L. McCarthy¹⁴⁹, T.G. McCarthy²⁹, N.A. McCubbin¹³⁰, K.W. McFarlane^{56,*}, J.A. Mcfayden⁷⁷,
G. Mchedlidge⁵⁴, T. McLaughlan¹⁸, S.J. McMahon¹³⁰, R.A. McPherson^{170,i}, A. Meade⁸⁵, J. Mechnich¹⁰⁶,
M. Medinnis⁴², S. Meehan³¹, S. Mehlhase³⁶, A. Mehta⁷³, K. Meier^{58a}, C. Meineck⁹⁹, B. Meirose⁸⁰, C. Melachrinis³¹,
B.R. Mellado Garcia^{146c}, F. Meloni^{90a,90b}, A. Mengarelli^{20a,20b}, S. Menke¹⁰⁰, E. Meoni¹⁶², K.M. Mercurio⁵⁷,
S. Mergelmeyer²¹, N. Meric¹³⁷, P. Mermod⁴⁹, L. Merola^{103a,103b}, C. Meroni^{90a}, F.S. Merritt³¹, H. Merritt¹¹⁰,
A. Messina^{30,v}, J. Metcalfe²⁵, A.S. Mete¹⁶⁴, C. Meyer⁸², C. Meyer³¹, J-P. Meyer¹³⁷, J. Meyer³⁰, R.P. Middleton¹³⁰,
S. Migas⁷³, L. Mijović¹³⁷, G. Mikenberg¹⁷³, M. Migestikova¹²⁶, M. Mikuz⁷⁴, D.W. Miller³¹, C. Mills⁴⁶, A. Milov¹⁷³,
D.A. Milstead^{147a,147b}, D. Milstein¹⁷³, A.A. Minaenko¹²⁹, M. Miñano Moya¹⁶⁸, I.A. Minashvili⁶⁴, A.I. Mincer¹⁰⁹,
B. Mindur^{38a}, M. Mineev⁶⁴, Y. Ming¹⁷⁴, L.M. Mir¹², G. Mirabelli^{133a}, T. Mitani¹⁷², J. Mitrevski⁹⁹, V.A. Mitsou¹⁶⁸,
S. Mitsui⁶⁵, A. Miucci⁴⁹, P.S. Miyagawa¹⁴⁰, J.U. Mjörnmark⁸⁰, T. Moa^{147a,147b}, K. Mochizuki⁸⁴, V. Moeller²⁸,
S. Mohapatra³⁵, W. Mohr⁴⁸, S. Molander^{147a,147b}, R. Moles-Valls¹⁶⁸, K. Mönig⁴², C. Monini⁵⁵, J. Monk³⁶,
E. Monnier⁸⁴, J. Montejo Berlingen¹², F. Monticelli⁷⁰, S. Monzani^{133a,133b}, R.W. Moore³, A. Moraes⁵³,
N. Morange⁶², J. Morel⁵⁴, D. Moreno⁸², M. Moreno Llácer⁵⁴, P. Moretini^{50a}, M. Morgenstern⁴⁴, M. Morii⁵⁷,
S. Moritz⁸², A.K. Morley¹⁴⁸, G. Mornacchi³⁰, J.D. Morris⁷⁵, L. Morvaj¹⁰², H.G. Moser¹⁰⁰, M. Mosidze^{51b},
J. Moss¹¹⁰, R. Mount¹⁴⁴, E. Mountricha²⁵, S.V. Mouraviev^{95,*}, E.J.W. Moyse⁸⁵, S.G. Muanza⁸⁴, R.D. Mudd¹⁸,
F. Mueller^{58a}, J. Mueller¹²⁴, K. Mueller²¹, T. Mueller²⁸, T. Mueller⁸², D. Muenstermann⁴⁹, Y. Munwes¹⁵⁴,
J.A. Murillo Quijada¹⁸, W.J. Murray^{171,130}, H. Musheghyan⁵⁴, E. Musto¹⁵³, A.G. Myagkov^{129,w}, M. Myska¹²⁷,
O. Nackenhorst⁵⁴, J. Nadal⁵⁴, K. Nagai⁶¹, R. Nagai¹⁵⁸, Y. Nagai⁸⁴, K. Nagano⁶⁵, A. Nagarkar¹¹⁰, Y. Nagasaka⁵⁹,
M. Nagel¹⁰⁰, A.M. Nairz³⁰, Y. Nakahama³⁰, K. Nakamura⁶⁵, T. Nakamura¹⁵⁶, I. Nakano¹¹¹, H. Namasivayam⁴¹,
G. Nanava²¹, R. Narayan^{58b}, T. Nattermann²¹, T. Naumann⁴², G. Navarro¹⁶³, R. Nayyar⁷, H.A. Neal⁸⁸,
P.Yu. Nechaeva⁹⁵, T.J. Neep⁸³, A. Negri^{120a,120b}, G. Negri³⁰, M. Negrini^{20a}, S. Nektarijevic⁴⁹, A. Nelson¹⁶⁴,
T.K. Nelson¹⁴⁴, S. Nemecek¹²⁶, P. Nemethy¹⁰⁹, A.A. Nepomuceno^{24a}, M. Nessi^{30,x}, M.S. Neubauer¹⁶⁶,
M. Neumann¹⁷⁶, R.M. Neves¹⁰⁹, P. Nevski²⁵, F.M. Newcomer¹²¹, P.R. Newman¹⁸, D.H. Nguyen⁶,
R.B. Nickerson¹¹⁹, R. Nicolaidou¹³⁷, B. Nicquevert³⁰, J. Nielsen¹³⁸, N. Nikiforou³⁵, A. Nikiforov¹⁶,
V. Nikolaenko^{129,w}, I. Nikolic-Audit⁷⁹, K. Nikolics⁴⁹, K. Nikolopoulos¹⁸, P. Nilsson⁸, Y. Ninomiya¹⁵⁶, A. Nisati^{133a},
R. Nisius¹⁰⁰, T. Nobe¹⁵⁸, L. Nodulman⁶, M. Nomachi¹¹⁷, I. Nomidis¹⁵⁵, S. Norberg¹¹², M. Nordberg³⁰,
J. Novakova¹²⁸, S. Nowak¹⁰⁰, M. Nozaki⁶⁵, L. Nozka¹¹⁴, K. Ntekas¹⁰, G. Nunes Hanninger⁸⁷, T. Nunnemann⁹⁹,
E. Nurse⁷⁷, F. Nuti⁸⁷, B.J. O'Brien⁴⁶, F. O'grady⁷, D.C. O'Neil¹⁴³, V. O'Shea⁵³, F.G. Oakham^{29,d}, H. Oberlack¹⁰⁰,
T. Obermann²¹, J. Ocariz⁷⁹, A. Ochi⁶⁶, M.I. Ochoa⁷⁷, S. Oda⁶⁹, S. Odaka⁶⁵, H. Ogren⁶⁰, A. Oh⁸³, S.H. Oh⁴⁵,
C.C. Ohm³⁰, H. Ohman¹⁶⁷, T. Ohshima¹⁰², W. Okamura¹¹⁷, H. Okawa²⁵, Y. Okumura³¹, T. Okuyama¹⁵⁶,
A. Olariu^{26a}, A.G. Olchevski⁶⁴, S.A. Olivares Pino⁴⁶, D. Oliveira Damazio²⁵, E. Oliver Garcia¹⁶⁸, A. Olszewski³⁹,
J. Olszowska³⁹, A. Onofre^{125a,125e}, P.U.E. Onyisi^{31,y}, C.J. Oram^{160a}, M.J. Oreglia³¹, Y. Oren¹⁵⁴,
D. Orestano^{135a,135b}, N. Orlando^{72a,72b}, C. Oropeza Barrera⁵³, R.S. Orr¹⁵⁹, B. Osculati^{50a,50b}, R. Ospanov¹²¹,
G. Otero y Garzon²⁷, H. Otono⁶⁹, M. Ouchrif^{136d}, E.A. Ouellette¹⁷⁰, F. Ould-Saada¹¹⁸, A. Ouraou¹³⁷,
K.P. Oussoren¹⁰⁶, Q. Ouyang^{33a}, A. Ovcharova¹⁵, M. Owen⁸³, V.E. Ozcan^{19a}, N. Ozturk⁸, K. Pachal¹¹⁹,
A. Pacheco Pages¹², C. Padilla Aranda¹², M. Pagáčová⁴⁸, S. Pagan Griso¹⁵, E. Paganis¹⁴⁰, C. Pahl¹⁰⁰, F. Paige²⁵,
P. Pais⁸⁵, K. Pajchel¹¹⁸, G. Palacino^{160b}, S. Palestini³⁰, D. Pallin³⁴, A. Palma^{125a,125b}, J.D. Palmer¹⁸, Y.B. Pan¹⁷⁴,
E. Panagiotopoulou¹⁰, J.G. Panduro Vazquez⁷⁶, P. Pani¹⁰⁶, N. Panikashvili⁸⁸, S. Panitkin²⁵, D. Pantea^{26a},
L. Paolozzi^{134a,134b}, Th.D. Papadopoulou¹⁰, K. Papageorgiou^{155,j}, A. Paramonov⁶, D. Paredes Hernandez³⁴,
M.A. Parker²⁸, F. Parodi^{50a,50b}, J.A. Parsons³⁵, U. Parzefall⁴⁸, E. Pasqualucci^{133a}, S. Passaggio^{50a}, A. Passeri^{135a},
F. Pastore^{135a,135b,*}, Fr. Pastore⁷⁶, G. Pásztor^{49,z}, S. Pataria¹⁷⁶, N.D. Patel¹⁵¹, J.R. Pater⁸³, S. Patricelli^{103a,103b},
T. Pauly³⁰, J. Pearce¹⁷⁰, M. Pedersen¹¹⁸, S. Pedraza Lopez¹⁶⁸, R. Pedro^{125a,125b}, S.V. Peleganchuk¹⁰⁸,
D. Pelikan¹⁶⁷, H. Peng^{33b}, B. Penning³¹, J. Penwell⁶⁰, D.V. Perepelitsa²⁵, E. Perez Codina^{160a},
M.T. Pérez García-Estañ¹⁶⁸, V. Perez Reale³⁵, L. Perini^{90a,90b}, H. Pernegger³⁰, R. Perrino^{72a}, R. Peschke⁴²,
V.D. Peshekhonov⁶⁴, K. Peters³⁰, R.F.Y. Peters⁸³, B.A. Petersen⁸⁷, J. Petersen³⁰, T.C. Petersen³⁶, E. Petit⁴²,
A. Petridis^{147a,147b}, C. Petridou¹⁵⁵, E. Petrolo^{133a}, F. Petrucci^{135a,135b}, M. Petteni¹⁴³, N.E. Pettersson¹⁵⁸,
R. Pezoa^{32b}, P.W. Phillips¹³⁰, G. Piacquadio¹⁴⁴, E. Pianori¹⁷¹, A. Picazio⁴⁹, E. Piccaro⁷⁵, M. Piccinini^{20a,20b},
R. Piegai²⁷, D.T. Pignotti¹¹⁰, J.E. Pilcher³¹, A.D. Pilkington⁷⁷, J. Pina^{125a,125b,125d}, M. Pinamonti^{165a,165c,aa},
A. Pinder¹¹⁹, J.L. Pinfold³, A. Pingel³⁶, B. Pinto^{125a}, S. Pires⁷⁹, M. Pitt¹⁷³, C. Pizio^{90a,90b}, M.-A. Pleier²⁵,

V. Pleskot¹²⁸, E. Plotnikova⁶⁴, P. Plucinski^{147a,147b}, S. Poddar^{58a}, F. Podlyski³⁴, R. Poettgen⁸², L. Poggioli¹¹⁶, D. Pohl²¹, M. Pohl⁴⁹, G. Polesello^{120a}, A. Policicchio^{37a,37b}, R. Polifka¹⁵⁹, A. Polini^{20a}, C.S. Pollard⁴⁵, V. Polychronakos²⁵, K. Pommès³⁰, L. Pontecorvo^{133a}, B.G. Pope⁸⁹, G.A. Popeneciu^{26b}, D.S. Popovic^{13a}, A. Poppleton³⁰, X. Portell Bueso¹², G.E. Pospelov¹⁰⁰, S. Pospisil¹²⁷, K. Potamianos¹⁵, I.N. Potrap⁶⁴, C.J. Potter¹⁵⁰, C.T. Potter¹¹⁵, G. Poulard³⁰, J. Poveda⁶⁰, V. Pozdnyakov⁶⁴, P. Pralavorio⁸⁴, A. Pranko¹⁵, S. Prasad³⁰, R. Pravahan⁸, S. Prell⁶³, D. Price⁸³, J. Price⁷³, L.E. Price⁶, D. Prieur¹²⁴, M. Primavera^{72a}, M. Proissl⁴⁶, K. Prokofiev¹⁰⁹, F. Prokoshin^{32b}, E. Protopapadaki¹³⁷, S. Protopopescu²⁵, J. Proudfoot⁶, M. Przybycien^{38a}, H. Przysieszniak⁵, E. Ptacek¹¹⁵, E. Pueschel⁸⁵, D. Puldon¹⁴⁹, M. Purohit^{25,ab}, P. Puzo¹¹⁶, J. Qian⁸⁸, G. Qin⁵³, Y. Qin⁸³, A. Quadt⁵⁴, D.R. Quarrie¹⁵, W.B. Quayle^{165a,165b}, D. Quilty⁵³, A. Qureshi^{160b}, V. Radeka²⁵, V. Radescu⁴², S.K. Radhakrishnan¹⁴⁹, P. Radloff¹¹⁵, P. Rados⁸⁷, F. Ragusa^{90a,90b}, G. Rahal¹⁷⁹, S. Rajagopalan²⁵, M. Rammensee³⁰, A.S. Randle-Conde⁴⁰, C. Rangel-Smith¹⁶⁷, K. Rao¹⁶⁴, F. Rauscher⁹⁹, T.C. Rave⁴⁸, T. Ravenscroft⁵³, M. Raymond³⁰, A.L. Read¹¹⁸, D.M. Rebuffi^{120a,120b}, A. Redelbach¹⁷⁵, G. Redlinger²⁵, R. Reece¹³⁸, K. Reeves⁴¹, L. Rehnisch¹⁶, A. Reinsch¹¹⁵, H. Reisin²⁷, M. Relich¹⁶⁴, C. Rembser³⁰, Z.L. Ren¹⁵², A. Renaud¹¹⁶, M. Rescigno^{133a}, S. Resconi^{90a}, B. Resende¹³⁷, P. Reznicek¹²⁸, R. Rezvani⁹⁴, R. Richter¹⁰⁰, M. Ridel⁷⁹, P. Rieck¹⁶, M. Rijssenbeek¹⁴⁹, A. Rimoldi^{120a,120b}, L. Rinaldi^{20a}, E. Ritsch⁶¹, I. Riu¹², F. Rizatdinova¹¹³, E. Rizvi⁷⁵, S.H. Robertson^{86,i}, A. Robichaud-Veronneau¹¹⁹, D. Robinson²⁸, J.E.M. Robinson⁸³, A. Robson⁵³, C. Roda^{123a,123b}, L. Rodrigues³⁰, S. Roe³⁰, O. Röhne¹¹⁸, S. Rolli¹⁶², A. Romaniouk⁹⁷, M. Romano^{20a,20b}, G. Romeo²⁷, E. Romero Adam¹⁶⁸, N. Rompotis¹³⁹, L. Roos⁷⁹, E. Ros¹⁶⁸, S. Rosati^{133a}, K. Rosbach⁴⁹, M. Rose⁷⁶, P.L. Rosendahl¹⁴, O. Rosenthal¹⁴², V. Rossetti^{147a,147b}, E. Rossi^{103a,103b}, L.P. Rossi^{50a}, R. Rosten¹³⁹, M. Rotaru^{26a}, I. Roth¹⁷³, J. Rothberg¹³⁹, D. Rousseau¹¹⁶, C.R. Royon¹³⁷, A. Rozanov⁸⁴, Y. Rozen¹⁵³, X. Ruan^{146c}, F. Rubbo¹², I. Rubinskiy⁴², V.I. Rud⁹⁸, C. Rudolph⁴⁴, M.S. Rudolph¹⁵⁹, F. Rühr⁴⁸, A. Ruiz-Martinez³⁰, Z. Rurikova⁴⁸, N.A. Rusakovich⁶⁴, A. Ruschke⁹⁹, J.P. Rutherford⁷, N. Ruthmann⁴⁸, Y.F. Ryabov¹²², M. Rybar¹²⁸, G. Rybkin¹¹⁶, N.C. Ryder¹¹⁹, A.F. Saavedra¹⁵¹, S. Sacerdoti²⁷, A. Saddique³, I. Sadeh¹⁵⁴, H.F.-W. Sadrozinski¹³⁸, R. Sadykov⁶⁴, F. Safai Tehrani^{133a}, H. Sakamoto¹⁵⁶, Y. Sakurai¹⁷², G. Salamanna⁷⁵, A. Salamon^{134a}, M. Saleem¹¹², D. Salek¹⁰⁶, P.H. Sales De Bruin¹³⁹, D. Salihagic¹⁰⁰, A. Salmikov¹⁴⁴, J. Salt¹⁶⁸, B.M. Salvachua Ferrando⁶, D. Salvatore^{37a,37b}, F. Salvatore¹⁵⁰, A. Salvucci¹⁰⁵, A. Salzburger³⁰, D. Sampsonidis¹⁵⁵, A. Sanchez^{103a,103b}, J. Sánchez¹⁶⁸, V. Sanchez Martinez¹⁶⁸, H. Sandaker¹⁴, R.L. Sandbach⁷⁵, H.G. Sander⁸², M.P. Sanders⁹⁹, M. Sandhoff¹⁷⁶, T. Sandoval²⁸, C. Sandoval¹⁶³, R. Sandstroem¹⁰⁰, D.P.C. Sankey¹³⁰, A. Sansoni⁴⁷, C. Santoni³⁴, R. Santonic^{134a,134b}, H. Santos^{125a}, I. Santoyo Castillo¹⁵⁰, K. Sapp¹²⁴, A. Sapronov⁶⁴, J.G. Saraiva^{125a,125d}, B. Sarrazin²¹, G. Sartisohn¹⁷⁶, O. Sasaki⁶⁵, Y. Sasaki¹⁵⁶, I. Satsounkevitch⁹¹, G. Sauvage^{5,*}, E. Sauvan⁵, P. Savard^{159,d}, D.O. Savu³⁰, C. Sawyer¹¹⁹, L. Sawyer^{78,k}, D.H. Saxon⁵³, J. Saxon¹²¹, C. Sbarra^{20a}, A. Sbrizzi³, T. Scanlon³⁰, D.A. Scannicchio¹⁶⁴, M. Scarella¹⁵¹, J. Schaarschmidt¹⁷³, P. Schacht¹⁰⁰, D. Schaefer¹²¹, R. Schaefer⁴², S. Schaepe²¹, S. Schaezel^{58b}, U. Schäfer⁸², A.C. Schaffer¹¹⁶, D. Schaile⁹⁹, R.D. Schamberger¹⁴⁹, V. Scharf^{58a}, V.A. Schegelsky¹²², D. Scheirich¹²⁸, M. Schernau¹⁶⁴, M.I. Scherzer³⁵, C. Schiavi^{50a,50b}, J. Schieck⁹⁹, C. Schillo⁴⁸, M. Schioppa^{37a,37b}, S. Schlenker³⁰, E. Schmidt⁴⁸, K. Schmieden³⁰, C. Schmitt⁸², C. Schmitt⁹⁹, S. Schmitt^{58b}, B. Schneider¹⁷, Y.J. Schnellbach⁷³, U. Schnoor⁴⁴, L. Schoeffel¹³⁷, A. Schoening^{58b}, B.D. Schoenrock⁸⁹, A.L.S. Schorlemmer⁵⁴, M. Schott⁸², D. Schouten^{160a}, J. Schovancova²⁵, M. Schram⁸⁶, S. Schramm¹⁵⁹, M. Schreyer¹⁷⁵, C. Schroeder⁸², N. Schuh⁸², M.J. Schultens²¹, H.-C. Schultz-Coulon^{58a}, H. Schulz¹⁶, M. Schumacher⁴⁸, B.A. Schumm¹³⁸, Ph. Schune¹³⁷, A. Schwartzman¹⁴⁴, Ph. Schwegler¹⁰⁰, Ph. Schwemling¹³⁷, R. Schwienhorst⁸⁹, J. Schwindling¹³⁷, T. Schwindt²¹, M. Schwoerer⁵, F.G. Sciacca¹⁷, E. Scifo¹¹⁶, G. Sciolla²³, W.G. Scott¹³⁰, F. Scuri^{123a,123b}, F. Scutti²¹, J. Searcy⁸⁸, G. Sedov⁴², E. Sedykh¹²², S.C. Seidel¹⁰⁴, A. Seiden¹³⁸, F. Seifert¹²⁷, J.M. Seixas^{24a}, G. Sekhniaidze^{103a}, S.J. Sekula⁴⁰, K.E. Selbach⁴⁶, D.M. Seliverstov^{122,*}, G. Sellers⁷³, N. Semprini-Cesari^{20a,20b}, C. Serfon³⁰, L. Serin¹¹⁶, L. Serkin⁵⁴, T. Serre⁸⁴, R. Seuster^{160a}, H. Severini¹¹², F. Sforza¹⁰⁰, A. Sfyrla³⁰, E. Shabalina⁵⁴, M. Shamim¹¹⁵, L.Y. Shan^{33a}, J.T. Shank²², Q.T. Shao⁸⁷, M. Shapiro¹⁵, P.B. Shatalov⁹⁶, K. Shaw^{165a,165b}, P. Sherwood⁷⁷, S. Shimizu⁶⁶, C.O. Shimmin¹⁶⁴, M. Shimojima¹⁰¹, T. Shin⁵⁶, M. Shiyakova⁶⁴, A. Shmeleva⁹⁵, M.J. Shochet³¹, D. Short¹¹⁹, S. Shrestha⁶³, E. Shulga⁹⁷, M.A. Shupe⁷, S. Shushkevich⁴², P. Sicho¹²⁶, D. Sidorov¹¹³, A. Sidoti^{133a}, F. Siegert⁴⁴, Dj. Sijacki^{13a}, O. Silbert¹⁷³, J. Silva^{125a,125d}, Y. Silver¹⁵⁴, D. Silverstein¹⁴⁴, S.B. Silverstein^{147a}, V. Simak¹²⁷, O. Simard⁵, Lj. Simic^{13a}, S. Simion¹¹⁶, E. Simioni⁸², B. Simmons⁷⁷, R. Simoniello^{90a,90b}, M. Simonyan³⁶, P. Sinervo¹⁵⁹, N.B. Sinev¹¹⁵, V. Sipica¹⁴², G. Siragusa¹⁷⁵, A. Sircar⁷⁸, A.N. Sisakyan^{64,*}, S.Yu. Sivoklokov⁹⁸, J. Sjölin^{147a,147b}, T.B. Sjørnsen¹⁴, H.P. Skottowe⁵⁷, K.Yu. Skovpen¹⁰⁸, P. Skubic¹¹², M. Slater¹⁸, T. Slavicek¹²⁷, K. Sliwa¹⁶², V. Smakhtin¹⁷³, B.H. Smart⁴⁶, L. Smestad¹⁴, S.Yu. Smirnov⁹⁷, Y. Smirnov⁹⁷, L.N. Smirnova^{98,ac}, O. Smirnova⁸⁰, K.M. Smith⁵³, M. Smizanska⁷¹, K. Smolek¹²⁷, A.A. Snesarev⁹⁵, G. Snidero⁷⁵, J. Snow¹¹², S. Snyder²⁵, R. Sobie^{170,i}, F. Socher⁴⁴, J. Sodomka¹²⁷, A. Soffer¹⁵⁴, D.A. Soh^{152,r}, C.A. Solans³⁰, M. Solar¹²⁷, J. Solc¹²⁷, E.Yu. Soldatov⁹⁷, U. Soldevila¹⁶⁸, E. Solfaroli Camillocci^{133a,133b}, A.A. Solodkov¹²⁹, O.V. Solovyanov¹²⁹, V. Solovyev¹²², P. Sommer⁴⁸, H.Y. Song^{33b}, N. Soni¹, A. Sood¹⁵, A. Sopczak¹²⁷, V. Sopko¹²⁷, B. Sopko¹²⁷, V. Sorin¹², M. Sosebee⁸, R. Soualah^{165a,165c}, P. Soueid⁹⁴, A.M. Soukharev¹⁰⁸, D. South⁴², S. Spagnolo^{72a,72b}, F. Spanò⁷⁶, W.R. Spearman⁵⁷, R. Spighi^{20a}, G. Spigo³⁰, M. Spousta¹²⁸, T. Spreitzer¹⁵⁹,

B. Spurlock⁸, R.D. St. Denis⁵³, S. Staerz⁴⁴, J. Stahlman¹²¹, R. Stamen^{58a}, E. Stanecka³⁹, R.W. Stanek⁶,
 C. Stanescu^{135a}, M. Stanescu-Bellu⁴², M.M. Stanitzki⁴², S. Stapnes¹¹⁸, E.A. Starchenko¹²⁹, J. Stark⁵⁵,
 P. Staroba¹²⁶, P. Starovoitov⁴², R. Staszewski³⁹, P. Stavina^{145a,*}, G. Steele⁵³, P. Steinberg²⁵, I. Stekl¹²⁷,
 B. Stelzer¹⁴³, H.J. Stelzer³⁰, O. Stelzer-Chilton^{160a}, H. Stenzel⁵², S. Stern¹⁰⁰, G.A. Stewart⁵³, J.A. Stillings²¹,
 M.C. Stockton⁸⁶, M. Stoebe⁸⁶, G. Stoicea^{26a}, P. Stolte⁵⁴, S. Stonjek¹⁰⁰, A.R. Stradling⁸, A. Straessner⁴⁴,
 J. Strandberg¹⁴⁸, S. Strandberg^{147a,147b}, A. Strandlie¹¹⁸, E. Strauss¹⁴⁴, M. Strauss¹¹², P. Strizenec^{145b},
 R. Ströhrmer¹⁷⁵, D.M. Strom¹¹⁵, R. Stroynowski⁴⁰, S.A. Stucci¹⁷, B. Stugu¹⁴, N.A. Styles⁴², D. Su¹⁴⁴, J. Su¹²⁴,
 HS. Subramania³, R. Subramaniam⁷⁸, A. Succurro¹², Y. Sugaya¹¹⁷, C. Suhr¹⁰⁷, M. Suk¹²⁷, V.V. Sulin⁹⁵,
 S. Sultansoy^{4c}, T. Sumida⁶⁷, X. Sun^{33a}, J.E. Sundermann⁴⁸, K. Suruliz¹⁴⁰, G. Susinno^{37a,37b}, M.R. Sutton¹⁵⁰,
 Y. Suzuki⁶⁵, M. Svatos¹²⁶, S. Swedish¹⁶⁹, M. Swiatlowski¹⁴⁴, I. Sykora^{145a}, T. Sykora¹²⁸, D. Ta⁸⁹, K. Tackmann⁴²,
 J. Taenzer¹⁵⁹, A. Taffard¹⁶⁴, R. Tafirout^{160a}, N. Taiblum¹⁵⁴, Y. Takahashi¹⁰², H. Takai²⁵, R. Takashima⁶⁸,
 H. Takeda⁶⁶, T. Takeshita¹⁴¹, Y. Takubo⁶⁵, M. Talby⁸⁴, A.A. Talyshv^{108,f}, J.Y.C. Tam¹⁷⁵, M.C. Tamsett^{78,ad},
 K.G. Tan⁸⁷, J. Tanaka¹⁵⁶, R. Tanaka¹¹⁶, S. Tanaka¹³², S. Tanaka⁶⁵, A.J. Tanasijczuk¹⁴³, K. Tan⁶⁶, N. Tannoury⁸⁴,
 S. Tapprogge⁸², S. Tarem¹⁵³, F. Tarrade²⁹, G.F. Tartarelli^{90a}, P. Tas¹²⁸, M. Tasevsky¹²⁶, T. Tashiro⁶⁷,
 E. Tassi^{37a,37b}, A. Tavares Delgado^{125a,125b}, Y. Tayalati^{136d}, F.E. Taylor⁹³, G.N. Taylor⁸⁷, W. Taylor^{160b},
 F.A. Teischinger³⁰, M. Teixeira Dias Castanheira⁷⁵, P. Teixeira-Dias⁷⁶, K.K. Temming⁴⁸, H. Ten Kate³⁰,
 P.K. Teng¹⁵², S. Terada⁶⁵, K. Terashi¹⁵⁶, J. Terron⁸¹, S. Terzo¹⁰⁰, M. Testa⁴⁷, R.J. Teuscher^{159,i}, J. Therhaag²¹,
 T. Theveneaux-Pelzer³⁴, S. Thoma⁴⁸, J.P. Thomas¹⁸, J. Thomas-Wilsker⁷⁶, E.N. Thompson³⁵, P.D. Thompson¹⁸,
 P.D. Thompson¹⁵⁹, A.S. Thompson⁵³, L.A. Thomsen³⁶, E. Thomson¹²¹, M. Thomson²⁸, W.M. Thong⁸⁷,
 R.P. Thun^{88,*}, F. Tian³⁵, M.J. Tibbetts¹⁵, V.O. Tikhomirov^{95,ae}, Yu.A. Tikhonov^{108,f}, S. Timoshenko⁹⁷,
 E. Tiouchichine⁸⁴, P. Tipton¹⁷⁷, S. Tisserant⁸⁴, T. Todorov⁵, S. Todorova-Nova¹²⁸, B. Toggerson¹⁶⁴, J. Tojo⁶⁹,
 S. Tokár^{145a}, K. Tokushuku⁶⁵, K. Tollefson⁸⁹, L. Tomlinson⁸³, M. Tomoto¹⁰², L. Tompkins³¹, K. Toms¹⁰⁴,
 N.D. Topilin⁶⁴, E. Torrence¹¹⁵, H. Torres¹⁴³, E. Torró Pastor¹⁶⁸, J. Toth^{84,z}, F. Touchard⁸⁴, D.R. Tovey¹⁴⁰,
 H.L. Tran¹¹⁶, T. Trefzger¹⁷⁵, L. Tremblet³⁰, A. Tricoli³⁰, I.M. Trigger^{160a}, S. Trincaz-Duvoid⁷⁹, M.F. Tripiana⁷⁰,
 N. Triplett²⁵, W. Trischuk¹⁵⁹, B. Trocmé⁵⁵, C. Troncon^{90a}, M. Trottier-McDonald¹⁴³, M. Trovatelli^{135a,135b},
 P. True⁸⁹, M. Trzebinski³⁹, A. Trzupek³⁹, C. Tsarouchas³⁰, J.C.-L. Tseng¹¹⁹, P.V. Tsiareshka⁹¹, D. Tsionou¹³⁷,
 G. Tsipolitis¹⁰, N. Tsirintanis⁹, S. Tsiskaridze¹², V. Tsiskaridze⁴⁸, E.G. Tskhadadze^{51a}, I.I. Tsukerman⁹⁶,
 V. Tsulaia¹⁵, S. Tsuno⁶⁵, D. Tsybychev¹⁴⁹, A. Tudorache^{26a}, V. Tudorache^{26a}, A.N. Tuna¹²¹, S.A. Tupputi^{20a,20b},
 S. Turchikhin^{98,ac}, D. Turecek¹²⁷, I. Turk Cakir^{4d}, R. Turra^{90a,90b}, P.M. Tuts³⁵, A. Tykhonov⁷⁴,
 M. Tylmad^{147a,147b}, M. Tyndel¹³⁰, K. Uchida²¹, I. Ueda¹⁵⁶, R. Ueno²⁹, M. Ughetto⁸⁴, M. Uglad¹⁴,
 M. Uhlenbrock²¹, F. Ukegawa¹⁶¹, G. Unal³⁰, A. Undrus²⁵, G. Unel¹⁶⁴, F.C. Ungaro⁴⁸, Y. Unno⁶⁵, D. Urbaniec³⁵,
 P. Urquijo²¹, G. Usai⁸, A. Usanova⁶¹, L. Vacavant⁸⁴, V. Vacek¹²⁷, B. Vachon⁸⁶, N. Valencic¹⁰⁶,
 S. Valentineti^{20a,20b}, A. Valero¹⁶⁸, L. Valery³⁴, S. Valkar¹²⁸, E. Valladolid Gallego¹⁶⁸, S. Vallecorsa⁴⁹,
 J.A. Valls Ferrer¹⁶⁸, R. Van Berg¹²¹, P.C. Van Der Deijl¹⁰⁶, R. van der Geer¹⁰⁶, H. van der Graaf¹⁰⁶,
 R. Van Der Leeuw¹⁰⁶, D. van der Ster³⁰, N. van Eldik³⁰, P. van Gemmeren⁶, J. Van Nieuwkoop¹⁴³, I. van Vulpen¹⁰⁶,
 M.C. van Woerden³⁰, M. Vanadia^{133a,133b}, W. Vandelli³⁰, R. Vanguri¹²¹, A. Vaniachine⁶, P. Vankov⁴²,
 F. Vannucci⁷⁹, G. Vardanyan¹⁷⁸, R. Vari^{133a}, E.W. Varnes⁷, T. Varol⁸⁵, D. Varouchas⁷⁹, A. Vartapetian⁸,
 K.E. Varvell¹⁵¹, V.I. Vassilakopoulos⁵⁶, F. Vazeille³⁴, T. Vazquez Schroeder⁵⁴, J. Veatch⁷, F. Veloso^{125a,125c},
 S. Veneziano^{133a}, A. Ventura^{72a,72b}, D. Ventura⁸⁵, M. Venturi⁴⁸, N. Venturi¹⁵⁹, A. Venturini²³, V. Vercesi^{120a},
 M. Verducci¹³⁹, W. Verkerke¹⁰⁶, J.C. Vermeulen¹⁰⁶, A. Vest⁴⁴, M.C. Vetterli^{143,d}, O. Viazlo⁸⁰, I. Vichou¹⁶⁶,
 T. Vickey^{146c,af}, O.E. Vickey Boeriu^{146c}, G.H.A. Viehhauser¹¹⁹, S. Viel¹⁶⁹, R. Vigne³⁰, M. Villa^{20a,20b},
 M. Villaplana Perez¹⁶⁸, E. Vilucchi⁴⁷, M.G. Vincter²⁹, V.B. Vinogradov⁶⁴, J. Virzi¹⁵, I. Vivarelli¹⁵⁰,
 F. Vives Vaque³, S. Vlachos¹⁰, D. Vladoiu⁹⁹, M. Vlasak¹²⁷, A. Vogel²¹, P. Vokac¹²⁷, G. Volpi⁴⁷, M. Volpi⁸⁷,
 H. von der Schmitt¹⁰⁰, H. von Radziewski⁴⁸, E. von Toerne²¹, V. Vorobel¹²⁸, K. Vorobev⁹⁷, M. Vos¹⁶⁸, R. Voss³⁰,
 J.H. Vossebeld⁷³, N. Vranjes¹³⁷, M. Vranjes Milosavljevic¹⁰⁶, V. Vrba¹²⁶, M. Vreeswijk¹⁰⁶, T. Vu Anh⁴⁸,
 R. Vuillermet³⁰, I. Vukotic³¹, Z. Vykydal¹²⁷, W. Wagner¹⁷⁶, P. Wagner²¹, S. Wahrenmund⁴⁴, J. Wakabayashi¹⁰²,
 J. Walder⁷¹, R. Walker⁹⁹, W. Walkowiak¹⁴², R. Wall¹⁷⁷, P. Waller⁷³, B. Walsh¹⁷⁷, C. Wang¹⁵², C. Wang⁴⁵,
 F. Wang¹⁷⁴, H. Wang¹⁵, H. Wang⁴⁰, J. Wang⁴², J. Wang^{33a}, K. Wang⁸⁶, R. Wang¹⁰⁴, S.M. Wang¹⁵², T. Wang²¹,
 X. Wang¹⁷⁷, C. Wanotayaroj¹¹⁵, A. Warburton⁸⁶, C.P. Ward²⁸, D.R. Wardrope⁷⁷, M. Warsinsky⁴⁸, A. Washbrook⁴⁶,
 C. Wasicki⁴², I. Watanabe⁶⁶, P.M. Watkins¹⁸, A.T. Watson¹⁸, I.J. Watson¹⁵¹, M.F. Watson¹⁸, G. Watts¹³⁹,
 S. Watts⁸³, B.M. Waugh⁷⁷, S. Webb⁸³, M.S. Weber¹⁷, S.W. Weber¹⁷⁵, J.S. Webster³¹, A.R. Weidberg¹¹⁹,
 P. Weigell¹⁰⁰, B. Weinert⁶⁰, J. Weingarten⁵⁴, C. Weiser⁴⁸, H. Weits¹⁰⁶, P.S. Wells³⁰, T. Wenaus²⁵, D. Wendland¹⁶,
 Z. Weng^{152,r}, T. Wengler³⁰, S. Wenig³⁰, N. Wermes²¹, M. Werner⁴⁸, P. Werner³⁰, M. Wessels^{58a}, J. Wetter¹⁶²,
 K. Whalen²⁹, A. White⁸, M.J. White¹, R. White^{32b}, S. White^{123a,123b}, D. Whiteson¹⁶⁴, D. Wicke¹⁷⁶,
 F.J. Wickens¹³⁰, W. Wiedenmann¹⁷⁴, M. Wielers¹³⁰, P. Wienemann²¹, C. Wiglesworth³⁶, L.A.M. Wiik-Fuchs²¹,
 P.A. Wijeratne⁷⁷, A. Wildauer¹⁰⁰, M.A. Wildt^{42,ag}, H.G. Wilkens³⁰, J.Z. Will⁹⁹, H.H. Williams¹²¹, S. Williams²⁸,
 C. Willis⁸⁹, S. Willocq⁸⁵, J.A. Wilson¹⁸, A. Wilson⁸⁸, I. Wingerter-Seez⁵, F. Winklmeier¹¹⁵, M. Wittgen¹⁴⁴,
 T. Wittig⁴³, J. Wittkowski⁹⁹, S.J. Wollstadt⁸², M.W. Wolter³⁹, H. Wolters^{125a,125c}, B.K. Wosiek³⁹, J. Wotschack³⁰,

M.J. Woudstra⁸³, K.W. Wozniak³⁹, M. Wright⁵³, M. Wu⁵⁵, S.L. Wu¹⁷⁴, X. Wu⁴⁹, Y. Wu⁸⁸, E. Wulf³⁵, T.R. Wyatt⁸³, B.M. Wynne⁴⁶, S. Xella³⁶, M. Xiao¹³⁷, D. Xu^{33a}, L. Xu^{33b,ah}, B. Yabsley¹⁵¹, S. Yacoub^{146b,ai}, M. Yamada⁶⁵, H. Yamaguchi¹⁵⁶, Y. Yamaguchi¹⁵⁶, A. Yamamoto⁶⁵, K. Yamamoto⁶³, S. Yamamoto¹⁵⁶, T. Yamamura¹⁵⁶, T. Yamanaka¹⁵⁶, K. Yamauchi¹⁰², Y. Yamazaki⁶⁶, Z. Yan²², H. Yang^{33e}, H. Yang¹⁷⁴, U.K. Yang⁸³, Y. Yang¹¹⁰, S. Yanush⁹², L. Yao^{33a}, W.-M. Yao¹⁵, Y. Yasu⁶⁵, E. Yatsenko⁴², K.H. Yau Wong²¹, J. Ye⁴⁰, S. Ye²⁵, A.L. Yen⁵⁷, E. Yildirim⁴², M. Yilmaz^{4b}, R. Yoosoofmiya¹²⁴, K. Yorita¹⁷², R. Yoshida⁶, K. Yoshihara¹⁵⁶, C. Young¹⁴⁴, C.J.S. Young³⁰, S. Youssef²², D.R. Yu¹⁵, J. Yu⁸, J.M. Yu⁸⁸, J. Yu¹¹³, L. Yuan⁶⁶, A. Yurkewicz¹⁰⁷, B. Zabinski³⁹, R. Zaidan⁶², A.M. Zaitsev^{129,w}, A. Zaman¹⁴⁹, S. Zambito²³, L. Zanello^{133a,133b}, D. Zanzi¹⁰⁰, A. Zaytsev²⁵, C. Zeitnitz¹⁷⁶, M. Zeman¹²⁷, A. Zemla^{38a}, K. Zengel²³, O. Zenin¹²⁹, T. Ženiš^{145a}, D. Zerwas¹¹⁶, G. Zevi della Porta⁵⁷, D. Zhang⁸⁸, F. Zhang¹⁷⁴, H. Zhang⁸⁹, J. Zhang⁶, L. Zhang¹⁵², X. Zhang^{33d}, Z. Zhang¹¹⁶, Z. Zhao^{33b}, A. Zhemchugov⁶⁴, J. Zhong¹¹⁹, B. Zhou⁸⁸, L. Zhou³⁵, N. Zhou¹⁶⁴, C.G. Zhu^{33d}, H. Zhu^{33a}, J. Zhu⁸⁸, Y. Zhu^{33b}, X. Zhuang^{33a}, A. Zibell¹⁷⁵, D. Zieminska⁶⁰, N.I. Zimine⁶⁴, C. Zimmermann⁸², R. Zimmermann²¹, S. Zimmermann²¹, S. Zimmermann⁴⁸, Z. Zinonos⁵⁴, M. Ziolkowski¹⁴², G. Zoernig¹⁷⁴, A. Zoccoli^{20a,20b}, M. zur Nedden¹⁶, G. Zurzolo^{103a,103b}, V. Zutshi¹⁰⁷, L. Zwalinski³⁰.

¹ Department of Physics, University of Adelaide, Adelaide, Australia

² Physics Department, SUNY Albany, Albany NY, United States of America

³ Department of Physics, University of Alberta, Edmonton AB, Canada

⁴ (a) Department of Physics, Ankara University, Ankara; (b) Department of Physics, Gazi University, Ankara; (c) Division of Physics, TOBB University of Economics and Technology, Ankara; (d) Turkish Atomic Energy Authority, Ankara, Turkey

⁵ LAPP, CNRS/IN2P3 and Université de Savoie, Annecy-le-Vieux, France

⁶ High Energy Physics Division, Argonne National Laboratory, Argonne IL, United States of America

⁷ Department of Physics, University of Arizona, Tucson AZ, United States of America

⁸ Department of Physics, The University of Texas at Arlington, Arlington TX, United States of America

⁹ Physics Department, University of Athens, Athens, Greece

¹⁰ Physics Department, National Technical University of Athens, Zografou, Greece

¹¹ Institute of Physics, Azerbaijan Academy of Sciences, Baku, Azerbaijan

¹² Institut de Física d'Altes Energies and Departament de Física de la Universitat Autònoma de Barcelona, Barcelona, Spain

¹³ (a) Institute of Physics, University of Belgrade, Belgrade; (b) Vinca Institute of Nuclear Sciences, University of Belgrade, Belgrade, Serbia

¹⁴ Department for Physics and Technology, University of Bergen, Bergen, Norway

¹⁵ Physics Division, Lawrence Berkeley National Laboratory and University of California, Berkeley CA, United States of America

¹⁶ Department of Physics, Humboldt University, Berlin, Germany

¹⁷ Albert Einstein Center for Fundamental Physics and Laboratory for High Energy Physics, University of Bern, Bern, Switzerland

¹⁸ School of Physics and Astronomy, University of Birmingham, Birmingham, United Kingdom

¹⁹ (a) Department of Physics, Bogazici University, Istanbul; (b) Department of Physics, Dogus University, Istanbul;

(c) Department of Physics Engineering, Gaziantep University, Gaziantep, Turkey

²⁰ (a) INFN Sezione di Bologna; (b) Dipartimento di Fisica e Astronomia, Università di Bologna, Bologna, Italy

²¹ Physikalisches Institut, University of Bonn, Bonn, Germany

²² Department of Physics, Boston University, Boston MA, United States of America

²³ Department of Physics, Brandeis University, Waltham MA, United States of America

²⁴ (a) Universidade Federal do Rio De Janeiro COPPE/EE/IF, Rio de Janeiro; (b) Federal University of Juiz de Fora (UFJF), Juiz de Fora; (c) Federal University of Sao Joao del Rei (UFSJ), Sao Joao del Rei; (d) Instituto de Física, Universidade de Sao Paulo, Sao Paulo, Brazil

²⁵ Physics Department, Brookhaven National Laboratory, Upton NY, United States of America

²⁶ (a) National Institute of Physics and Nuclear Engineering, Bucharest; (b) National Institute for Research and Development of Isotopic and Molecular Technologies, Physics Department, Cluj Napoca; (c) University Politehnica Bucharest, Bucharest; (d) West University in Timisoara, Timisoara, Romania

²⁷ Departamento de Física, Universidad de Buenos Aires, Buenos Aires, Argentina

²⁸ Cavendish Laboratory, University of Cambridge, Cambridge, United Kingdom

²⁹ Department of Physics, Carleton University, Ottawa ON, Canada

³⁰ CERN, Geneva, Switzerland

³¹ Enrico Fermi Institute, University of Chicago, Chicago IL, United States of America

³² (a) Departamento de Física, Pontificia Universidad Católica de Chile, Santiago; (b) Departamento de Física,

Universidad Técnica Federico Santa María, Valparaíso, Chile

³³ ^(a) Institute of High Energy Physics, Chinese Academy of Sciences, Beijing; ^(b) Department of Modern Physics, University of Science and Technology of China, Anhui; ^(c) Department of Physics, Nanjing University, Jiangsu; ^(d) School of Physics, Shandong University, Shandong; ^(e) Physics Department, Shanghai Jiao Tong University, Shanghai, China

³⁴ Laboratoire de Physique Corpusculaire, Clermont Université and Université Blaise Pascal and CNRS/IN2P3, Clermont-Ferrand, France

³⁵ Nevis Laboratory, Columbia University, Irvington NY, United States of America

³⁶ Niels Bohr Institute, University of Copenhagen, Kobenhavn, Denmark

³⁷ ^(a) INFN Gruppo Collegato di Cosenza, Laboratori Nazionali di Frascati; ^(b) Dipartimento di Fisica, Università della Calabria, Rende, Italy

³⁸ ^(a) AGH University of Science and Technology, Faculty of Physics and Applied Computer Science, Krakow; ^(b) Marian Smoluchowski Institute of Physics, Jagiellonian University, Krakow, Poland

³⁹ The Henryk Niewodniczanski Institute of Nuclear Physics, Polish Academy of Sciences, Krakow, Poland

⁴⁰ Physics Department, Southern Methodist University, Dallas TX, United States of America

⁴¹ Physics Department, University of Texas at Dallas, Richardson TX, United States of America

⁴² DESY, Hamburg and Zeuthen, Germany

⁴³ Institut für Experimentelle Physik IV, Technische Universität Dortmund, Dortmund, Germany

⁴⁴ Institut für Kern- und Teilchenphysik, Technische Universität Dresden, Dresden, Germany

⁴⁵ Department of Physics, Duke University, Durham NC, United States of America

⁴⁶ SUPA - School of Physics and Astronomy, University of Edinburgh, Edinburgh, United Kingdom

⁴⁷ INFN Laboratori Nazionali di Frascati, Frascati, Italy

⁴⁸ Fakultät für Mathematik und Physik, Albert-Ludwigs-Universität, Freiburg, Germany

⁴⁹ Section de Physique, Université de Genève, Geneva, Switzerland

⁵⁰ ^(a) INFN Sezione di Genova; ^(b) Dipartimento di Fisica, Università di Genova, Genova, Italy

⁵¹ ^(a) E. Andronikashvili Institute of Physics, Iv. Javakishvili Tbilisi State University, Tbilisi; ^(b) High Energy Physics Institute, Tbilisi State University, Tbilisi, Georgia

⁵² II Physikalisches Institut, Justus-Liebig-Universität Giessen, Giessen, Germany

⁵³ SUPA - School of Physics and Astronomy, University of Glasgow, Glasgow, United Kingdom

⁵⁴ II Physikalisches Institut, Georg-August-Universität, Göttingen, Germany

⁵⁵ Laboratoire de Physique Subatomique et de Cosmologie, Université Joseph Fourier and CNRS/IN2P3 and Institut National Polytechnique de Grenoble, Grenoble, France

⁵⁶ Department of Physics, Hampton University, Hampton VA, United States of America

⁵⁷ Laboratory for Particle Physics and Cosmology, Harvard University, Cambridge MA, United States of America

⁵⁸ ^(a) Kirchhoff-Institut für Physik, Ruprecht-Karls-Universität Heidelberg, Heidelberg; ^(b) Physikalisches Institut, Ruprecht-Karls-Universität Heidelberg, Heidelberg; ^(c) ZITI Institut für technische Informatik, Ruprecht-Karls-Universität Heidelberg, Mannheim, Germany

⁵⁹ Faculty of Applied Information Science, Hiroshima Institute of Technology, Hiroshima, Japan

⁶⁰ Department of Physics, Indiana University, Bloomington IN, United States of America

⁶¹ Institut für Astro- und Teilchenphysik, Leopold-Franzens-Universität, Innsbruck, Austria

⁶² University of Iowa, Iowa City IA, United States of America

⁶³ Department of Physics and Astronomy, Iowa State University, Ames IA, United States of America

⁶⁴ Joint Institute for Nuclear Research, JINR Dubna, Dubna, Russia

⁶⁵ KEK, High Energy Accelerator Research Organization, Tsukuba, Japan

⁶⁶ Graduate School of Science, Kobe University, Kobe, Japan

⁶⁷ Faculty of Science, Kyoto University, Kyoto, Japan

⁶⁸ Kyoto University of Education, Kyoto, Japan

⁶⁹ Department of Physics, Kyushu University, Fukuoka, Japan

⁷⁰ Instituto de Física La Plata, Universidad Nacional de La Plata and CONICET, La Plata, Argentina

⁷¹ Physics Department, Lancaster University, Lancaster, United Kingdom

⁷² ^(a) INFN Sezione di Lecce; ^(b) Dipartimento di Matematica e Fisica, Università del Salento, Lecce, Italy

⁷³ Oliver Lodge Laboratory, University of Liverpool, Liverpool, United Kingdom

⁷⁴ Department of Physics, Jožef Stefan Institute and University of Ljubljana, Ljubljana, Slovenia

⁷⁵ School of Physics and Astronomy, Queen Mary University of London, London, United Kingdom

⁷⁶ Department of Physics, Royal Holloway University of London, Surrey, United Kingdom

⁷⁷ Department of Physics and Astronomy, University College London, London, United Kingdom

⁷⁸ Louisiana Tech University, Ruston LA, United States of America

⁷⁹ Laboratoire de Physique Nucléaire et de Hautes Energies, UPMC and Université Paris-Diderot and

CNRS/IN2P3, Paris, France

⁸⁰ Fysiska institutionen, Lunds universitet, Lund, Sweden

⁸¹ Departamento de Fisica Teorica C-15, Universidad Autonoma de Madrid, Madrid, Spain

⁸² Institut für Physik, Universität Mainz, Mainz, Germany

⁸³ School of Physics and Astronomy, University of Manchester, Manchester, United Kingdom

⁸⁴ CPPM, Aix-Marseille Université and CNRS/IN2P3, Marseille, France

⁸⁵ Department of Physics, University of Massachusetts, Amherst MA, United States of America

⁸⁶ Department of Physics, McGill University, Montreal QC, Canada

⁸⁷ School of Physics, University of Melbourne, Victoria, Australia

⁸⁸ Department of Physics, The University of Michigan, Ann Arbor MI, United States of America

⁸⁹ Department of Physics and Astronomy, Michigan State University, East Lansing MI, United States of America

⁹⁰ ^(a) INFN Sezione di Milano; ^(b) Dipartimento di Fisica, Università di Milano, Milano, Italy

⁹¹ B.I. Stepanov Institute of Physics, National Academy of Sciences of Belarus, Minsk, Republic of Belarus

⁹² National Scientific and Educational Centre for Particle and High Energy Physics, Minsk, Republic of Belarus

⁹³ Department of Physics, Massachusetts Institute of Technology, Cambridge MA, United States of America

⁹⁴ Group of Particle Physics, University of Montreal, Montreal QC, Canada

⁹⁵ P.N. Lebedev Institute of Physics, Academy of Sciences, Moscow, Russia

⁹⁶ Institute for Theoretical and Experimental Physics (ITEP), Moscow, Russia

⁹⁷ Moscow Engineering and Physics Institute (MEPhI), Moscow, Russia

⁹⁸ D.V.Skobel'tsyn Institute of Nuclear Physics, M.V.Lomonosov Moscow State University, Moscow, Russia

⁹⁹ Fakultät für Physik, Ludwig-Maximilians-Universität München, München, Germany

¹⁰⁰ Max-Planck-Institut für Physik (Werner-Heisenberg-Institut), München, Germany

¹⁰¹ Nagasaki Institute of Applied Science, Nagasaki, Japan

¹⁰² Graduate School of Science and Kobayashi-Maskawa Institute, Nagoya University, Nagoya, Japan

¹⁰³ ^(a) INFN Sezione di Napoli; ^(b) Dipartimento di Fisica, Università di Napoli, Napoli, Italy

¹⁰⁴ Department of Physics and Astronomy, University of New Mexico, Albuquerque NM, United States of America

¹⁰⁵ Institute for Mathematics, Astrophysics and Particle Physics, Radboud University Nijmegen/Nikhef, Nijmegen, Netherlands

¹⁰⁶ Nikhef National Institute for Subatomic Physics and University of Amsterdam, Amsterdam, Netherlands

¹⁰⁷ Department of Physics, Northern Illinois University, DeKalb IL, United States of America

¹⁰⁸ Budker Institute of Nuclear Physics, SB RAS, Novosibirsk, Russia

¹⁰⁹ Department of Physics, New York University, New York NY, United States of America

¹¹⁰ Ohio State University, Columbus OH, United States of America

¹¹¹ Faculty of Science, Okayama University, Okayama, Japan

¹¹² Homer L. Dodge Department of Physics and Astronomy, University of Oklahoma, Norman OK, United States of America

¹¹³ Department of Physics, Oklahoma State University, Stillwater OK, United States of America

¹¹⁴ Palacký University, RCPTM, Olomouc, Czech Republic

¹¹⁵ Center for High Energy Physics, University of Oregon, Eugene OR, United States of America

¹¹⁶ LAL, Université Paris-Sud and CNRS/IN2P3, Orsay, France

¹¹⁷ Graduate School of Science, Osaka University, Osaka, Japan

¹¹⁸ Department of Physics, University of Oslo, Oslo, Norway

¹¹⁹ Department of Physics, Oxford University, Oxford, United Kingdom

¹²⁰ ^(a) INFN Sezione di Pavia; ^(b) Dipartimento di Fisica, Università di Pavia, Pavia, Italy

¹²¹ Department of Physics, University of Pennsylvania, Philadelphia PA, United States of America

¹²² Petersburg Nuclear Physics Institute, Gatchina, Russia

¹²³ ^(a) INFN Sezione di Pisa; ^(b) Dipartimento di Fisica E. Fermi, Università di Pisa, Pisa, Italy

¹²⁴ Department of Physics and Astronomy, University of Pittsburgh, Pittsburgh PA, United States of America

¹²⁵ ^(a) Laboratório de Instrumentação e Física Experimental de Partículas - LIP, Lisboa; ^(b) Faculdade de Ciências, Universidade de Lisboa, Lisboa; ^(c) Department of Physics, University of Coimbra, Coimbra; ^(d) Centro de Física Nuclear da Universidade de Lisboa, Lisboa; ^(e) Departamento de Física, Universidade do Minho, Braga; ^(f)

Departamento de Física Teórica y del Cosmos and CAFPE, Universidad de Granada, Granada (Spain); ^(g) Dep

Física and CEFITEC of Faculdade de Ciências e Tecnologia, Universidade Nova de Lisboa, Caparica, Portugal

¹²⁶ Institute of Physics, Academy of Sciences of the Czech Republic, Praha, Czech Republic

¹²⁷ Czech Technical University in Prague, Praha, Czech Republic

¹²⁸ Faculty of Mathematics and Physics, Charles University in Prague, Praha, Czech Republic

¹²⁹ State Research Center Institute for High Energy Physics, Protvino, Russia

¹³⁰ Particle Physics Department, Rutherford Appleton Laboratory, Didcot, United Kingdom

- 131 Physics Department, University of Regina, Regina SK, Canada
- 132 Ritsumeikan University, Kusatsu, Shiga, Japan
- 133 (a) INFN Sezione di Roma; (b) Dipartimento di Fisica, Sapienza Università di Roma, Roma, Italy
- 134 (a) INFN Sezione di Roma Tor Vergata; (b) Dipartimento di Fisica, Università di Roma Tor Vergata, Roma, Italy
- 135 (a) INFN Sezione di Roma Tre; (b) Dipartimento di Matematica e Fisica, Università Roma Tre, Roma, Italy
- 136 (a) Faculté des Sciences Ain Chock, Réseau Universitaire de Physique des Hautes Energies - Université Hassan II, Casablanca; (b) Centre National de l'Energie des Sciences Techniques Nucleaires, Rabat; (c) Faculté des Sciences Semlalia, Université Cadi Ayyad, LPHEA-Marrakech; (d) Faculté des Sciences, Université Mohamed Premier and LPTPM, Oujda; (e) Faculté des sciences, Université Mohammed V-Agdal, Rabat, Morocco
- 137 DSM/IRFU (Institut de Recherches sur les Lois Fondamentales de l'Univers), CEA Saclay (Commissariat à l'Energie Atomique et aux Energies Alternatives), Gif-sur-Yvette, France
- 138 Santa Cruz Institute for Particle Physics, University of California Santa Cruz, Santa Cruz CA, United States of America
- 139 Department of Physics, University of Washington, Seattle WA, United States of America
- 140 Department of Physics and Astronomy, University of Sheffield, Sheffield, United Kingdom
- 141 Department of Physics, Shinshu University, Nagano, Japan
- 142 Fachbereich Physik, Universität Siegen, Siegen, Germany
- 143 Department of Physics, Simon Fraser University, Burnaby BC, Canada
- 144 SLAC National Accelerator Laboratory, Stanford CA, United States of America
- 145 (a) Faculty of Mathematics, Physics & Informatics, Comenius University, Bratislava; (b) Department of Subnuclear Physics, Institute of Experimental Physics of the Slovak Academy of Sciences, Kosice, Slovak Republic
- 146 (a) Department of Physics, University of Cape Town, Cape Town; (b) Department of Physics, University of Johannesburg, Johannesburg; (c) School of Physics, University of the Witwatersrand, Johannesburg, South Africa
- 147 (a) Department of Physics, Stockholm University; (b) The Oskar Klein Centre, Stockholm, Sweden
- 148 Physics Department, Royal Institute of Technology, Stockholm, Sweden
- 149 Departments of Physics & Astronomy and Chemistry, Stony Brook University, Stony Brook NY, United States of America
- 150 Department of Physics and Astronomy, University of Sussex, Brighton, United Kingdom
- 151 School of Physics, University of Sydney, Sydney, Australia
- 152 Institute of Physics, Academia Sinica, Taipei, Taiwan
- 153 Department of Physics, Technion: Israel Institute of Technology, Haifa, Israel
- 154 Raymond and Beverly Sackler School of Physics and Astronomy, Tel Aviv University, Tel Aviv, Israel
- 155 Department of Physics, Aristotle University of Thessaloniki, Thessaloniki, Greece
- 156 International Center for Elementary Particle Physics and Department of Physics, The University of Tokyo, Tokyo, Japan
- 157 Graduate School of Science and Technology, Tokyo Metropolitan University, Tokyo, Japan
- 158 Department of Physics, Tokyo Institute of Technology, Tokyo, Japan
- 159 Department of Physics, University of Toronto, Toronto ON, Canada
- 160 (a) TRIUMF, Vancouver BC; (b) Department of Physics and Astronomy, York University, Toronto ON, Canada
- 161 Faculty of Pure and Applied Sciences, University of Tsukuba, Tsukuba, Japan
- 162 Department of Physics and Astronomy, Tufts University, Medford MA, United States of America
- 163 Centro de Investigaciones, Universidad Antonio Narino, Bogota, Colombia
- 164 Department of Physics and Astronomy, University of California Irvine, Irvine CA, United States of America
- 165 (a) INFN Gruppo Collegato di Udine, Sezione di Trieste, Udine; (b) ICTP, Trieste; (c) Dipartimento di Chimica, Fisica e Ambiente, Università di Udine, Udine, Italy
- 166 Department of Physics, University of Illinois, Urbana IL, United States of America
- 167 Department of Physics and Astronomy, University of Uppsala, Uppsala, Sweden
- 168 Instituto de Física Corpuscular (IFIC) and Departamento de Física Atómica, Molecular y Nuclear and Departamento de Ingeniería Electrónica and Instituto de Microelectrónica de Barcelona (IMB-CNM), University of Valencia and CSIC, Valencia, Spain
- 169 Department of Physics, University of British Columbia, Vancouver BC, Canada
- 170 Department of Physics and Astronomy, University of Victoria, Victoria BC, Canada
- 171 Department of Physics, University of Warwick, Coventry, United Kingdom
- 172 Waseda University, Tokyo, Japan
- 173 Department of Particle Physics, The Weizmann Institute of Science, Rehovot, Israel
- 174 Department of Physics, University of Wisconsin, Madison WI, United States of America
- 175 Fakultät für Physik und Astronomie, Julius-Maximilians-Universität, Würzburg, Germany
- 176 Fachbereich C Physik, Bergische Universität Wuppertal, Wuppertal, Germany

- ¹⁷⁷ Department of Physics, Yale University, New Haven CT, United States of America
- ¹⁷⁸ Yerevan Physics Institute, Yerevan, Armenia
- ¹⁷⁹ Centre de Calcul de l'Institut National de Physique Nucléaire et de Physique des Particules (IN2P3), Villeurbanne, France
- ^a Also at Department of Physics, King's College London, London, United Kingdom
- ^b Also at Institute of Physics, Azerbaijan Academy of Sciences, Baku, Azerbaijan
- ^c Also at Particle Physics Department, Rutherford Appleton Laboratory, Didcot, United Kingdom
- ^d Also at TRIUMF, Vancouver BC, Canada
- ^e Also at Department of Physics, California State University, Fresno CA, United States of America
- ^f Also at Novosibirsk State University, Novosibirsk, Russia
- ^g Also at CPPM, Aix-Marseille Université and CNRS/IN2P3, Marseille, France
- ^h Also at Università di Napoli Parthenope, Napoli, Italy
- ⁱ Also at Institute of Particle Physics (IPP), Canada
- ^j Also at Department of Financial and Management Engineering, University of the Aegean, Chios, Greece
- ^k Also at Louisiana Tech University, Ruston LA, United States of America
- ^l Also at Institutio Catalana de Recerca i Estudis Avancats, ICREA, Barcelona, Spain
- ^m Also at CERN, Geneva, Switzerland
- ⁿ Also at Ochadai Academic Production, Ochanomizu University, Tokyo, Japan
- ^o Also at Manhattan College, New York NY, United States of America
- ^p Also at Institute of Physics, Academia Sinica, Taipei, Taiwan
- ^q Also at Department of Physics, Nanjing University, Jiangsu, China
- ^r Also at School of Physics and Engineering, Sun Yat-sen University, Guangzhou, China
- ^s Also at Academia Sinica Grid Computing, Institute of Physics, Academia Sinica, Taipei, Taiwan
- ^t Also at Laboratoire de Physique Nucléaire et de Hautes Energies, UPMC and Université Paris-Diderot and CNRS/IN2P3, Paris, France
- ^u Also at School of Physical Sciences, National Institute of Science Education and Research, Bhubaneswar, India
- ^v Also at Dipartimento di Fisica, Sapienza Università di Roma, Roma, Italy
- ^w Also at Moscow Institute of Physics and Technology State University, Dolgoprudny, Russia
- ^x Also at Section de Physique, Université de Genève, Geneva, Switzerland
- ^y Also at Department of Physics, The University of Texas at Austin, Austin TX, United States of America
- ^z Also at Institute for Particle and Nuclear Physics, Wigner Research Centre for Physics, Budapest, Hungary
- ^{aa} Also at International School for Advanced Studies (SISSA), Trieste, Italy
- ^{ab} Also at Department of Physics and Astronomy, University of South Carolina, Columbia SC, United States of America
- ^{ac} Also at Faculty of Physics, M.V.Lomonosov Moscow State University, Moscow, Russia
- ^{ad} Also at Physics Department, Brookhaven National Laboratory, Upton NY, United States of America
- ^{ae} Also at Moscow Engineering and Physics Institute (MEPhI), Moscow, Russia
- ^{af} Also at Department of Physics, Oxford University, Oxford, United Kingdom
- ^{ag} Also at Institut für Experimentalphysik, Universität Hamburg, Hamburg, Germany
- ^{ah} Also at Department of Physics, The University of Michigan, Ann Arbor MI, United States of America
- ^{ai} Also at Discipline of Physics, University of KwaZulu-Natal, Durban, South Africa
- * Deceased